ESTIMATION OF ECOLOGICALLY RELEVANT LAND COVER VARIABLES FROM IMAGING SPECTROSCOPY

Dissertation

zur

Erlangung der naturwissenschaftlichen Doktorwürde
(Dr. sc. nat.)

vorgelegt der

Mathematischen-naturwissenschaftlichen Fakultät

der

Universität Zürich

von

Silvia Huber Gharib

von Schübelbach SZ

Promotionskomitee

Prof. Dr. Klaus I. Itten (Vorsitz)
Dr. Niklaus E. Zimmermann
Dr. Mathias Kneubühler

Zürich, 2008

Abstract

The terrestrial biosphere is a key part of the global climate system. In particular vegetation strongly affects exchanges of energy and moisture between land and the atmosphere by influencing temperature, evapotranspiration, convective transfer of heat and moisture and atmospheric composition. The structure, type and condition of vegetation canopies are of high relevance for all the interactions. Currently, the dynamics of land-atmosphere interactions are not well quantified at regional or global scales, constituting one of the major limitations for large-scale climate projection. Refined information on vegetated land cover and its change, phenology, structure and moreover function is therefore critical to enhance our understanding and modeling ability of exchanges between the Earth's surface and the adjacent atmosphere.

This thesis presents two aspects of information on vegetated land covers outlined above: first, the determination of functional vegetation properties namely foliar biochemistry and second, on a regional level, the classification of land cover and plant functional types. The major goal of the presented work is to derive vegetation and land cover properties from directional and/or hyperspectral Earth observations relevant to ecosystem and Earth system modeling emphasizing novel statistical methods. In a first part, the thesis focuses on the development of statistical models from airborne hyperspectral (HyMap) and spaceborne spectrodirectional (CHRIS) data with a newly introduced subset selection algorithm to derive quantitative information on foliar biochemistry (nitrogen, carbon and water concentration) at the canopy level within mixed forests in the Swiss Plateau region. The second part addresses the use of support vector machines (SVM) to classify land cover and plant functional types from spectrodirectional observations. Hence, a major part of this dissertation deals with the combined exploitation of the two information dimensions (spectral and directional) provided by the innovative hyperspectral and multidirectional Earth observation system CHRIS-PROBA.

The work on foliar biochemistry has demonstrated the feasibility to develop statistical models of sufficient accuracy among three study sites and eleven species belonging to three functional types to predict foliar chemistry with airborne HyMap data. The utility of the newly introduced subset selection method is shown with enhanced results compared to a standard procedure. The additional information contained in multidirectional CHRIS data had a positive impact on model accuracy to estimate biochemistry: model fits augmented and prediction errors declined considerably. With this study the improved use of the directional dimension not only for structural estimates, as shown in previous studies, but indirectly also for biochemical estimates is proven. The developed models allow us to generate regional maps of biochemical concentration, which may serve as an important tool for monitoring forest health and status.

The second part of the dissertation was designed to investigate non-parametric support vector machines (SVM) to classify multidirectional CHRIS data into land cover classes and plant functional types. The results of this investigation show that support vector machines achieved higher classification accuracies than standard methods such as the maximum

likelihood classifier. Further, this study has demonstrated that directional data improved classification accuracies in general.

More broadly, this work has shown the usefulness of introducing novel statistical algorithms to the hyperspectral remote sensing community. The findings of this dissertation emphasize the beneficial value of spectrodirectional measurements for application-oriented studies in the field of environmental remote sensing and they enhance our understanding in using these data.

Zusammenfassung

Terrestrische Ökosysteme nehmen eine zentrale Rolle ein im globalen Klimasystem. Insbesondere die Vegetation beeinflusst durch ihren Stoff- und Energiehaushalt die Interaktionen zwischen Land und Atmosphäre massgeblich. Das Wissen über das Ausmass und die Dynamik dieser Wechselwirkungen ist noch ungenügend, was eine der grossen Unsicherheiten für grossräumige Klimaprojektionen darstellt. Detaillierte Information über die Art der Bodenbedeckung, deren saisonale und langfristige Veränderung sowie Struktur und Physiologie ist eine wichtige Voraussetzung um Interaktionen besser zu verstehen und um Ökosystem- und Klimamodelle weiterzuentwickeln, sowohl für die globale wie auch für die regionale Skala. Eine kontinuierliche und grossflächige Beschreibung von Ökosystemparametern kann jedoch nur durch Fernerkundungstechniken erreicht werden.

Das Ziel dieser Arbeit ist die Herleitung von Ökosystemparametern aus Fernerkundungsdaten mittels innovativer statistischer Methoden. Neben der Benutzung des flugzeuggetragenen Hyperspektralsensors HyMap werden in dieser Dissertation die Daten des satellitengetragenen CHRIS-Sensors verwendet, der zwei Informationsdimensionen (spektral und direktional) gleichzeitig verfügbar macht. Der Beitrag von multiangularer Information für verschiedene Anwendungen wird in dieser Arbeit umfassend diskutiert.

Im ersten Teil der Arbeit werden statistische Modelle mit einem für die Fernerkundung neuen Variablen Selektionsalgorithmus entwickelt, um quantitative Information über biochemische Blattparameter (Stickstoff-, Kohlenstoff- und Wasserkonzentration) aus HyMap und CHRIS-Daten herzuleiten. Die Daten für die Methodenentwicklung wurden in drei Mischwäldern (zwei im Kanton Aargau, einer im Kanton Solothurn) im Schweizer Mittelland erhoben. Die erzielten Resultate haben gezeigt, dass statistische Modelle mit genügender Genauigkeit über mehrere Untersuchungsgebiete und Baumarten kalibriert werden können, um die Blattchemie aus HyMap-Daten herzuleiten. Der Nutzen des neu eingeführten Selektionsalgorithmus konnte anhand von verbesserten Resultaten im Vergleich zu einer herkömmlichen Methode demonstriert werden. Die Zusatzinformation die in multidirektionalen CHRIS Daten enthalten ist, hatte einen positiven Einfluss auf die Genauigkeit der Modelle. Mit dieser Untersuchung konnte dargelegt werden, dass die direktionale Dimension in Fernerkundungsdaten nicht nur für die Herleitung von Strukturparametern (bspw. Blattflächenindex) verwendet werden kann, sondern ebenso gut für die genauere Abschätzung von biochemischen Parametern geeignet ist. Mit den entwickelten statistischen Modellen können regionale Biochemiekarten hergestellt werden, die der Überwachung des Waldzustands oder als Eingangsgrössen in Ökosystemmodelle dienen können.

Im zweiten Teil der Arbeit wird der Nutzen von Support Vektor Maschinen für die Klassifikation der Bodenbedeckung sowie funktionellen Vegetationstypen aus spektrodirektionalen CHRIS-Daten untersucht. Insbesondere wird der Einfluss der spektralen und der direktionalen Komponente der Fernerkundungsdaten auf das Klassifikationsresultat betrachtet. Das verwendete Untersuchungsgebiet liegt im Kanton Aargau, südlich von Rothrist und umfasst den grössten Wald des Schweizer Mittellandes, kleinräumige

Ackerbauflächen, Wiesen und Siedlungsgebiete. Die Resultate dieser Untersuchung haben gezeigt, dass Klassifikationen mit Support Vektor Maschinen genauer sind als solche, die mit einer herkömmlichen Methode (Maximum Likelihood Classifier) durchgeführt werden. Auch in dieser Analyse führte der Gebrauch von multidirektionalen Daten zu einem verbesserten Produkt verglichen mit Klassifikationen basierend auf Nadir-Daten.

Insgesamt hat diese Dissertation das Potential von innovativen statistischen Algorithmen für die hyperspektrale Fernerkundung aufgezeigt. Die Eignung multiangularer Erdbeobachtungsdaten für praktische Anwendungen im Bereich der Umweltüberwachung konnte dargelegt und das Verständnis für den Gebrauch dieser Daten verbessert werden.

Table of Contents

List of Figures

List of Tables

List of Acronyms

Adj.-R^2	Adjusted coefficient of determination
AEON	Australian Ecosystem Observation Network
AIC	Akaike's Information Criterion
ALL	dataset with samples from all three study sites and tree species
ANIF	Anisotropy Factor
ANIX	Anisotropy Index
APEX	Airborne Prism EXperiment
ASD	Analytical Spectral Devices
ATCOR	Atmospheric and Topographic CORrection software
ATSR	Along-Track Scanning Radiometer
B&B	Branch-and-Bound algorithm
BDD	dataset with all broadleaf deciduous samples
BET	Bettlachstock study site
BNC	Band depths Normalized to the waveband Center of the absorption feature
CAO	Carnegie Airborne Observatory
CASI	Compact Airborne Spectrographic Imager
CBD	Convention on Biological Diversity
CCD	Convention to Combat Desertification
CHRIS	Compact High Resolution Imaging Spectrometer
C:N ratio	Carbon to Nitrogen ratio
CRDR	Continuum-Removed Derivative Reflectance
CV	Cross-Validation
CV-RMSE	Cross-Validated Root Mean Squared Error
DSM	Digital Surface Model
DTM	Digital Terrain Model
ENVI	ENvironment for Visualizing Images (software)
EO	Earth Observation
ESA	European Space Agency
FCCC	Framework Convention on Climate Change
FDR	First Derivative Reflectance
FOV	Field Of View
FSD	dataset with all European beech (*Fagus sylvatica*) samples
FZA	Fly-by Zenith Angle
GCP	Ground Control Point
GEO	Group on Earth Observation
GEOSS	Global Earth Observation System of Systems
GLP	Global Land Project
GMES	Global Monitoring for Environment and Security
GPS	Global Positioning System
HyMap	Hyperspectral Mapping imaging spectrometer
IFOV	Instantaneous Field Of View
imageSVM	an IDL based SVM tool to classify remote sensing data
INDIVIDUAL	Individual parameter set for every binary problem (SVM)
IPCC	Intergovernmental Panel on Climate Change
K	Kappa coefficient
KUT	Kuettigen study site
LAD	Leaf Angle Distribution
LAI	Leaf Area Index
LIBSVM	integrated software for support vector classification, regression and distribution estimation
MEA	Multilateral Environmental Agreement

MEAN	Single parameter set for all binary problems (SVM)
MISR	Multiangle Imaging SpectroRadiometer
MLC	Maximum Likelihood Classifier
MSPI	Multiangle SpectroPolarimetric Imager
NASA	National Aeronautics and Space Administration
NBDI	Normalized Band Depth Index
NED	dataset with all needle-leaf evergreen samples
NEON	National Ecological Observatory Network
NIR	Near-Infrared
NIRS	Near-Infrared spectroscopy
OA	Overall Accuracy
OAA	One-Against-ALL (SVM)
OAO	One-Against-One (SVM)
PARGE	PARametric GEocoding software
PFT	Plant Functional Type
POLDER	Polarization and Directionality of the Earth's Reflectance
PROBA	PRoject for On-Board Autonomy
R^2	Coefficient of determination
RBF	Radial Basis Function
RMSE	Root Mean Squared Error
ROI	Region Of Interest (ENVI)
RTM	Radiative Transfer Model
SPEC	dataset with untransformed reflectance values
SVM	Support Vector Machine
TM	Thematic Mapper (Landsat)
TOPS	Terrestrial Observation and Prediction System
UNEP	United Nations Environment Program
VOR	Vordemwald study site
WSSD	World Summit on Sustainable Development

1 Introduction

Society depends on ecosystems in the same way it depends on the weather, water resources and agriculture. Earth's ecosystems perform numerous functions that regulate climate and maintain habitable conditions for life on Earth. The extent, structure and functioning of the ecosystems have been considerably transformed over the last three centuries mainly through human activity (Vitousek et al., 1997; Solomon et al., 2007). The most significant change in the structure of ecosystems has been the transformation of approximately one quarter of the terrestrial surface to cultivated systems (Millennium Ecosystem Assessment, 2005). Change and variability in land cover and land use are significant drivers of climate change through feedbacks to the atmosphere (Feddema et al., 2005; Foley et al., 2005; Pielke Sr, 2005), influencing biodiversity (Koh, 2007), ecosystem processes and services (Defries and Bounoua, 2004) and are therefore of high socio-economic relevance (Stern, 2007). The loss of biodiversity threatens food supplies, health and security (Secretariat of the Convention on Biological Diversity., 2006) and thus may undermine many ecosystem services in the long run (Foley et al., 2005).

Local and regional climates and hydrology are fundamentally driven by the exchanges of gases, heat, water and small particles between the land and the atmosphere (Mooney et al., 1987; Schimel et al., 2001). In particular vegetation is the driving force of all terrestrial biological processes and builds 29 % of the interface of the global surface with the atmosphere (Graetz, 1990). Most of these exchange processes that take place between plant surfaces and the atmosphere are driven by the incoming energy from the sun and controlled by both surface factors and the structural characteristics of the canopy itself (McPherson, 2007). Therefore, accurate characterisation of land surface properties and temporal dynamics serve as key components to many land cover schemes that form part of Earth system models, ecosystem process models, water interception models or carbon cycle process models, which in turn are used as prediction tools in climate and ecosystem research. Currently, the dynamics of land surface properties and land-atmosphere interactions are not well quantified at regional or global scales, constituting one of the major limitations for large-scale climate projections (European Space Agency, 2006; Solomon et al., 2007). Because repeated and continuous coverage is not feasible with ground measurements over large spatial areas, remotely sensed data usually provide the only means to characterize such extents. Detailed vegetation characterization will improve the predictive capabilities of available Earth system and climate models and allow a more consistent understanding of the relevant processes of terrestrial ecosystems. The predictive character of land-surface schemes is necessary in order to fully couple the dynamics of surface and atmosphere in global climate models (European Space Agency, 2006).

1.1 Remote sensing of land ecosystems

Earth observation in general is an excellent tool for monitoring the environmental state over space and time. It provides spatially continuous and temporally frequent information products

in manifold spectral and directional settings (=four information dimensions). Hence, remote sensing enabled exceptional advances in the modelling, mapping and understanding of ecosystems (Turner et al., 2004; Ustin et al., 2004) because it allowed ecologists to investigate new spatial and temporal scales: for example by discerning large-scale patterns in ecological systems, by measuring large-scale processes near real time (Graetz, 1990) and to access longer term, quasi-continuous data over much wider regions than has previously been monitored using ground-based assessments (Roughgarden et al., 1991). Consequently, the use of Earth observation (EO) in ecological research, ecosystem monitoring and management has significantly increased in recent years (Fassnacht et al., 2006).

The successful integration of remote sensing derived products with ecology began with the launch of Landsat in 1972 (Cohen and Goward, 2004). Ever since then, a considerable amount of publications reflects the use of such data for a wide range of ecological applications with spatial and temporal context (Roughgarden et al., 1991; Wickland, 1991; Cohen and Goward, 2004; Schaepman, 2007). One of the first and most commonly used applications in the field of remote sensing was land cover classification. Over the last two decades substantial research efforts have been devoted to extracting land cover information from remote sensing data (Swain and Davis, 1978; Defries and Townshend, 1999; Waske and Benediktsson, 2007). Land cover mapping provides key environmental information needed for scientific analyses, resource management and policy development at regional, continental and global levels (Bartholome and Belward, 2005). Characterization of land cover resulted in products with spatial extent ranging from ecosystems (Held et al., 2003; Johansen et al., 2007) to habitats (Zimmermann et al., 2007) and with thematic resolution ranging from forest mapping and inventories (Darvishsefat, 1995; Kellenberger, 1996; Schlerf and Hill, 2005; McRoberts and Tomppo, 2007) to those containing detailed information about plant functional types and species (Cochrane, 2000; Kokaly et al., 2003; Clark et al., 2005). Some studies focused on continuous fields incorporating biophysical and biochemical variables (Schwarz and Zimmermann, 2005) while others have shown the value of EO to map temporal phenomena, such as land cover changes (Lenney et al., 1996), successional stages (Koetz et al., 2007) or phenology (Kneubühler, 2002). Further more, remote sensing techniques were used for biodiversity studies (Carlson et al., 2007) and finally for general environmental monitoring and management (Phinn et al., 2000; Fassnacht et al., 2006).

1.1.1 Imaging spectroscopy

With the advent of imaging spectroscopy, also known as hyperspectral remote sensing, in the mid-1980s, a significant advancement was achieved in monitoring quantitative characteristics of terrestrial ecosystems due to the extended spectral dimension. In contrast to multispectral sensors, imaging spectrometers sample contiguously in the visible and infrared part of the electromagnetic spectrum using dozens to hundreds of narrow spectral bands (Goetz et al., 1985). Using the reflectance information from these narrow spectral bands (usually only few nanometers wide) it is possible to assess plant conditions manifested in foliar biochemical status, for example, by developing statistical relationships sensitive to biochemistry. That is because the spectral reflectance features result from harmonics and overtones of absorptions

by foliar biochemicals (Murray and Willliams, 1987; Curran, 1989; Elvidge, 1990).

The findings between plant chemical constituents and the absorption of electromagnetic radiation evolved from the research field of laboratory near-infrared spectroscopy (NIRS) to the remote sensing community (Norris et al., 1976). A number of studies proved that there are strong relationships between the concentration of key biochemicals, including nitrogen concentration and the level of radiation across spectral absorption features in dry ground leaves (Elvidge, 1990; McLellan et al., 1991) as well as in fresh whole leaves (Curran et al., 1992; Martin and Aber, 1994). However, the increasing complexity at the canopy level complicates the application of laboratory- or monoculture-tested methods so that these relationships become weaker at the canopy level. Yet further research in this field is needed to improve the methodology to deal with complex natural environments such as mixed forests.

Ecological applications to which hyperspectral sensing has been contributing significantly (Goodenough et al., 2006) are forest disaster detection (Lawrence and Labus, 2003), invasive species mapping (Underwood et al., 2003; Asner and Vitousek, 2005), Kyoto protocol information provision (Kurz and Apps, 2006), forest health monitoring (Goodenough et al., 2004) or global change studies (Goetz et al., 2005). Accurate remotely sensed estimates of foliar biochemical concentrations of vegetation canopies have been used to aid understanding of ecosystem function over a wide range of scales (Peterson et al., 1988; Wessman et al., 1988; Martin and Aber, 1997; Dawson et al., 1999; Ollinger et al., 2002). In addition, information about foliar biochemistry provides us with indicators of plant productivity, rate of litter decomposition and availability of nutrient in space and time (Curran, 1989). Hence, imaging spectroscopy permits the extraction of unprecedented information about the terrestrial environment (Curran, 2001; Ustin et al., 2004).

Currently, several airborne systems provide hyperspectral Earth observations (e.g., the compact airborne spectrographic imager (CASI) or the Hyperspectral Mapping Imaging Spectrometer (HyMap)), but only two non-military spaceborne hyperspectral sensors are operating: ESA's Compact High Resolution Imaging Spectrometer (CHRIS) and NASA's Hyperion. At present, several hyperspectral sensors are under development or at the planning stage, such as the Airborne Prism Experiment (APEX) (Nieke et al., 2005), the Airborne Reflective Emissive Spectrometer (ARES) (Richter et al., 2005), the Environmental Mapping and Analysis Program (EnMap) (Stuffler et al., 2007), the South African Multi Sensor Micro-satellite Imager (MSMI) (http://www.sunspace.co.za), the Canadian Hyperspectral Environment and Resources Observer (HERO) (Hollinger et al., 2006) or the Flora satellite mission (Asner et al., 2005).

1.1.2 Multidirectional remote sensing

Apart from the spatial, spectral and temporal information dimension of Earth observations, the directional dimension is an additional information source which permits the anisotropy of land surfaces to be documented. Multidirectional reflectance observations of terrestrial ecosystems contain additional and unique information beyond that acquired with nadir or single-angle spectral measurements (Barnsley et al., 1997; Asner et al., 1998; Diner et al., 1999; Schönermark et al., 2004; Diner et al., 2005).

So far, the exploitation of passive optical observations largely focused on characterizing the spatial heterogeneity (horizontal dimensions). However, the radiative transfer in complex three-dimensional vegetation canopies cannot fully be represented with nadir or monodirectional systems. Due to the complex three-dimensional nature of vegetation canopies, independent observations are necessary for its comprehensive and robust characterization. Hyperspectral and multidirectional measurements from space offer new and unique opportunities to access the complexity of light scattering on the surface and hence to the structural and optical information contained therein (Schönermark et al., 2004).

It has been recognized that the anisotropy of the scattered radiation field is intimately related to the structural properties of the observed surfaces (e.g., Minnaert, 1941; Hapke, 1981). Hence, a number of studies have investigated how to relate surface anisotropy to surface vegetation structure (e.g., Chen et al., 2003; Chopping et al., 2003). Sandmeier and co-workers (1999) developed two quantities, the anisotropy factor (ANIF) and the anisotropy index (ANIX) to derive canopy structural characteristics from directional hyperspectral data (Sandmeier and Deering, 1999). These two quantities allow a direct comparison of the anisotropic effect and its spectral variability for various land cover classes. In another study, physically based interpretations were used to relate the anisotropy of multi-directional reflectance measurements to the structure and heterogeneity of the underlying surface (Widlowski et al., 2001; Pinty et al., 2002; Widlowski et al., 2004).

Some authors found that the use of directional observations could improve the retrieval of relevant ecological parameters such as leaf area index (LAI) (Diner et al., 1999), gap fraction and leaf orientation (Chen et al., 2003; Ustin et al., 2004), tree cover and tree height (Heiskanen, 2006; Kimes et al., 2006) or wheat yield maps (Begiebing et al., 2007). It was also shown that the separability of land cover types may improve when using multiangular data (Barnsley et al., 1997; Gobron et al., 2000; Brown de Colstoun and Walthall, 2006). However, the impact of multidirectional data on the estimation of canopy biochemistry was never investigated to date. Because canopy reflectance is influenced by many factors including leaf optical properties and canopy structure, it seems obvious that also biochemical estimates are affected by surface anisotropy.

These research findings express the relevance of multiangular measurements also to a variety of societal themes, such as improving weather forecasting, addressing climate variability and change, supporting global land observations, assisting measurements of water supply and air quality (Macauley and Diner, 2007).

Most exact measurements of anisotropic reflectance characteristics are captured with goniometer systems. By comparing goniometric data of a particular target with directional satellite data we obtain detailed information that may contribute to more accurate bi-directional reflectance models (Schopfer et al., 2007). However, such detailed measurements are only feasible for a few selected targets. Directional data acquired from air- or spaceborne platforms is thus vital for large-scale and application-oriented projects. Currently, there is only one spaceborne instrument with the capability of acquiring hyperspectral and multiangular data simultaneously: the Compact High Resolution Imaging Spectrometer (CHRIS) on-board of the PROBA (Project for On-board Autonomy) platform (Barnsley et al.,

2004). Other multispectral sensors capable of simultaneously measuring multiangular reflectance are the Multiangle Imaging SpectroRadiometer (MISR) (Diner et al., 2002), the Along-Track Scanning Radiometer (ATSR-2/AATSR) (Stricker et al., 1995) or the Polarization and Directionality of the Earth's Reflectances (POLDER) (Deschamps et al., 1994). A successor of MISR is currently under planning, the Multiangle SpectroPolarimetric Imager (MSPI) (Diner et al., 2007).

1.2 Societal and political awareness

Human-induced environmental change has accelerated over the last three decades and this enhanced awareness at the global governance level for environmental policy. Consequently, a rapid growth in the number of environmental agreements and treaties since the 1972 Stockholm Conference on the Environment was observed and the Earth Summit in 1992 led to the establishment of multilateral environmental agreements (MEAs), with the formation of three major conventions: the Convention on Biological Diversity (CBD), the Convention to Combat Desertification (CCD) and the UN Framework Convention on Climate Change (FCCC). The World Summit on Sustainable Development (WSSD) in 2002 in Johannesburg finally highlighted the urgent need for coordinated observations relating to the state of the Earth for achieving sustainable development (United Nations, 2002).

Many existing MEAs involve environmental factors that could be assessed remotely and efforts are underway to use remote sensing technology in relation to such agreements, for example to examine changes in biodiversity in the context of the CBD (Strand et al., 2007) or to monitor carbon sequestration under the UNFCCC Kyoto Protocol (Kurz and Apps, 2006). The Kyoto Protocol's effectiveness will strongly depend on whether the emission data used to assess compliance are reliable. Remote sensing can provide substantial support to the protocol by providing spatially referenced, systematic and continuous observations of large areas (Rosenqvist et al., 2003; IPCC, 2007). Earth observation can also significantly contribute to global environmental assessments in support of MEAs, including the Millenium Ecosystem Assessment (Millennium Ecosystem Assessment, 2005) or the Global Environmental Outlook (United Nations Environment Programme, 2007).

The increased emphasis being given to meeting societal benefits within the EO community is reflected in several agreements. The agreement at the Third Earth Observations Summit in 2005 to establish a Global Earth Observation System of Systems (GEOSS) could facilitate and contribute to the implementation and surveillance of all treaties described above. The purpose of GEOSS is to achieve comprehensive, coordinated and sustained observations of the Earth system, in order to improve monitoring of the state of the Earth, increase understanding of Earth processes and enhance prediction of the behavior of the Earth system (GEO, 2005). GEOSS will focus on nine societal benefit areas, two of which address biodiversity and ecosystem management and protection.

Another agreement that directly serves society, is the international charter on 'Space and Major Disasters', initiated by global space agency members. The charter aims at providing satellite data free of charge to rescue authorities responding to major natural or man-made disasters anywhere in the world (http://www.disasterscharter.org).

Finally, the Global Monitoring for Environment and Security (GMES), a joint initiative of the European Commission and the European Space Agency, is a particular example of how remote sensing should make environmental and security-related EO information available to the people and organizations who need it (GENACS Consortium, 2005).

1.3 Objectives and structure of thesis

The major goal of the presented PhD dissertation is to derive vegetation and land cover properties from directional and/or hyperspectral Earth observations relevant to ecosystem and Earth systems modeling. This thesis has been divided into two thematic parts. The first part will focus on the development of statistical models from airborne hyperspectral (HyMap) and spaceborne spectrodirectional (CHRIS) data to derive quantitative information on foliar biochemistry at the canopy level within mixed forests. The second part will address the use of support vector machines (SVM) to classify land cover and plant functional types from spectrodirectional CHRIS observations. Hence, a major part of this dissertation deals with the combined exploitation of the two information dimensions (spectral and directional) provided by the innovative hyperspectral and multidirectional EO system CHRIS-PROBA.

The following research questions have been developed and will be investigated in this dissertation:

Part 1: Biochemistry assessment

- Can statistical models be developed among a broad range of species and multiple study sites to predict foliar nitrogen, carbon and water concentration with sufficient accuracy? (chapter 4)
- Can predictive statistical models be improved by using novel variable selection methods? (chapter 4)
- How do statistical models perform when built only on causal wavebands? (chapter 4)
- Do multiangular measurements improve statistical models to predict foliar biochemistry at the canopy level? (chapter 5)
- How do different viewing angles (and their combination) influence the predictive quality of statistical models to estimate foliar biochemistry at the canopy level? (chapter 5)
- Is added information contained in multiangular data still present after continuum removal and normalization procedures have been applied to reflectance data? (chapter 5)

Part 2: Land cover and plant functional types classification

- How does the support vector machines classifier perform compared to a standard method? (chapter 6)
- To what extent do the spectral and directional data dimensions affect the classification results? (chapter 6)

The dissertation has been organized in the following way: chapter two introduces the study sites and describes the used material including field and laboratory measurements as well as the acquisition and preprocessing of airborne HyMap and spaceborne CHRIS image data. Chapter three lays out the intrinsic properties of models in general, outlines the methodologies used to derive biochemical canopy attributes and evaluates at the approach applied to classify land cover and pant functional types. Chapters four and five present results of the biochemistry assessment with airborne HyMap and spaceborne CHRIS data, respectively, and chapter six imparts the results of the land cover and plant functional types classification with support vector machines. Chapter seven concludes with main findings derived from the research and a last chapter (eight) provides an outlook.

2 Material

A broad variety of material is needed to elaborate environmental remote sensing analyses. This chapter addresses the study sites, field and laboratory data, sensors and imagery as well as data preprocessing. Comparably big efforts are needed to obtain leaf material from the tree crowns in order to relate foliar biochemical concentrations with remotely sensed information.

2.1 Study sites

The ground data used in this study was collected in 2004 in three different sites on the Swiss Plateau: Vordemwald (VOR) 7°53' E, 47°16'N, Kuettigen (KUT) 8°02' E, 47°25'N and Bettlachstock (BET) 7°25' E, 47°13'N (Fig. 2.1). The investigations described in chapter 4 involve data of all three study sites whereas the studies shown in the chapters 5 and 6 are solely based on data sampled at the Vordemwald site.

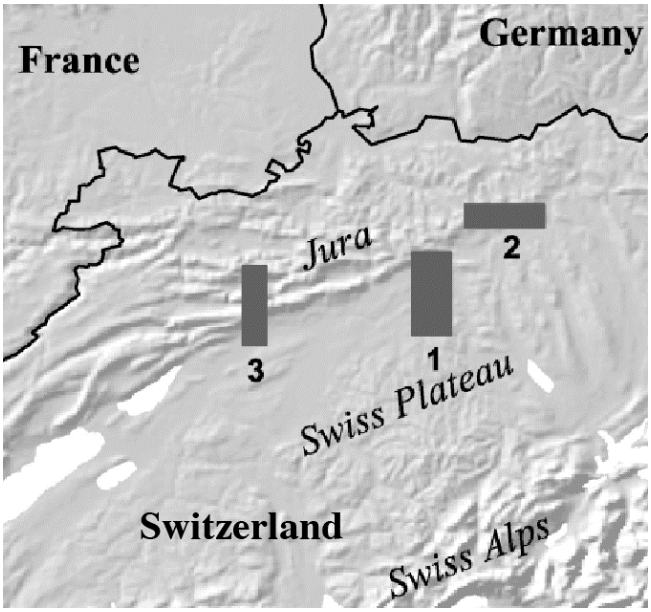

Fig. 2.1. Study sites of the field campaign 2004 in Switzerland. The three areas (1: Vordemwald; 2: Kuettigen; 3: Bettlachstock) represent the coverage of the acquired HyMap images. Field data were collected at different subplots located at the three sites.

The Swiss Plateau includes a broad variety of vegetation and soil types and covers flat areas as well as mountainous regions. This variety enabled the collection of a wide range of species composition and foliar chemistry. Study sites stretch from an altitude of ~400 to 1200 meters above see level. In all three sites the canopy is composed of a mixture of plant fuctional types. The most important tree species include European beech (*Fagus sylvatica* L.), English oak (*Quercus robur* L.), European ash (*Fraxinus excelsior* L.), sycamore maple (*Acer pseudoplatanus* L.), silver fir (*Abies alba* Mill.), Norway spruce (*Picea abies* L.) and Scots pine (*Pinus sylvestris* L.). Additionally, black alder (*Alnus glutinosa* (L.) Gaertn.), littleleaf linden (*Tilia cordata* Mill.), northern red oak (*Quercus rubra* L.) and European larch (*Larix decidua* Mill.) were sampled. A total of eleven different species were sampled belonging to

three plant functional types, namely: needleleaf evergreen, needleleaf deciduous (*Larix* only) and broadleaf deciduous.

At the three study sites (VOR, KUT and BET) 15, 8 and 5 subplots, respectively, were determined where field sampling took place. The subplots for the best sampled site VOR are indicated in Fig. 2.2. The subplots were chosen according to their species composition, to

Fig. 2.2. Study site Vordemwald (VOR) that represents the best sampled site, seen by the HyMap sensor. White squares indicate subplots where field data were collected including foliar material, crown dimensions and Leaf Area Index.

cover a broad variety of species and hence to gain a broad range of biochemical concentrations, and their within-stand species homogeneity to obtain either pure coniferous or deciduous subplots. The species were selected according to their proportion in the forest surrounding the subplots so that they were dominant within a group of neighboring trees and accordingly the spatial scale of several CHRIS pixels (18 m). Only those trees were selected for foliar sampling with large crown dimension.

2.2 Field data sampling

In July 2004, field data were sampled to determine leaf biochemistry in the laboratory and to obtain additional biophysical and positional tree properties. At each subplot of the three study sites 3–10 tree crowns were climbed for foliar material sampling in the crown top. A tree climber excised three different upper sunlit canopy branches from a total of 132 trees (60 at the Vordemwald site), whereof 52 were conifers and 80 broadleaves. To obtain representative samples, the field assistants collected in total 45 leaves from the three deciduous branches and 50–60 needles from all selected needle-leaved branches including the first three needle years. For each sampled tree the collected leaf material was pooled, sealed in bags and stored in a cool box for transportation.

Further, height and crown dimensions of all sampled trees were assessed using a Forestor Vertex Hypsometer (Haglof Inc.). A transponder was temporarily attached to the trunk at breast height and with the hand unit the operator measured the distance from the trunk and treetop by sonic pulses. To determine the projection of the crown to the ground, the radii along the four main axes were measured. The heights of the trees ranged from 18 m to 46 m with a mean of 31 m. The mean radii of a broad-leaved and a needle-leaved tree crown were found to be 4.7 m and 3.0 m, respectively. Leaf Area Index (LAI) was determined using a LAI-2000 Plant Canopy Analyzer (LI-COR, 1992). Measures of LAI ranged from 3.8–6.5. Also for the closest neighboring trees to the sampled trees geographical positions, species name and few canopy structural properties (height, diameter) were measured, but no foliar material was collected.

To geo-locate the sampled individual tree crowns later in the remotely sensed images, the trunk position of each tree was measured during the field campaign with a Trimble GeoXT GPS receiver, which corrects for multipath biases. The positional precision was improved by recording 20 to 40 GPS measurements per trunk and by applying a post processing differential correction to the recorded data using the Pathfinder Office software (Trimble, 2005). For each GPS position, horizontal precision estimates were calculated using an algorithm that accounts for the number and configuration of the satellites in view to the receiver (Trimble, 2005). For a sampled tree the horizontal precision estimate represents the radius (from the mean GPS position of the trunk) of a circle within which the positional value lies at least 95 % of the time. The GPS horizontal precision estimates among all trees and study sites varied between 1.2 and 9.8 m with a mean value of 2.7 m (for more details see Table 4.1 in chapter 4).

2.3 Laboratory analyses

In the laboratory, the leaf area, the fresh and dry weight and the biochemical composition was determined for all 132 collected leaf samples. An LI-3100 Area Meter (LI-COR, 1987) was used to obtain the projected leaf area of the samples. Fresh and dry mass were determined by weighing the samples before and after being oven dried at 85° C until a constant weight was achieved and from the difference between the fresh and dry masses divided by the area, water content per cm^2 was calculated. For C:N analyses the samples were dried at 65 °C until a

constant weight was achieved, then ground to powder and finally injected into an elemental analyzer (NA 2500; CE Instruments, Milan, Italy). These analyses were performed by the WSL laboratory. From each sample, two sub-samples were analyzed and checked for within-sample variation. None of the samples exceeded a threshold of 3 % variation between the two sub-sample measurements and its mean.

2.4 Hyperspectral data acquisition and processing

The characterization of quantitative forest properties from remote sensing data requires acquisition and preprocessing of image data. This section outlines the acquisition and processing of airborne HyMap data and spaceborne directional CHRIS data.

2.4.1 Airborne HyMap data acquisition and processing

On 29 July 2004, imaging spectrometer data were recorded for all three study sites using HyVista's Hyperspectral Mapping Imaging Spectrometer (HyMap) (Cocks et al., 1998). The HyMap sensor was flown on a Dornier Do-228 aircraft at an altitude of 3000 m a.s.l. and acquired data in 126 wavebands (15–20 nm in bandwidth), from 450 to 2480 nm at a spatial resolution of 5 m. Its instantaneous field of view (IFOV) is 2.5 mrad along-track and 2.0 mrad across-track and the field of view (FOV) is 60 degrees (512 pixels). Four 2.5x12 km scenes were acquired covering the three study sites under cloud free conditions. HyMap at-sensor radiance data were transformed to apparent surface reflectance using the ATCOR4 software (Richter and Schlaepfer, 2002). ATCOR4 performs a combined atmospheric/topographic correction, where effects of terrain such as slope, aspect and elevation of the observed surface is accounted for. The imaging spectrometer data were orthorectified based on the parametric geocoding procedure PARGE, which considers the terrain geometry and allows attitude (roll, pitch and heading) and flightpath dependent distortions to be corrected (Schläpfer and Richter, 2002; Schläpfer, 2005). The Swisstopo-DHM25 was used to geo-register the HyMap data – a digital terrain model (DTM) with a horizontal and vertical resolution of 25 m and 1.5 m, respectively. A DTM used for geo-registration has to be in accordance with the optical resolution and spatial accuracy of the HyMap data to be processed on the DTM. Therefore, the DTM was resampled to 5 m using the bilinear interpolated gaps method (Schläpfer et al., 2007).

The resulting surface reflectance datasets were compared to field spectroradiometer data, which were simultaneously taken during the overflights with an Analytical Spectral Devices (ASD) field spectrometer from a range of different ground objects (asphalt, dense lawn and water). The mean of several ASD measurements was then used for comparison with HyMap spectra (Fig. 2.3). For water bodies, the absolute difference between the reflectance derived from the imaging spectrometer HyMap and from ground measurements was 1 % at 740 nm and 0.5 % at 1500 nm. For the asphalt and lawn targets the maximum relative deviation was in the same range.

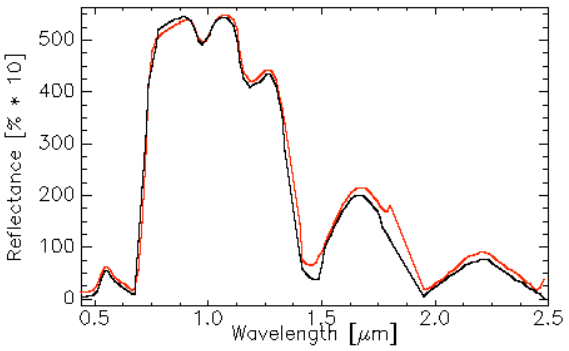

Fig. 2.3. Comparison of a mean vegetation spectrum measured with an ASD spectroradiometer at ground (red) and a preprocessed HyMap spectral signature (black).

A digital surface model (DSM) is deemed the best source for geometric correction as it is considered to be optically most relevant (Schläpfer 2003). Since no DSM was available, a DTM was used instead. As a consequence, there was a need to correct the HyMap viewing geometry for high objects such as trees in order to adjust positional shifts originating from the DTM-based geometric correction. Otherwise, it is not possible to find the exact position of tree crowns in the HyMap image. A trigonometric function was used for incorporating sensor viewing angles and tree heights to calculate the resulting shifts of each tree crown relative to the DTM corrections. Then the geographic tree positions were adjusted by subtracting the positional shifts from the ground-measured positions. The further away the trees were positioned from nadir the bigger was the distortion. The applied corrections ranged from 0.5 to 10 m.

Before spectral information was extracted from the HyMap images and transformed using the continuum removal procedure, all sampled tree crowns were localized in each image. To enable an accurate geographic localization of the crowns, all HyMap images were resampled to a spatial resolution of one meter using a bilinear interpolation algorithm. Then, the crown radius of each tree was displayed on the image as a circle (Fig. 2.4).

Fig. 2.4. Zoomed portion of a HyMap image showing tree crowns (white circles), trunk positions as measured using GPS (+) and the inner radii of the safe crown positions (95 % likelihood of correct representation) as derived from the GPS horizontal precision (black circles). Only HyMap spectral data inside of the inner (black) circle was used for analysis in order to reduce the effects of positional uncertainty. The ID's of the sampled trees are listed next to the tree centers.

Then, a *safe* crown projection was applied to the image by incorporating the horizontal positional precision of the GPS measurements. By this, the portion of the image that is safely (95 % likelihood) associated to the target tree crown irrespective of the direction of the positional error was displyed. This reduces the risk of linking the spectral response to understory vegetation or to a neighboring tree crown. The mean reflectance of all pixels which were positioned within the GPS safe crown projection of a selected tree crown were then extracted using the Region of Interest (ROI) Tool in the ENVI package (Research Systems, 2004). In most cases, the mean GPS precision estimates were clearly smaller than the crown circumferences.

2.4.2 Spaceborne CHRIS-PROBA data acquisition and processing

For the investigation of impacts of directionality on canopy biochemistry estimation and land cover classification, data of the spaceborne ESA-mission CHRIS (Compact High Resolution Imaging Spectrometer) on-board PROBA-1 were used (Barnsley et al., 2004). PROBA-1 was launched in October 2001 and it is equipped with five instruments including CHRIS, which provides multiangular data in the range from 447 nm to 1035 nm in 37 bands with a spatial resolution of 18 m at nadir (= land mode 5 configuration). CHRIS simultaneously supplies five viewing angles with the nominal fly-by zenith angles (FZA's) at ±36°, ±55° and 0° (nadir). The images were acquired on July 1, 2006, over the study site Vordemwald and covered an area of 6.5x13 km (Fig. 2.5).

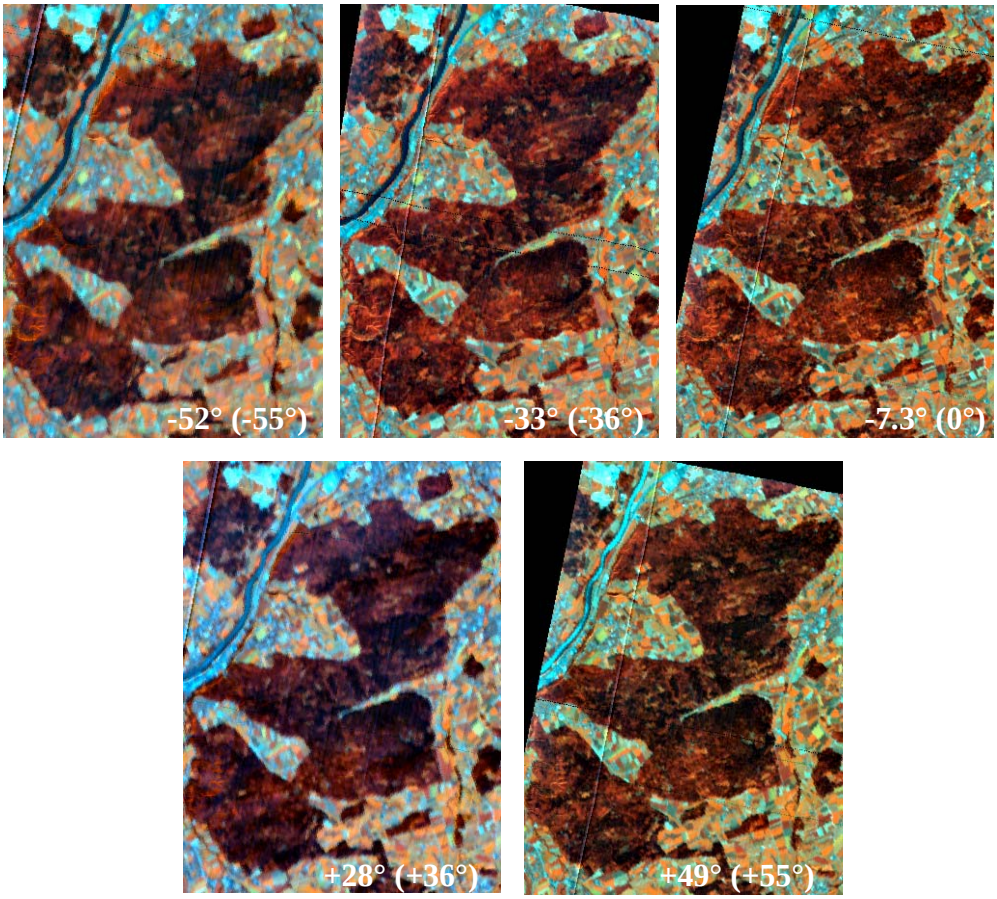

Fig. 2.5. Five CHRIS images acquired over the Vordemwald study site on July 1, 2006. In parenthesis are the nominal and aside the true fly-by zenith angles listed.

However, the actual viewing zenith angles of CHRIS data acquisitions do rarely represent the nominal FZA's due to uncertainties in pointing (Davidson and Vuilleumier, 2005). The actual viewing angle for the nadir image was for instance -7.3° in the backward scattering viewing direction (Fig. 2.6). In addition, Figure 2.6 shows that the acquisition has not occurred accurately in the solar principal plane where anisotropic effects are most pronounced for vegetation.

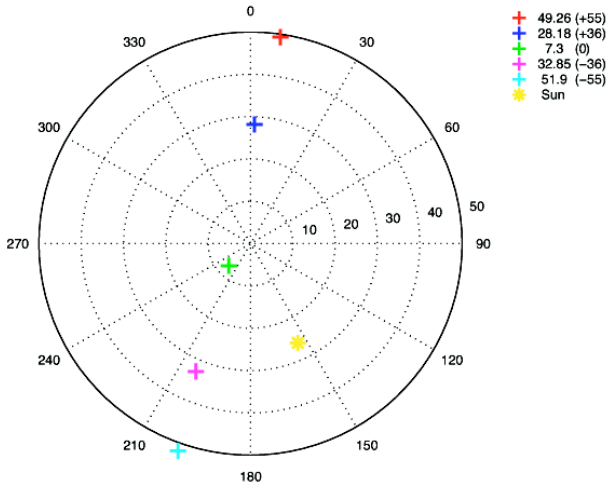

Fig. 2.6. Acquisition geometries and illumination angles for the five CHRIS images acquired on July 1, 2006. The nominal fly-by zenith angles are listed in brackets. The center of the plot represents the target.

The five CHRIS multiangular acquisitions were orthorectified and radiometrically corrected. Geometric correction was based on a three-dimensional physical model (Toutin, 2004), which is implemented in the commercially available image processing software PCI/OrthoEngine (PCI Geomatics, 2006). High positional accuracy of the respective multiangular products after geometric correction was a prerequisite for a reliable extraction of spectral information from the five images. To achieve a high geometric accuracy and a co-registration of the multiangular image cubes, georegistration was carried out on all five cubes using a digital surface model (DSM) (swisstopo ©) with 2 m resolution (Schläpfer et al., 2003). The resulting RMSEs derived from Ground Control Points (GCP's) were at 0.46–0.79 pixels along track and 0.39–0.73 pixels across track. Subsequent atmospheric correction of the CHRIS radiance data was performed using ATCOR-3 (Richter, 1998), which is based on MODTRAN-4. ATCOR-3 enables the processing of data from tilted sensors by accounting for varying path lengths through the atmosphere, varying transmittance and for terrain effects by incorporating digital terrain model (DTM) data and their derivatives such as slope and aspect, sky view factor and cast shadow. For the atmospheric processing a laser-based DTM with 2 m spatial resolution (swisstopo ©) was resampled to 18 m using bilinear interpolation (Schläpfer et al., 2007).

After geometric and atmospheric correction, canopy reflectances corresponding to the 60 field-sampled tree crowns (at the Vordemwald site) were extracted from the five CHRIS images thus obtaining a total of five sets each consisting of 60 spectral signatures. The geographical trunk positions (vector data) of the sampled trees were used to locate the pixels in the images (Gorodetzky, 2005) and extract spectral data with the *Region of interest* (ROI)-tool in the ENVI image processing package (Research Systems, 2004). Fig. 2.7. illustrates the viewing angle dependant spectral signatures extracted from a co-registered pixel which represents a tree crown of silver fir.

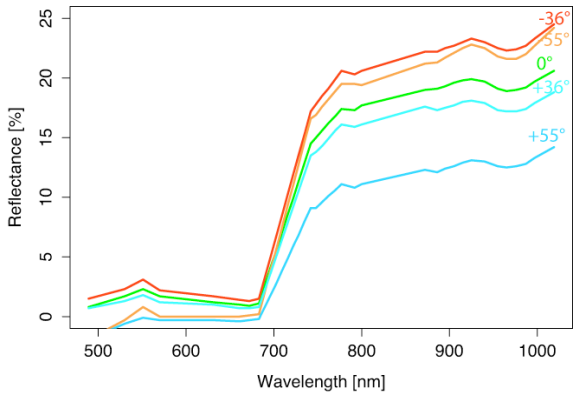

Fig. 2.7. Spectral signatures of one silver fir site from processed CHRIS data of the nominal viewing zenith angles at ±36°, ±55° and 0°. Negative viewing zenith angles correspond to the backward scattering direction, positive viewing zenith angles represent the forward scattering direction.

2.4.2.1 CHRIS data processing for land cover and plant functional types classification

The section below describes the additional data processing necessary for the land cover study presented in chapter 6, including data preprocessing in ATCOR-3, convolution of CHRIS data to Landsat Thematic Mapper specifications and calculation of the anisotropy factor.

2.4.2.1.1 CHRIS data preprocessing

The images used for the land cover mapping were processed differently. Prior to the geometric and radiometric correction of the five CHRIS multiangular acquisitions, stripes were removed and missing pixels filled using the software HDFclean (Cutter, 2006). Temperature-varying calibration errors in the CHRIS imaging system result in a striping effect in the along track direction. The processing readjusts the relative brightness of different columns to minimize the effect (Cutter, 2006). Afterwards, geometric and atmospheric correction were conducted as described in section 2.4.2 except that the ATCOR-3 parameters file was set to interpolate wavebands in the 760 nm oxygen region, whereas the wavebands in the 725–825 and 940–1130 nm water vapor region were not set to interpolate. With the default parameter file, all three spectral regions are interpolated. Fig. 2.8 shows two vegetation spectra: the first was processed in ATCOR-3 with the default parameter file (interpolated) whereas the second was processed without any interpolation.

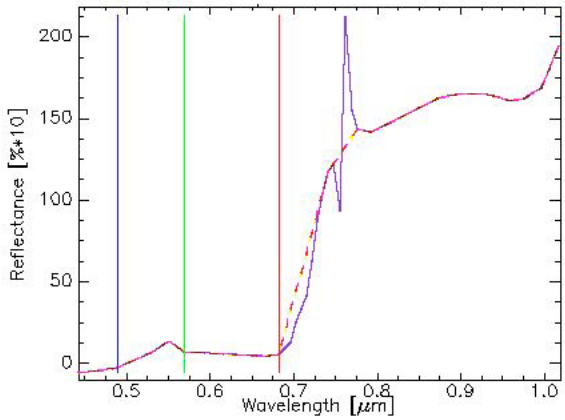

Fig. 2.8. Two CHRIS spectra of a vegetation target are shown. The first was processed in ATCOR-3 by interpolating the reflectance values (- - -) at wavebands in the 760 nm oxygen and the 725–825 and 940–1130 nm water vapor regions, whereas the second spectrum was processed without any interpolation (——).

2.4.2.1.2 Convolution of CHRIS data to Landsat Thematic Mapper (TM)

One of the objectives of the land cover study presented in chapter 6 was to investigate the spectral and directional contribution upon the classification result. Therefore, datasets were generated beforehand that differed regarding spectral and directional resolution. In order to compare different spectral resolutions the CHRIS spectra were convoluted to the spectral specifications of Landsat Thematic Mapper (TM) in the ENVI image processing package (Research Systems, 2004). Due to the limited spectral range of CHRIS (447–1035 nm) the convolution was performed for the first four TM bands at 479, 561, 661 and 835 nm. A comparison between convolved and original CHRIS spectra for a vegetation and soil target is given in Fig. 2.9.

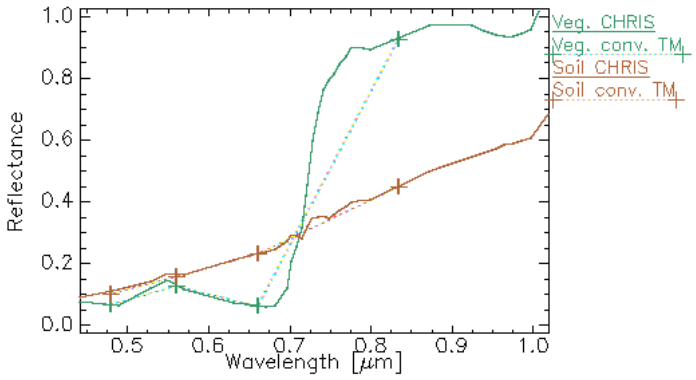

Fig. 2.9. Original (—) and convolved (+) CHRIS spectra for a vegetation (green) and soil (brown) target, respectively. Apparently, convolution causes large information loss for vegetation targets, whereas for soil targets the loss is minimal.

Image stacks were created in ENVI to compare classifications based on different directional datasets, by adding all 36 bands of the nadir image and additionally, the wavebands at 489 nm and 682 nm of the off-nadir angles (±35° and ±55°), resulting in a dataset with 44 layers in total. Only the bands at these distinctive wavelengths were used because directional information is most apparent there. In addition, processing time can be significantly reduced with a smaller dataset in the subsequent classification procedure.

I also created a directional dataset with the convolved CHRIS data. Due to the already reduced spectral dimensions all four spectral bands were used for each of the five FZAs, resulting in a dataset of 20 layers.

2.4.2.1.3 Anisotropy factor (ANIF)

Besides using spectrodirectional CHRIS information for the land cover study, the anisotropy factor (ANIF) was calculated for all CHRIS off-nadir angles and generated an additional ANIF dataset to investigate its impact on classifications. The ANIF is a measure for the reflectance anisotropy and it is calculated as follows (Sandmeier et al., 1998):

$$ANIF(\lambda,\theta_s,\phi_s,\theta_v,\phi_v) = \frac{\rho(\lambda,\theta_s,\phi_s,\theta_v,\phi_v)}{\rho_0(\lambda,\theta_s,\phi_s)} \text{ [dimensionless]}, \quad (2.1)$$

where ρ = bi-directional reflectance factor, ρ_0 = nadir reflectance factor, λ = wavelength, θ = zenith angle, ϕ = azimuth angle, s = illumination direction and v = viewing direction.

The anisotropy factor describes the portion of radiation reflected into a specific view direction relative to the nadir reflectance and is sometimes called relative reflectance. Interestingly, the ANIFs show very distinctive patterns for different viewing angles and land cover types (Fig. 2.10). Hence, land cover classes with similar spectral signatures (e.g., crops and grasslands) become in classifications distinguishable by the use of ANIFs.

To obtain an ANIF dataset for the land cover classification (chapter 6) all 37 spectral bands of the CHRIS nadir image were stacked with the ANIFs at three wavelengths (489, 682 and 735 nm) of all off-nadir angles (±36°, ±55°). This dataset was termed *CHRIS nadir ANIF* and contained in total 49 layers.

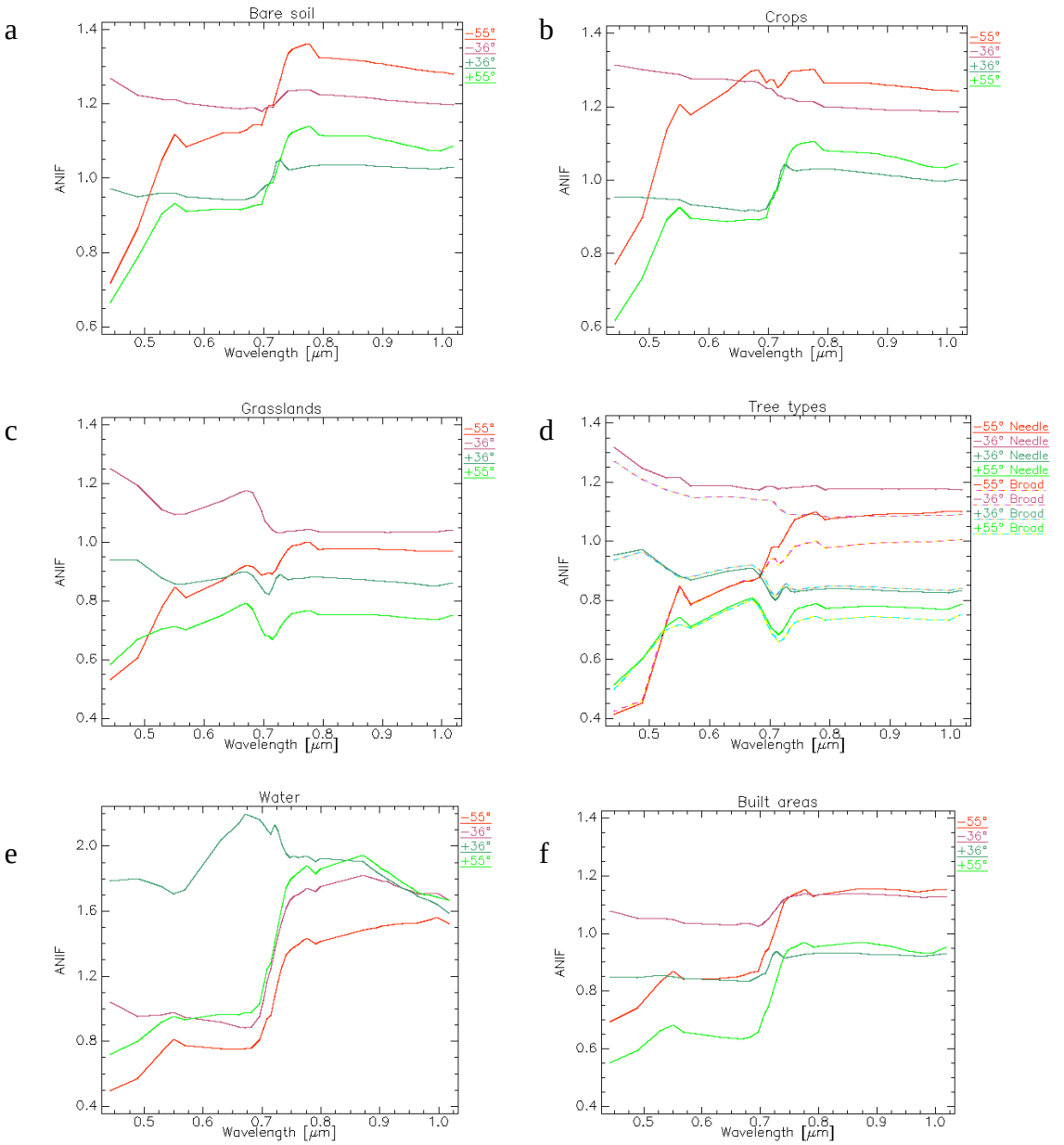

Fig. 2.10. Anisotropy factors (ANIFs) for different land cover types. All ANIFs were calculated for the nominal CHRIS angles at ±36° and ±55°, for (a) bare soils, (b) crops, (c) grasslands, (d) coniferous and broadleaf forests, (e) water bodies and (f) built-up areas.

3 Methods

In this chapter the methods to develop statistical models for biochemistry retrieval from airborne and spaceborne hyperspectral measurements and the approach to classify land cover and plant functional types are presented. The applied techniques range from parametric to non-parametric statistical approaches to subset selection and spectral transformation procedures. I start with a brief introduction to the intrinsic properties of models.

3.1 Introduction

3.1.1 Precision, generality and reality

With the advancement of the computing environment and the advent of new statistical techniques the development and use of a wide array of models has grown rapidly also in environmental remote sensing. Different approaches to modeling evolved due to the limitations when handling *precision*, *generality* and *reality* (Sharpe, 1990). It was suggested that it is not possible to maximize all three desirable properties in a single model (Levins, 1966) (Fig. 3.1).

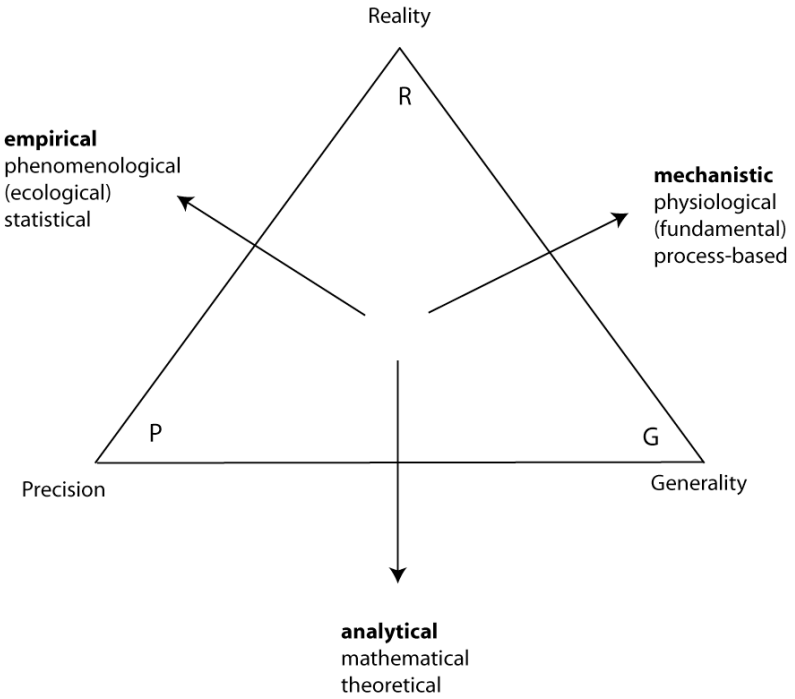

Fig. 3.1. A classification of models based on their intrinsic properties (Guisan and Zimmermann, 2000).

This trade-off led to the distinction of three different groups of models (empirical, mechanistic, analytical) and its associated constraints are consequential when selecting modeling approaches for specific project goals (Guisan and Zimmermann, 2000).

Also models commonly used in remote sensing underlie the trade-off between *precision*, *generality* and *reality*. Radiative Transfer Models (RTMs), on the leaf and canopy level, can

be assigned to the process-based category. RTMs help to understand the way in which light interacts with plant canopies and to infer structural and chemical characteristics from reflectance measurements (Ustin et al., 1999). RTMs represent a basis for developing physically based methods. They are complex and demanding to parameterize. Therefore, operational techniques often remain on products derived from empirical studies (statistical approach) because they are faster and easier to apply (Ustin et al., 1999; Asner et al., 2003). For such statistical approaches, one collects data on the spectral signatures of a variety of objects, then fits a statistical relationship between the objects and their signatures and finally uses statistical techniques (such as regression analysis) to determine the characteristics of an object from its signature.

3.1.2 Bias, variance and model complexity

A key aspect of any learning model is the success with which it forms generalizations from training data, as measured by its accuracy in classifying further data from the same source. However, this accuracy is not maximized by modeling training data as accurately as possible. An extremely close fit to training data tends to generalize poorly to independent test data, because such a fit inevitably entails fitting random (noise) aspects of the sample as well as regular, replicable trends – a phenomenon known as overfitting (high variance as well as low bias). Inversely, a model that fits the training data too poorly will miss regular trends as well as noise, called underfitting (high bias) (Hastie et al., 2001; Briscoe and Feldman, 2006). The phenomenon can be seen schematically by plotting model complexity against accuracy as measured from an independent test dataset. Accuracy first rises to some optimum, but then declines again (Fig. 3.2).

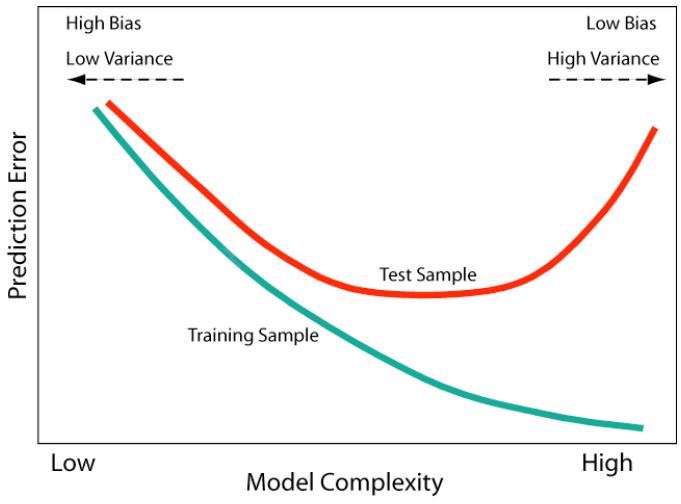

Fig. 3.2. Behavior of test sample and training sample error as the model complexity is varied (Hastie et al., 2001).

Normally, model development is a two-step procedure: first we select a model by estimating the performance of different models in order to choose the (approximate) best one and second, we assess the final model assessment by estimating its prediction error (generalization

error) on new and independent data. If we are in a data-rich situation (what is hardly ever the case for ground measurements in remote sensing), the best approach for both problems is to randomly divide the dataset into three parts: a training set, a validation set and a test data set. The training set is used to fit the models; the validation set is used to estimate prediction error for model selection; the test data set is used for assessment of the generalization error of the final chosen model. A typical split might be 50 % for training and 25 % each for validation and testing (Hastie et al., 2001). However, in most cases there is insufficient data to split into three parts. Hence, the validation step can be approximated either analytically (e.g., Akaike's Information Criterion (AIC)) or by efficient sample re-use (cross-validation and the bootstrap) (Hastie et al., 2001).

3.2 Statistical methods for foliar biochemistry estimation

In this study multiple linear regression was used to develop statistical models between foliar biochemistry and hyperspectral measurements. The statistical approach assumes that a foliar spectrum is the sum of each chemical constituent, weighted by its concentration. A calibration equation between the chemical of interest (e.g., nitrogen and carbon concentrations) and the spectral signature at different wavelengths (explanatory variables) is developed. Regression analysis is extensively explained in Draper and Smith (1966).

Also in multiple linear regression the number of explanatory variables can not be arbitrarily high. Especially when using high-dimensional hyperspectral signatures to develop regression models the number of bands used in the model must be reduced to a reasonable number and be in due proportion to the number of observations. This has to be done to avoid data overfitting, to optimize the accuracy and predictive power (generalization) of a model (see section 3.1.2) and to remove irrelevant and redundant data to reduce computational costs. It is recommended that no more than $m/10$ predictors should be included in the final model, where m is the total number of observations (Hruschka, 1987; Guisan and Zimmermann, 2000).

One of the most difficult tasks is to decide, which explanatory variables, or combination thereof, should enter the model (Guisan and Zimmermann, 2000). The selection of predictors (feature subset selection or variable selection) can be made arbitrarily, automatically, by following physiological principles, or by following specific shrinkage rules.

3.2.1 Feature subset selection

The problem of dimensionality reduction is old (Hocking and Leslie, 1967) and it is a research area at the intersection of several disciplines, including statistics, pattern recognition, machine learning and artificial intelligence. The term *feature subset selection* is taken to refer to algorithms that select a subset of the existing features without a transformation (Jain and Zongker, 1997). There is a large number of search strategies, which can be grouped in three categories: complete (e.g., branch-and-bound, beam search), heuristic (e.g., forward selection, bidirectional search) or random search (e.g., simulated annealing, genetic algorithms) (Dash and Liu, 1997).

This study employed two statistical subset selection methods, namely a forward variable selection and an enumerative branch-and-bound (B&B) procedure to limit the number of spectral wavebands used in the regression and to create parsimonious models to predict foliar biochemistry at the canopy level.

Heuristic search strategies, such as the forward selection procedure, are easy to explain, inexpensive to compute and therefore most widely used, also in most studies dealing with dimensionality reduction and hyperspectral remote sensing data (Weisberg, 1980). For a detailed explanation of these algorithms, the reader is referred to Miller (2002). The basic characteristics of B&B methods have been addressed in previous studies (Mitten, 1970; Furnival and Wilson, 1974; Narendra and Fukunaga, 1977; Miller, 2002). B&B algorithms are efficient because they avoid exhaustive enumeration by rejecting suboptimal subsets without direct evaluation and guarantee optimality if the features obey monotonicity (Narendra and Fukunaga, 1977). The name *branch-and-bound* arises from the two basic operations: *branching*, which consists of dividing collections of sets of solutions into subsets and *bounding*, which consists of establishing bounds on the value of the objective function over the subsets of solutions (Mitten, 1970).

As a result of both procedures (forward search and B&B), a number of wavelengths are selected that explain canopy biochemical properties. For both methods, Akaike's Information Criterion (AIC) (Akaike, 1973; Akaike, 1974) was used to evaluate whether adding a variable improved the models significantly. AIC is an efficient standard method to evaluate the effect of adding or removing variables to a model (Burnham and Anderson, 1998). By adding an additional variable to a model, a penalty for compensating the loss of a degree of freedom is added. If the gain by the new variable is larger than the penalty, then the variable is considered significant and thus reduces the AIC. The final model has AIC minimized.

3.2.2 Cross-validation

As discussed in section 3.1.2, in situations with insufficient independent observations for model validation, the validation step can be approximated with cross-validation (CV). Cross-validation is a simple and widely used method for estimating prediction errors. The CV method uses part of the original data to fit the model (training set) and a different part to test it (testing set). A *k*-fold CV splits a dataset randomly into *k* bins (subsamples), then iteratively determines regression parameters using a sample of *k*-1 bins and tests the resulting model against the left out bin. This procedure is repeated such that each bin has been used *k*-1 times for fitting parameters and once for testing. Finally, the *k* CV results can be averaged to produce a single error estimation. Typical choices of *k* are 5 or 10. The case $k = m$ (where m is the total number of observations in the original sample) is known as *leave-one-out* cross-validation (Guisan and Zimmermann, 2000; Hastie et al., 2001).

All models were tested using a 10-fold CV procedure with random splitting order of the data (Hastie et al., 2001). The average error over all *k* bins determines the CV error. For increased stability, the 10-fold cross-validation was repeated 10 times and the model evaluation measures were averaged for final comparison. The root mean square error of each cross-validated model (CV-RMSE) was calculated to evaluate each model and to assess its

predictive capability.

3.3 Support vector machines for land cover classification

For the land cover and plant functional types classification (chapter 6) support vector machines (SVMs) were used, a set of non-parametric methods used for classification and regression. SVM algorithms were inspired by the statistical learning theory which began in the 1960s to solve pattern recognition problems (Cortes and Vapnik, 1995; Vapnik, 2000). The theoretical development of SVMs has been addresses by Vapnik (2000) and several other papers (Burges, 1989; Huang et al., 2002; Bazi and Melgani, 2006). An extensive description is also given in (Cristianini and Shawe-Taylor, 2000).

The basic idea of SVM algorithms is to locate the optimal boundaries between linearly separable classes. If classes are separable in two dimensions they can be split by a line. For linearly non-separable cases, the original data is mapped into higher-dimensional feature space through nonlinear transformations (*kernel* functions) (Fig. 3.3). Then, in this new feature space, an optimal linearly separating *hyperplane* is constructed.

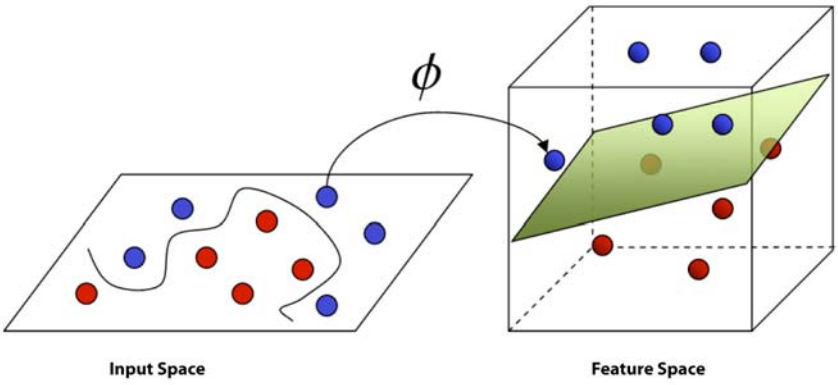

Fig. 3.3. The idea of support vector machines is to map the training data nonlinearly into a higher-dimensional feature space via ϕ and construct a separating hyperplane with maximum margin there. This yields a nonlinear decision boundary in input space. By the use of *kernel* functions, it is possible to compute the separating hyperplane without explicitly carrying out the map into the feature space (Hearst, 1998).

There are many possible solutions for a separating *hyperplane*, the problem is to find the optimal one (= ill-posed problem). The optimal *hyperplane* is the one with maximal margin of separation between the two classes (Vapnik, 2000). For SVMs only “difficult points” close to the decision boundary influence optimality, whereas in linear regression all points are involved. These points that lie closest to the decision surface (*hyperplane*) are termed "support vectors" (Fig. 3.4). They carry all relevant information about the classification problem and they have direct bearing on the optimum location of the decision surface by changing the position of the dividing *hyperplane* if removed. The number of support vectors is thus small as the decision surface is fitted only to these vectors (Vapnik, 2000). Therefore, SVMs are

independent of the dimensionality of feature space, a major advantage of this method (Pal and Mather, 2003).

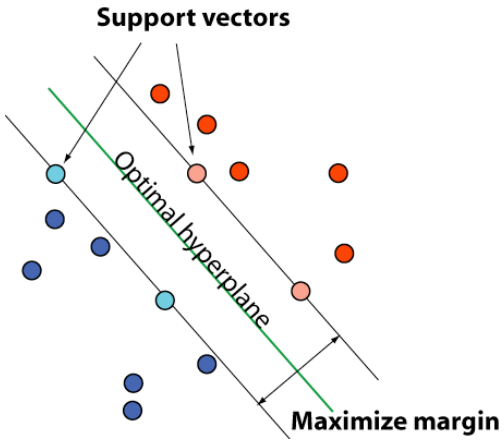

Fig. 3.4. Schematic representation of support vectors and optimal *hyperplane*, after (Burges, 1989).

By the use of *kernels*, original data is mapped into higher-dimensional feature space, but all necessary computations are performed directly in input space (Hearst, 1998). Though new *kernels* are being proposed, the four basic types of *kernels* are: (1) linear, (2) polynomial, (3) radial basis function (RBF) and (4) sigmoid.

For the SVM training, some *kernel* and regularization parameters have to be set initially (Schölkopf et al., 2000). Because it is not known beforehand which parameters are the best for one problem, a parameter search (= grid search) must be performed with the goal to identify good parameters so that the classifier can accurately predict unknown data (Hsu et al., 2001).

SVMs are binary classifiers; they always separate only two classes (or two groups of classes). There are two main strategies to solve multi-class problems: the one-against-one (OAO) and the one-against-all (OAA) strategy (Foody and Mathur, 2004). OAO applies a set of individual classifiers to all possible pairs of classes and performs a majority vote to assign the winning class. In the case of OAA, a set of binary classifiers is trained to separate each class from the rest; the maximum decision value determines the final class label (van der Linden and Janz, 2007).

Like in any model training process, it is not useful to achieve too high training accuracy to avoid overfitting the model (see section 3.1). With cross-validation the overfitting problem can be prevented and prediction accuracy assessed at once.

3.3.1 Classification accuracy

The most common way to express classification accuracy is the preparation of a so-called error (confusion, contingency) matrix. Different measures and statistics can be derived from the values in an error matrix: for example the producer's accuracy, the user's accuracy and the overall accuracy, a combination of producer's and user's accuracies. The producer's accuracy measures how well a certain area has been classified. The user's accuracy is a measure of the

reliability of the map. It informs the user how well the map represents what is really on the ground (Banko, 1998). For a detailed description of the error matrix and the computation of accuracy measures the reader is referred to the literature (Congalton and Green, 1999; Czaplewski, 2003).

Developed by Cohen (1960) the Kappa coefficient (*K*) is another measure of accuracy which determines the proportion of agreement after chance agreements have been removed from considerations. It was introduced to the remote sensing community in the early 1980s (Congalton et al., 1983) and has become a widely used measure for classification accuracy.

3.4 Spectral transformations based on continuum removal

The spectral reflectance of a vegetation canopy is known to be primarly a function of the foliage optical properties, the canopy structure, the understory and soil background reflectance, the illumination conditions and finally the viewing geometry (e.g., Myneni et al., 1989; Disney et al., 2000). In order to minimize some of the effects of spectral variability that is independent on biochemical concentration and to better relate hyperspectral information to canopy biochemical composition, a range of spectral transformation methods have been proposed. Among these methods, continuum removal analysis yielded the most promising results in estimating foliar chemistry (Shi et al., 2003). Continuum removal was successfully used in the field of geology (Clark and Roush, 1984) until Kokaly and Clark (1999) demonstrated its use for foliar biochemistry retrieval: the foliar biochemical concentrations could be accurately predicted with continuum removal applied to lab-measured spectra taken from dried and ground leaves. Later the methodology was successfully tested on fresh leaves (Curran et al., 2001).

Continuum removal normalizes reflectance spectra to allow comparison of individual absorption features from a common baseline (Kokaly, 2001). The continuum is a convex hull fitted over a spectrum. The hull can be fitted either over the whole spectrum or absorption features of interest by using straight-line segments that connect local spectral maxima (endpoints of continuum lines). The observed spectral continuum is considered an estimate of the other absorptions present in the spectrum, not including the one of interest (Clark and Roush, 1984).

Continuum-removed spectra were calculated for all extracted tree spectra (HyMap and CHRIS) by dividing the original reflectance values by the corresponding values of the continuum line (Kokaly and Clark, 1999) (Fig. 3.5a). Additionally, normalization procedures were applied on the continuum-removed data to minimize extraneous influences. For both, HyMap and CHRIS spectra, band depths were normalized to the waveband at the center of the absorption feature (BNC), as proposed by Kokaly and Clark (1999). CHRIS spectra were also normalized with 1) the normalized band depth index (NBDI), as proposed by Mutanga et al. (2004) and 2) the continuum-removed derivative reflectance CRDR (Tsai and Philpot, 1998; Mutanga et al., 2004).

3.4.1 Continuum removal on HyMap data

The extracted HyMap mean spectra of the sampled tree crowns (n=132) were processed for continuum removal at seven pre-selected wavelength ranges according to known chlorophyll, nitrogen, protein, cellulose, lignin, starch and water absorption features (Table 3.1). To approximate the continuum lines, straight-line segments were used that connect local spectral maxima as defined in Table 3.1.

Table 3.1 Pre-selected wavelength ranges for continuum removal analysis and their associated causal absorption features (Murray and Willliams, 1987; Curran, 1989; Elvidge, 1990; Penuelas et al., 1994; Fourty et al., 1996; Kokaly, 2001; Kokaly et al., 2003).

Endpoints of continuum lines [nm]	**Causal absorption features [nm] related to foliar biochemicals**			
	Chlorophyll (a,b)	Nitrogen/Protein	Cellulose/Lignin/Starch	Water
452–528	460			
558–756	570, 640, 660, 680, red edge (700–750)	570 red edge (700–750)		
877–1069		910, 1020	970, 990	970, 980
1084–1287			1120, 1200, 1220	1200
1329–1783		1510, 1640, 1690, 1730	1420, 1450, 1480, 1490, 1530, 1540, 1560, 1680, 1690, 1700, 1736, 1754, 1770, 1780	1400, 1450, 1580
1806–2205		1940, 1980, 2054, 2060, 2130, 2172, 2180	1820, 1900, 1924, 1930, 1940, 1950, 1960, 2000, 2050-2140, 2080, 2100	1940
2223–2388		2240, 2300, 2350	2250, 2262, 2270, 2280, 2320, 2330, 2340, 2350	

The band depth normalized to the center (BNC) was calculated by dividing the band depth of each band by the band depth at the band center (Eq. 3.1):

$$\mathrm{BNC} = \left(1-\left(R/R_i\right) / 1-\left(R_c/R_{ic}\right)\right) , \tag{3.1}$$

where R is the reflectance of the sample at the waveband of interest, R_i is the reflectance of the continuum line at the waveband of interest, R_c is the reflectance of the sample at the absorption feature center and R_{ic} is the reflectance of the continuum line at the absorption feature center (Curran et al., 2001) (Fig. 3.5b). The band center is the minimum of the continuum-removed absorption feature (Kokaly and Clark, 1999). The band center was determined for each spectrum separately and could therefore vary between different spectra.

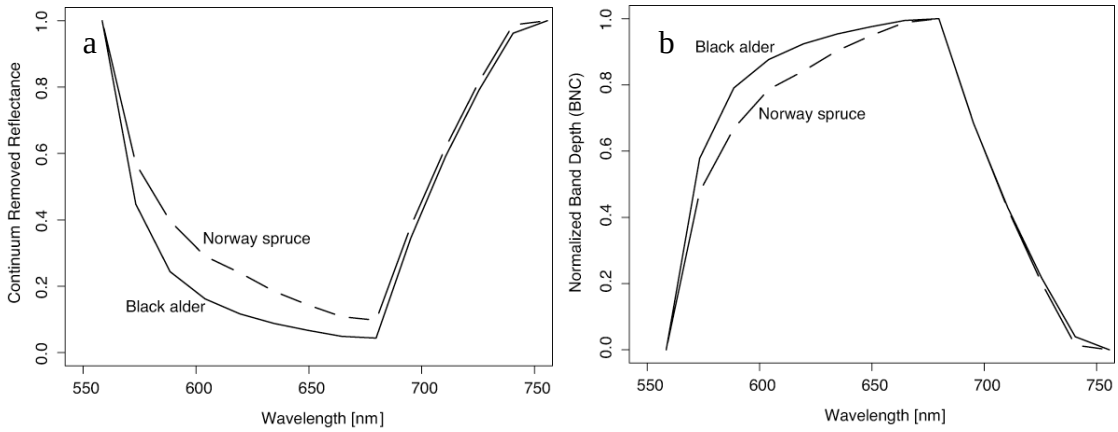

Fig. 3.5. Example of data transformation in the 670 nm absorption feature region: (a) continuum-removed reflectance, (b) normalized band depth reflectance.

3.4.2 Continuum removal on CHRIS data

For the multidirectional analysis with CHRIS data (chapter 5) four datasets were generated per viewing angle, consisting of differently transformed spectral data of tree canopies (n=60). One of the four datasets consisted of original reflectance (termed SPEC) and the other three of continuum-removed data using different algorithms. The second dataset (BNC) represented band depths normalized to the waveband at the center of the absorption feature, calculated as described in section 3.3.1 (Eq. 3.1). The third dataset (NBDI) represented normalized band depth index values. NBDI was calculated by subtracting the band center, which is the maximum band depth, from the band depth and dividing it by their sum (Eq. 3.2):

$$\text{NBDI} = \frac{\left(1-\left(R/R_i\right)\right) - \left(1-\left(R_c/R_{ic}\right)\right)}{\left(1-\left(R/R_i\right)\right)+\left(1-\left(R_c/R_{ic}\right)\right)} \tag{3.2}$$

The last dataset was termed CRDR for Continuum-removed derivative reflectance. It was calculated by applying the first difference transformation described in Equation 3.3 to the continuum-removed reflectances.

$$FDR_{(i)} = \left(R_{(j+1)} - R_{(j)}\right) \Big/ \Delta_{\lambda} \tag{3.3}$$

where FDR is the first derivative reflectance at wavelength i situated in the middle between wavebands j and $j + 1$. $R_{(j)}$ is the reflectance at waveband j, $R_{(j+1)}$ is the reflectance at waveband

j + 1 and Δ_λ is the difference in wavelengths between bands j and j + 1 (Tsai and Philpot, 1998; Mutanga et al., 2004).

To approximate the continuum lines, straight-line segments were used that connect local spectra maxima of absorption features in the regions of 551–755 nm and 925–1019 nm. For the first absorption feature, the different unprocessed and processed signatures of a Norway spruce canopy obtained from five CHRIS viewing angles are illustrated in Fig. 3.6.

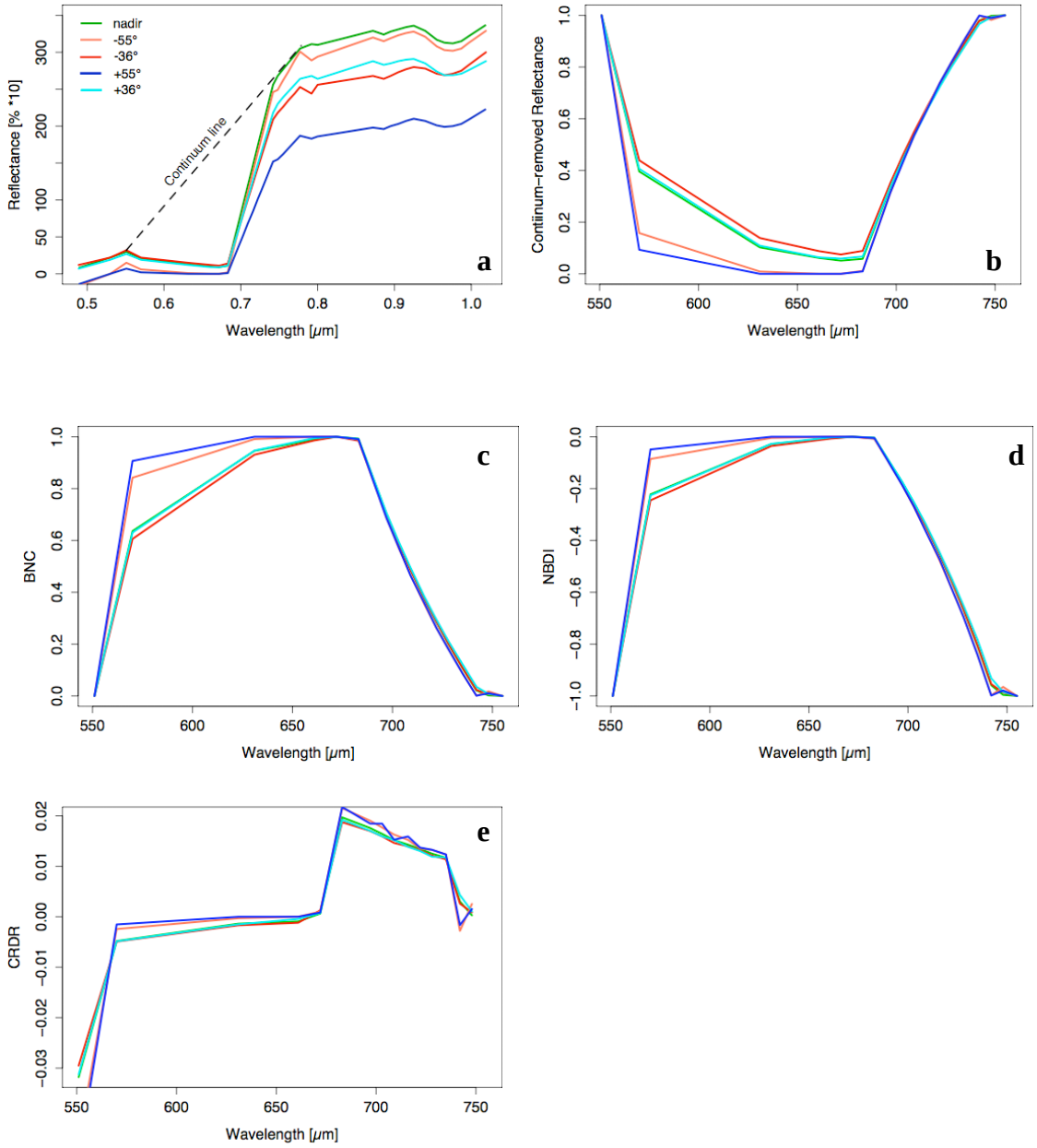

Fig. 3.6. Unprocessed (a) and processed (b-e) signatures of a Norway spruce canopy obtained from five CHRIS viewing angles at nominal ±36°, ±55° and 0°. For the absorption feature between 551 and 755 nm continuum-removed signatures (b), band depths normalized to the waveband at the center of the absorption feature (BNC) (c), normalized band depth index values (d) and continuum-removed derivative reflectances are shown. Note that the nadir and +36° signatures are for all processing procedures nearly identical.

Continuum removal for nitrogen concentration (C_N) was applied to the absorption feature located between 551 and 755 nm where the leaf water effect is minimal. Several studies have shown a strong nitrogen-pigment relationship in this region because the chlorophyll content in foliage is highly correlated with total protein and, hence with total nitrogen content (Field and Mooney, 1986; Evans, 1989; Yoder and Pettigrew-Crosby, 1995; Johnson and Billow, 1996). The reason for this is that proteins are the major nitrogen bearing leaf constituents, typically holding 70–80 % of all nitrogen. An additional 5–10 % of nitrogen is allocated to chlorophyll and lipoproteins (Chapin and Kedrowski, 1983). Moreover, the red edge region of the spectrum (680–740 nm) is sensitive to chlorophyll concentration (Gates et al., 1965; Horler et al., 1983; Rock et al., 1988; Moss and Rock, 1991). An increase of chlorophyll concentration causes a broadening of the chlorophyll absorption feature centered around 680 nm, resulting in a shift of the point of maximum slope (termed the red edge position) towards longer wavelengths (Gates et al., 1965). Finally, reflectance ratios in the red edge were positively correlated with chlorophyll and nitrogen concentrations (Moss and Rock, 1991; Gitelson et al., 1996; Sims and Gamon, 2002).

For the estimation of water content (C_W) I was restricted to using the weak liquid water absorption feature at 970 nm (Curran, 1989) owing to the sensor's spectral range. The regression results solely based on this feature were not satisfactory. The calibration for C_W estimates could be improved by additionally using the feature between 551–755 nm.

4 Estimating Biochemical Concentration in Mixed Forests from HyMap Data using Band-Depth Analyses and Subset Regression Algorithms

4.1 Introduction

Biochemical processes, such as photosynthesis, respiration and litter decomposition are affected by the foliar chemistry of plants. Traditional measurements of leaf chemistry at the forest canopy level are time-consuming, expensive and spatially constrained. Remote sensing allows for repeatable and continuous retrieval of biochemical information over a wide spatial scale and thus facilitates the understanding of ecosystem functions. Imaging spectroscopy can be used for a range of environmental applications (Curran, 2001; Ustin et al., 2004; Asner and Vitousek, 2005), including e.g. the identification and mapping of invasive species (Underwood et al., 2003; Asner and Vitousek, 2005; Lawrence et al., 2006) or the detection of the spatial variability of soil carbon to nitrogen (C:N) ratios through related patterns in canopy chemistry (Ollinger et al., 2002). Spatial estimates of foliar chemistry have the potential to improve ecosystem models (Martin and Aber, 1997; Pan et al., 2004; Turner et al., 2004) or to indicate the forest health status. The latter carries an important economic component not only regarding forest products (Goodenough et al., 2003; Goodenough et al., 2004) but also in terms of protection forests, which are able to protect people, settlement, traffic routes, other infrastructures and agricultural land against natural hazards, such as snow avalanches, rock falls or surface erosion (Brang et al., 2001).

The most important chemical components of green foliage are the concentration of nitrogen (C_N) and carbon (C_C) and the content of water (C_W). Foliar C_N is closely related to the maximum photosynthetic rate and ecosystem productivity (Field and Mooney, 1986). Moreover, C_N of leaf litter strongly affects the soil respiration and the decay rate of leaf litter (Merrill and Cowling, 1966; Melillo et al., 1982). Proteins are the major nitrogen bearing leaf constituents, typically holding 70–80 % of all nitrogen. An additional 5–10 % of nitrogen is allocated to chlorophyll and lipoproteins (Chapin and Kedrowski, 1983). Carbon is allocated mainly to cellulose (up to 65 %) and lignin (up to 20 %). Water content accounts for 40 to 80 % of the fresh weight of green leaves (Elvidge, 1990). Leaves use water for photosynthesis or release the water for cooling the plant. Lack of water restricts the transpiration, which induces closure of stomata and results in reduced evaporation from the leaf surface and thus decreases photosynthesis (Dubey, 2005).

Relationships between foliar chemistry and nitrogen cycling of individual species revealed interesting differences between species and plant functional types (Ollinger et al., 2002; Lovett et al., 2004). It has been shown that the decomposability of leaf litter varies among species (Daubenmire and Prusso, 1963). These findings implicate the importance of distinguishing individual tree species and plant functional types (e.g. broadleaf deciduous, needleleaf evergreen) when investigating mixed forests using remote sensing. Yet, accurate geo-location of individual tree crowns in mixed stands (Piedallu and Gegout, 2005) and

precise geo-registration of images remains a problem for matching field-sampled crowns with remotely sensed images for training and evaluation purposes.

Canopy biochemistry can be associated to hyperspectral information by regression analyses (section 3.2). A range of spectral transformation methods has been proposed to better relate hyperspectral information to canopy biochemical composition and other ground-measured structures. Among these methods, continuum-removal analysis (section 3.3) yielded the most promising results in estimating foliar chemistry (Shi et al., 2003). Kokaly and Clark (1999) demonstrated that with continuum removal applied to lab-measured spectra taken from dried and ground leaves the foliar biochemical concentrations could be accurately predicted. At the scale of remotely sensed images additional difficulties arise originating from atmospheric conditions, solar illumination, understory vegetation, canopy architecture variability and – especially – leaf water (Dawson et al., 1999) since leaf water obscures the absorption features of nitrogen and carbon (Elvidge, 1990). Additional uncertainties arise from scaling point field measurements of foliar chemistry to the canopy scale. Continuum removal analysis was shown to reduce both influences (Kokaly and Clark, 1999). The scaling from controlled laboratory conditions to field-based measurements has been successfully demonstrated for grasslands (Mutanga et al., 2004; Mutanga et al., 2005) and for a pure eucalypt stand (Huang et al., 2004). Huang's analyses were carried out using a single tree species only when estimating foliar C_N from airborne hyperspectral data. So far, continuum removal has not been evaluated in mixed species forests on an individual tree level, facing the problem of mixed pixels due to overlapping crowns of different species. Also, most studies have been conducted on remotely sensed images of a single region only, thus avoiding the inter-regional comparison of foliar chemistry assessments (Matson et al., 1994) or inter-regional predictions were conducted at a canopy-level by averaging multiple tree crowns (Martin and Aber, 1997).

The main goal of this analysis was to train a set of inter-regional models (data of study sites Bettlachstock, Kuettigen and Vordemwald; section 2.1) of canopy biochemical concentration in mixed species forests based on hyperspectral data in combination with continuum removal analyses. Besides using the standard variable selection method of stepwise forward selection in linear regression modeling, novel methods were tested based on branch-and-bound (B&B) variable search algorithms (section 3.2.1). Additional minor goals of this study included (a) testing the accordance of statistically significant wavebands with causal absorption features found in laboratory investigations and (b) testing the stability of the models evaluated from a 10-fold cross-validation procedure. Finally, models were trained from lab-derived causal wavebands for estimating biochemical concentrations. These models were then compared with the B&B optimized models, using all wavebands. These tests were applied in three different regions and also examined the potential of extrapolating predictions of biochemical concentration from one area to another using independent test data.

4.2 Statistical analyses

Multiple linear regression analyses were used in order to train models to predict C_N, C_C and C_W from continuum-removed spectra (BNC) (chapter 3). To limit the number of spectral wavebands used in the regression and to create parsimonious models, this study employed two statistical variable selection methods, namely an enumerative branch-and-bound (B&B) and a forward variable selection procedure (section 3.2.1). Both procedures selected wavebands that best explained the biochemical concentrations.

For training models of biochemical canopy properties the 132 biochemistry samples collected in three different study sites were split into five subsets (Table 4.1). Separate regression models were trained from these subsets and labeled as follows: ALL included all data irrespective of study site, species or leaf type (n=132); VOR included all samples from the study site Vordemwald, irrespective of leaf type and species (n=60); NED included all needleleaf (evergreen) samples across all study sites (n=52); BDD included all broadleaf (deciduous) samples across all study sites (n=80) and FSD included all European beech (*Fagus sylvatica*) samples across all study sites (n=42).

The resulting model fit is reported by means of the adjusted coefficient of determination (adj.-R^2). Regression R^2 values report how well the model explains the variation of the dependent variable. The adj.-R^2 accounts for the number of predictors and sample points used, which influence the effective degrees of freedom (Weisberg 1980). It does so by lowering the regression R^2 accordingly. Therefore, it is better suited to compare the strengths of model fit that include differing numbers of observations and predictors (Weisberg, 1980). The wavebands selected in the regression were examined for accordance with lab-based absorption features known from literature. The ± 12 nm range was used, defined by Curran et al. (2001), to indicate causal relation. Causal relation is indicated when selected wavebands are located within ± 12 nm of an absorption feature of the biochemical of interest.

Next to using subset selection methods based on all wavebands, it was evaluated how well biochemical concentrations can be estimated based exclusively on causal wavebands reported in the literature. Therefore, the B&B subset algorithm was forced to select only from the wavebands listed in Table 3.1, for C_N, C_C and C_W, respectively. The selected models were then compared with the models based on all wavebands. To assess the power of the models to extrapolate between regions, both the ALL and the NED dataset were divided into three subsets, one per region. The subsets of study sites were now grouped pairwise (e.g. VOR and KUT), then a search using the B&B procedure to select a subset of wavebands was performed and finally C_N of the third independent study site (e.g. BET) was predicted.

The root mean square error (RMSE) was calculated of each cross-validated model to evaluate a model and to assess its predictive capability (section 3.2.2).

4.3 Results

4.3.1 Chemistry data

The analyzed foliar samples revealed distinct differences in terms of biochemical composition of the three functional types (Table 4.1). Nitrogen concentration and data range were clearly higher for broadleaf than for needle-leaved species (Fig. 4.1a).

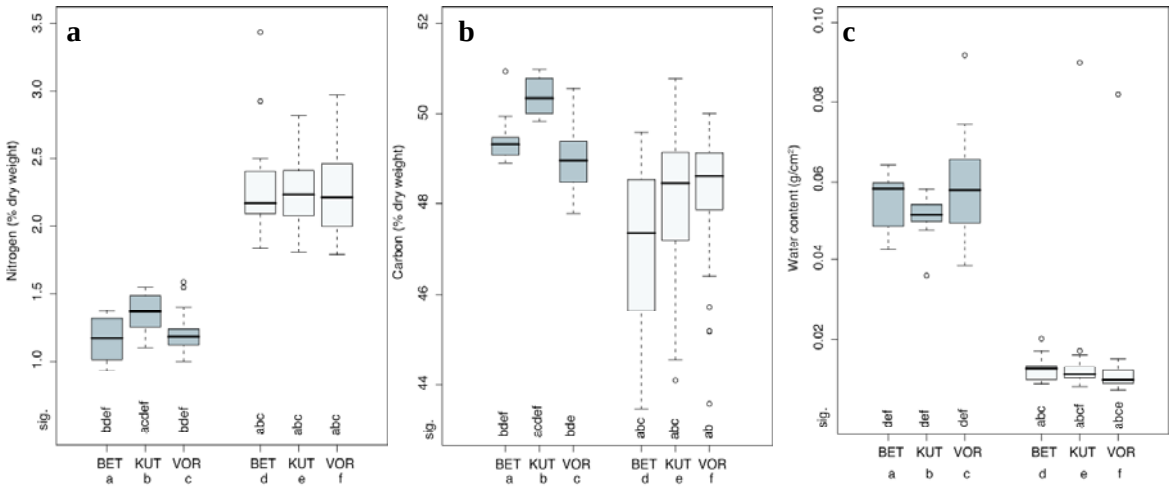

Fig. 4.1. (a) Nitrogen concentration, (b) carbon concentration and (c) leaf water content of needle-leaved (grey) and broad-leaved species (white) by study sites (BET: Bettlach; KUT: Kuettigen; VOR: Vordemwald). The box of the plots encloses the middle half of the samples, with an end at each quartile (lower and upper quartiles). The median of each dataset is indicated by the black center line. Whiskers sprout from the two ends of each box until the sample maximum and minimum. Potential outliers are plotted as circles. Significance (sig.) of difference in medians ($\alpha < 0.05$) compared to the other datasets is indicated by letters a - f.

Linden and alder, a nitrogen-fixing tree, had the highest and spruce the lowest C_N among all species. Because larch behaved like broadleaf deciduous trees regarding C_N it was included in the latter functional type for C_N prediction. It can be seen from the boxplots in Figure 4.1 that some populations were non-symmetrical (non-centered median lines and unequal whisker lengths). Therefore, details are subsequently reported in median values.

Median values of broad-leaved trees were nearly identical among the three study sites, but Vordemwald revealed a higher range in measured values than the other two sites. The median values of needle-leaved species were nearly identical for Bettlachstock and Vordemwald, but both differed significantly from the median of data from Kuettigen. This may be explained by the higher proportion of pine samples taken at Kuettigen, since pine needles are higher in C_N compared to fir and spruce. The smallest within-site variability of C_N was observed at Vordemwald for needle-leaved species.

Table 4.1. Summary statistics of biochemical and structural properties, GPS horizontal precision and dataset size (n), grouped by datasets (ALL, VOR, NED, BDD and FSD).

Dataset	n	Min	Max	Mean	St. Dev.
ALL	**120† / 132‡**				
Nitrogen (% dry weight)		0.93	3.44	1.85	0.57
Carbon (% dry weight)		43.46	50.98	48.48	1.49
Water (g/cm^2)		0.007	0.092	0.030	0.024
Crown radius (m)		1.4	8.2	4.0	1.4
Height (m)		18	46	31	5.2
GPS precision (m)		1.2	9.8	2.7	1.1
VOR	**50† / 60‡**				
Nitrogen (% dry weight)		1.00	2.97	1.68	0.58
Carbon (% dry weight)		43.57	50.56	48.56	1.20
Water (g/cm^2)		0.007	0.092	0.038	0.026
Crown radius (m)		1.4	8.1	4.1	1.4
Height (m)		26	46	34	4.0
GPS precision (m)		1.4	5.0	2.5	0.7
NED	**50† / 52‡**				
Nitrogen (% dry weight)		0.93	1.59	1.22	0.15
Carbon (% dry weight)		47.78	50.95	49.31	0.78
Water (g/cm^2)		0.036	0.092	0.056	0.01
Crown radius (m)		1.4	5.0	3.0	0.8
Height (m)		18	42	32	5.8
GPS precision (m)		1.5	5.2	2.5	0.8
BDD	**71† / 80‡**				
Nitrogen (% dry weight)		1.79	3.44	2.26	0.30
Carbon (% dry weight)		43.46	50.77	47.91	1.59
Water (g/cm^2)		0.007	0.09	0.013	0.013
Crown radius (m)		1.8	8.2	4.7	1.3
Height (m)		20	46	30	4.6
GPS precision (m)		1.2	9.8	2.9	1.2
FSD	**40† / 42‡**				
Nitrogen (% dry weight)		1.81	2.56	2.14	0.19
Carbon (% dry weight)		47.15	50.77	48.88	0.68
Water (g/cm^2)		0.007	0.013	0.010	0.001
Crown radius (m)		2.4	8.2	4.8	1.4
Height (m)		22	46	31	5.2
GPS precision (m)		1.2	5.0	2.5	1.0

† corresponds to the C_W dataset; ‡ corresponds to the C_C & C_N dataset;

C_C exhibited a remarkably larger range for broadleaves than for needle-leaved species (Fig. 4.1b). In Bettlachstock, the largest range was observed for needle-leaved and the smallest range for broad-leaved species, respectively. In general, needle-leaved species had higher C_C. Among all tree species, ash and maple revealed the smallest and pine the highest C_C values. Among all sites and functional types divergent median values were found. The highest median was found at Kuettigen among needle-leaved species and the smallest at Bettlachstock among broadleaves. At Kuettigen again the highest C_C values were observed due to higher number of pine samples taken.

Analyses of C_W revealed higher median values and a larger range in measured C_W values

for needle-leaved compared to broad-leaved species (Fig. 4.1c), where C_W was calculated on an area-basis. Larch showed the highest C_W, it was therefore included in the needle-leaved group for C_W prediction. Among the three study sites, the highest variability was found at Vordemwald for needle-leaved species whereas for broad-leaved trees a nearly identical range for all study sites was observed.

4.3.2 Building and cross-validating regression models

Figure 4.2 gives an example of both the B&B and the forward selected regression models between the BNC reflectance values and the chemical concentrations of different datasets. Mostly, both algorithms selected the same first waveband, as can be seen in the given example (waveband at 1157.8nm), but the following waveband selections differ considerably. Characteristic for the forward search algorithm is that once a waveband was selected it stays in the model not as for the B&B approach.

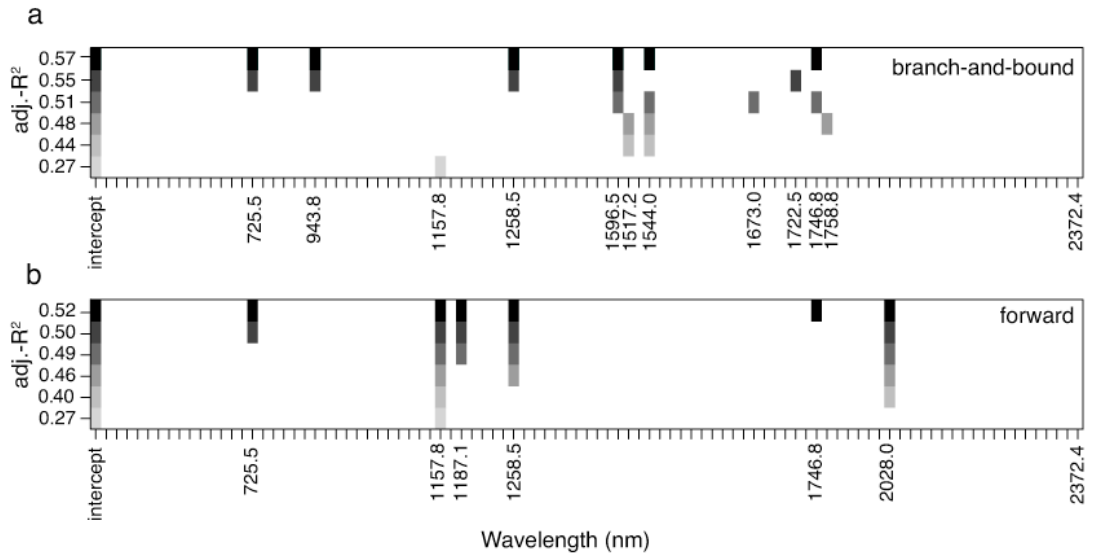

Fig. 4.2. Example of a result of selected wavebands using a branch-and-bound (a) and a forward search (b) algorithm for C_N using the ALL dataset. The x-axis shows HyMap wavebands and the y-axis expresses the resulting model fit (adj.-R^2) in increasing number of bands selected. The Figure shows the selected wavebands, starting with a model with the intercept and one predictor variable (x = 1157.8 nm, adj.-R^2 = 0.27).

Table 4.2 illustrates that prediction accuracies of B&B models were always higher (RMSE lower) than those of the forward and the causal models for all datasets and biochemical concentrations. Hence, the findings of the B&B models are subsequently shown for presenting tested (cross-validated) models graphically.

Table 4.2. Model fit (adj.-R^2) and cross-validated accuracy (RMSE) of regression models of biochemical concentration. Three regression approaches are presented, differing in the way variable subsets are selected: forward: forward search algorithm; B&B: branch-and-bound algorithm; causal: B&B algorithm using only lab identified wavebands.

Dataset	Subset method	Nitrogen		Carbon		Water	
		adj.-R^2	*RMSE*	adj.-R^2	*RMSE*	adj.-R^2	*RMSE*
ALL	forward	0.49	*0.397*	0.30	*1.210*	0.41	*0.018*
	B&B	0.53	*0.381*	0.31	*1.215*	0.49	*0.016*
	causal	0.45	*0.411*	0.28	*1.240*	-	-
VOR	forward	0.53	*0.376*	0.46	*0.837*	0.49	*0.017*
	B&B	0.63	*0.334*	0.47	*0.831*	0.53	*0.016*
	causal	0.51	*0.384*	0.40	*0.884*	-	-
NED	forward	0.44	*0.105*	0.35	*0.600*	0.36[2]	*0.008*
	B&B	0.45	*0.104*	0.50	*0.519*	0.37[2]	*0.008*
	causal	0.31	*0.117*	0.40	*0.581*	-	-
BDD	forward	0.16[1]	*0.239*	0.25	*1.332*	0.30	*0.002*
	B&B	0.29[1]	*0.218*	0.29	*1.286*	0.38	*0.002*
	causal	0.14[1]	*0.242*	0.25	*1.327*	-	-
FSD	forward	0.16	*0.170*	0.05	*0.624*	0.47	*0.001*
	B&B	0.50	*0.125*	0.30	*0.525*	0.48	*0.001*
	causal	0.38	*0.141*	0.00	*0.683*	-	-

[1] dataset excl. linden; [2] dataset incl. larch;

The VOR dataset demonstrates that a model for mixed forest canopies (nine species for the study site VOR) consisting of three functional types could be trained reasonably using the B&B subset method. Model fits for the three biochemical concentrations C_N, C_C and C_W reached adj.-R^2 values of 0.63, 0.47 and 0.53, respectively. The results for a similar model using data from all three regions (Table 4.2) showed that training a model using the dataset ALL proved to be less accurate, especially for estimating C_C (adj.-R^2 = 0.31). However, for C_N and C_W the predictive capability of the models could be improved by partitioning the ALL data into sets of functional types (coniferous and deciduous). For C_C, only the NED data revealed smaller RMSEs after partitioning.

For all biochemical concentrations, models could be trained for the needle-leaved evergreen dataset (NED). Model fits for biochemical concentration yielded adj.-R^2 values of 0.45 for C_N and of 0.50 for C_C. Models developed from the broadleaf dataset (BDD) from all three study sites performed comparably poor. Splitting up the BDD dataset further into a species set for *Fagus sylvatica* (FSD) improved the models markedly (not for C_C). Here, cross-validated errors dropped roughly by 50% for all three biochemicals. On average, best model fits and lowest errors among all datasets were achieved for C_N, whereas C_C was shown

to be the most difficult to estimate. Figures 4.3 and 4.4 illustrate some of the models presented.

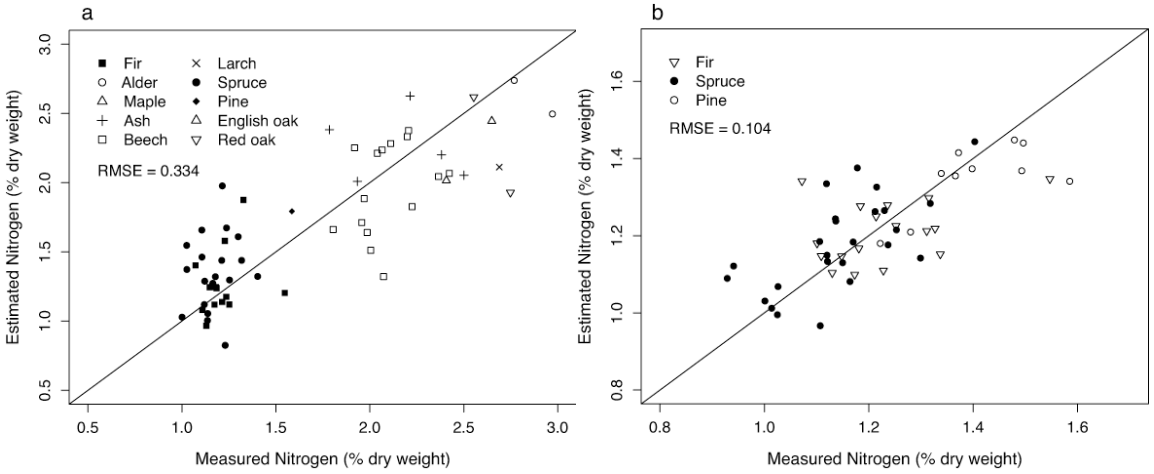

Fig. 4.3. Measured vs. estimated foliar nitrogen concentration (C_N) using branch-and-bound subset regression as estimation for: a) the dataset (VOR) consisting of samples from the study site Vordemwald (n=60); b) the needleleaf dataset (NED) consisting of samples from all three study sites (n=52).

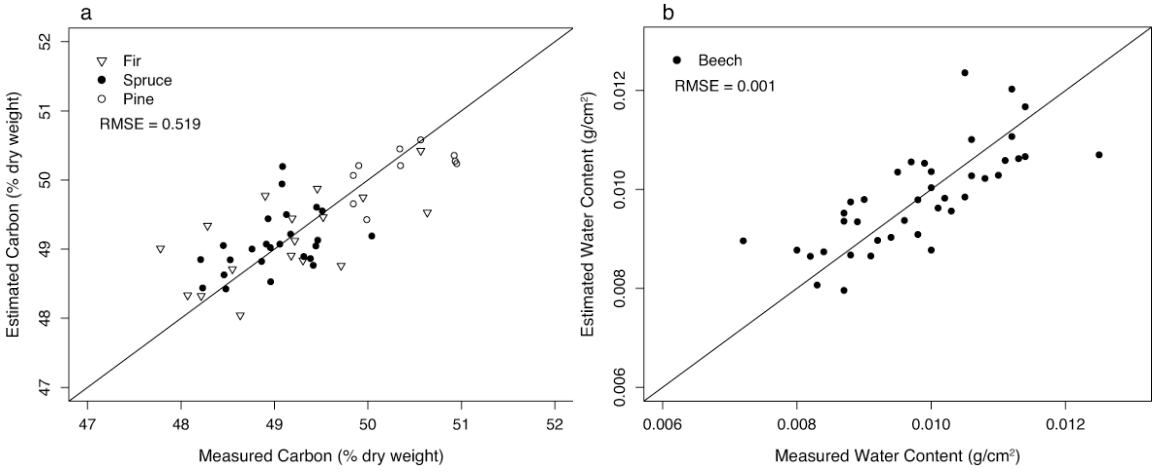

Fig. 4.4. Measured vs. estimates of a) foliar carbon concentration (C_C) in the needleleaf dataset (NED) consisting of samples from all three study sites (n=52) and of b) foliar water content (C_W) in the European beech dataset (FSD) consisting of samples from all three study sites (n=40). Estimates are derived using a branch-and-bound subset regression method.

4.3.3 Accordance and performance of models from causal wavebands

The accordance between statistically selected wavebands and causally known absorption features was evaluated for the B&B and forward search algorithms. For C_N models the B&B algorithm selected ~47 %, whereas the forward search algorithm chose ~43 % of wavebands known from literature. For the C_C model ~27 % and ~47 % of the selected wavebands from the B&B and forward search algorithms, respectively, were related to known absorption features. When considering both subset selection methods, ~28 % of the selected causal

wavebands fell within the red edge range for C_N and about 47 % fell within the range of 2050–2140 nm (lignin feature) for C_C models. The selected bands for C_W were not directly attributable to known absorption features. When evaluating all developed models, neither model fit (adj.-R^2) nor error (RMSE) did correlate significantly with the number of selected causal wavebands.

In order to test how well biochemical concentration can be estimated by using only causal wavebands in regression models, the B&B algorithm was forced to select only from these known wavebands. These models were found to be inferior (adj.-R^2 = 0.0–0.51) to B&B models based on all wavebands (adj.-R^2 = 0.29–0.63) for all datasets and biochemical concentrations used (Table 4.2). However, when compared with forward search model results, some causal models achieved similar or (in two cases) even slightly higher adj.-R^2 values and smaller RMSEs. Interestingly, the results of the C_C models trained from the datasets ALL and BDD were quite similar for all three subset methods (forward, B&B and causal). By investigating the models optimized from causal wavebands alone the study revealed that the absorption features at 570 nm, 740 nm, 1980 nm and 2054 nm were most often selected by C_N models. Similarly, the absorption features at 1700 nm, 1960 nm and 2050 nm were often selected by C_C models.

4.3.4 Extrapolating predictions

The capability to extrapolate C_N spatially was tested by developing models from data of any two study sites and then predicting the foliar biochemistry of the third independent study site (independent test). Table 4.3 shows the results for the datasets ALL and NED by study site, for tested models based on the B&B and the causal waveband selection. There were not enough observations for training and testing the models of the remaining datasets.

Table 4.3. Accuracy assessment of extrapolated predictions for C_N models. Training samples (*Train*) comprise the data of two study sites, test samples (*Test*) contain data of the third independent study site (VOR: Vordemwald, KUT: Kuettigen, BET: Bettlachstock). Results are reported in terms of model accuracy (RMSE).

Dataset / model	*Train*: VOR+KUT (n=109) *Test*: BET (n=23)	*Train*: VOR+BET (n=83) *Test*: KUT (n=49)	*Train*: KUT+BET (n=72) *Test*: VOR (n=60)
ALL / B&B	*0.604*	*0.430*	*0.486*
ALL / causal bands	*0.597*	*0.394*	*0.528*
	Train: n=43 / *Test*: n=9	*Train*: n=42 / *Test*: n=10	Training set too small.
NED / B&B	*0.179*	*0.155*	-
NED / causal bands	*0.127*	*0.103*	-

It is apparent from Table 4.3 that predictions generally resulted in higher RMSE values. Interestingly, predictions based on models using only causal wavebands achieved lower errors than did B&B models based on all wavebands. Best predictions were achieved with models based on the dataset NED using either the data of Vordemwald and Kuettigen or Vordemwald and Bettlachstock to train the models. Here, model accuracies were very close to those obtained when using data from all study sites.

4.4 Discussion and conclusions

Differences in biochemical concentrations between the three study sites were mainly due to the proportion and dominance of species available at each site. In Vordemwald the higher range in C_N for broadleaves can be explained by the presence of the nitrogen-fixing black alder, which has only been sampled at this site. The site Kuettigen often differs from the other two sites because of the higher proportion of Scots pines. The latter deviates from the other needle-leaved species in this study with respect to leaf structural and biochemical properties.

Because models trained for ALL resulted in moderate accuracies in terms of predicted biochemical concentrations, the dataset ALL was split into functional types. This study confirms previous findings that partitioning data by functional groups yielded lower errors (Serrano et al., 2002; Mutanga et al., 2004). Yet, it was also discovered that splitting by functional types may be of limited benefit if many species are involved per functional type (as is the case with the broadleaf group in this study). NED and BDD were composed of three and eight different species, respectively. The moderate results yielded from BDD may be explained by the fact that a higher number of species lead to a higher variability in leaf angle distribution (LAD). LAD significantly affects the representation of leaf optical properties at canopy scales (Asner, 1998). Asner (1998) showed that a smaller range of LAD leads to a higher relative contribution of leaf optical properties to the canopy-level reflectance since leaf optical properties – and thus the biochemical composition of leaf material – are generally underrepresented at canopy scales, unless LAI is quite high.

Additional uncertainties arose from scaling point field measurements of foliar chemistry to canopy scale and comparing laboratory measurements to field concentrations because the two may differ significantly (Curran, 1989). Yet, the main constraint for biochemistry estimation of green foliage remains leaf water since it obscures the absorption features of interest (Elvidge, 1990; Kokaly and Clark, 1999). In particular C_C was difficult to assess because the impact of leaf water on the estimation errors is higher for C_C than for C_N. Already a small amount of leaf water (e.g. 20 %) leads to an increase of the errors in biochemistry estimates (Kokaly and Clark, 1999). However, Cc also showed the least variation among all measured compounds across sites, functional types and species. Therefore it is not truly problematic for environmental applications if models do not improve much beyond the sample mean (null model). An alternative to avoid the leaf water problem might be a prior removal of water from absorption features of interest using a nonlinear least squares spectral matching technique (Gao and Goetz, 1994). It has been shown that water removed spectra may enhance absorption features during the upscaling from leaf to canopy spectra (Schlerf et al., 2005).

Estimating C_N was more successful because many selected wavebands were positioned in the red-edge region of the spectrum, which is less influenced by leaf water. This is in agreement with findings that the red edge slope is sensitive to a variation in foliar chemistry (Gates et al., 1965; Horler et al., 1983; Yoder and Pettigrew-Crosby, 1995; Mutanga et al., 2005).

The findings from the extrapolation predictions demonstrated clear differences between the three study sites because the quality of prediction depended on training sets. It seems

important that the training set covers the whole data range of the variables to be predicted (Miller, 2002). Contrary to the model accuracy assessment by cross-validation, the dataset NED performed best regarding accuracy when extrapolated to new areas. This proves the above statement regarding calibration range. Models solely based on causal wavebands performed best when predictions were extrapolated. This is interesting and represents a clear proof of the usefulness of using conceptual rather than empirical models for predictive purposes outside of the training area. Additional improvements may originate from mapping tree species (or functional type) from remotely sensed data prior to predicting the canopy biochemistry.

The accordance between statistically selected and causal wavebands exhibited a drawback of statistical subset selection methods. More than 50 % of the selected wavebands were not directly attributable to known absorption features relevant to targeted biochemical compounds. The performance of the tested branch-and-bound algorithm was encouraging because estimates of C_N, C_C and C_W based on the models of this algorithm achieved lowest RMSE and highest adj.-R^2 values. However, a disadvantage of the enumerative search was the processing time. The higher the number of variables to be searched, the longer was the processing time. Still, and most importantly, for extrapolating predictions and when testing with independent test datasets causal models retrieved better results than B&B models.

In summary, the following four statements conclude this study: (1) individual tree spectra were successfully extracted from remotely sensed images originating from differing test sites and models of sufficient accuracy were trained among three study sites and eleven species belonging to three functional types; (2) of the two regression methods tested, models derived from branch-and-bound algorithm explained the variation in biochemical concentration better; (3) predictions of models trained from data pooled across all three study sites could partly be improved by prior splitting data into functional types and species; (4) models solely based on causal wavebands can achieve similar or better results when extrapolating biochemistry predictions to other areas.

5 Contribution of Directional CHRIS/PROBA Data for Estimating Foliar Biochemistry in Mixed Forest

5.1 Introduction

Sun and sensor geometries cause directional effects in remotely sensed reflectance data which may influence the estimates of biophysical and biochemical variables. For instance, the anisotropic reflectance behavior of plant canopies implies that remote sensing observations vary without a change in the physical or chemical properties of the material observed. This complicates the interpretation of remotely sensed data of the same geographic location collected by different instruments at varying spatial scales or sampling times (Asner, 2004). The bidirectional variability is often considered as noise and its impact on the estimation of plant biochemical and structural variables remains unknown in many cases. However, several studies have shown that directional measurements contain added information about vegetation structure (Meyer et al., 1995; Asner et al., 1998), such as leaf area index (LAI) (Diner et al., 1999), gap fraction and leaf orientation (Chen et al., 2003; Ustin et al., 2004), or tree cover and tree height (Heiskanen, 2006) and that separability of land cover types may improve when using multiangular data (Barnsley et al., 1997; Gobron et al., 2000; Brown de Colstoun and Walthall, 2006; Kneubühler et al., 2006).

The complex vertical and horizontal structure of vegetation communities limits the ability to accurately derive biochemical estimates from remotely sensed data without accounting for canopy structure (Ustin et al., 2004). It has been shown that LAI and leaf orientation have a strong effect on leaf optical properties and thus the biochemistry of foliar material, at canopy scales (Asner, 1998). For canopies with a small LAI the foliar biochemistry is generally underrepresented in the canopy reflectance signal. In particular the NIR region, which shows the strongest multiple-scattering in green foliage canopies has the best potential for enhancement of the leaf-level signal if multiangular data is used (Asner, 1998). So far, little attention has been given to using directional information to the assessment of biochemical properties, such as nitrogen concentration (C_N) and water content (C_W). These two biochemicals belong to the most relevant components of green foliage due to their direct relation to photosynthesis. Their spatial characterization is valuable for a broad range of environmental applications (Curran, 2001; Ustin et al., 2004; Asner and Vitousek, 2005) (see section 5.1).

The objective of this study was to investigate the contribution of directional CHRIS data for the estimation of C_N and C_W by evaluating regression models based on various combinations of CHRIS viewing angles. Specifically, it was investigated: a) whether the information contained in remotely sensed multiangular data improves C_N and C_W estimates, b) if certain sensor viewing angles emerge to be beneficial for estimating C_N and C_W and finally c) whether additional directional information remains present after continuum removal and normalization have been applied to reflectance data. Explicitly no modeling study was

performed to demonstrate the potential of spectrodirectional EO information to application-oriented users including all inherent ambiguities.

For these investigations four datasets were generated per viewing angle (±36°, ±55° and nadir). One of the four datasets consisted of original reflectance, as extracted from each of the five CHRIS images and the other three of continuum-removed data using different algorithms as described in the method's chapter in section 3.3.2. The datasets were termed as follows: SPEC represented original reflectance values; BNC represented band depths normalized to the waveband at the center of the absorption feature; CRDR represented continuum-removed derivative reflectance and NBDI represented normalized band depth index values. Multidirectional CHRIS data were used in this study which were acquired over the Vordemwald (VOR) study site (section 2.1) and in-situ measurements as described in the sections 2.2 and 2.3. The CHRIS acquisition happened two years after field data collection but during the same phenological period (July). We assumed a stable C_N (Martin and Aber, 1997) and C_W (Gond et al., 1999) level during July and only small inter-annual variability for nitrogen concentration (Grassi et al., 2005) and leaf water status (Leuschner et al., 2001) due to similar climatic conditions in the years 2004 and 2006 (Swiss Federal Office of Meteorology and Climatology MeteoSchweiz, 2006). This assumption was confirmed by repeated leaf sample collections taken on one subplot over 10 years, which belongs to the framework of the IPC Forest monitoring. Summary statistics of biochemical and structural attributes of the Vordemwald site are given in Table 4.1.

5.2 Statistical analyses

Multiple linear regression analysis was applied to fit models between the dependent variables (C_N and C_W) and all possible viewing angle combinations of the four spectral datasets (SPEC, BNC, CRDR, NBDI). To limit the number of spectral wavebands used in the regression models, this study employed a statistical variable selection method, namely an enumerative branch-and-bound (B&B) search procedure (section 3.2.1). The regression was constrained to five selected wavelengths that best explained C_N and C_W. This limitation was applied in order to avoid overfitting of the models. The F statistic for all presented models was significant at the 5 % significance level.

An objective of this experiment was to determine whether assessing canopy C_N and C_W could be improved with additional directional information. Therefore, the model fitting was started on data extracted from one viewing angle (e.g., nadir). Next, models were developed for all possible combinations of two viewing angles (e.g., nadir and -36°) and the analysis was continued with three and four viewing angles to finally introduce the data of all five viewing angles as independent variables. This resulted in a total of 31 viewing angle combinations, which were evaluated for each spectral dataset. The models were evaluated by comparing the mean regression R^2 (measure of model fit termed coefficient of determination) from models with the same number of viewing angles. To test the models and to assess its predictive capability, a 10-fold cross-validation was applied with random splitting order of the data (section 3.2.2), from which the root mean square errors (CV-RMSE) was calculated. All

analyses were implemented within the R statistical package, a free software environment for statistical computing and graphics (R Development Core Team, 2005) under the GNU public license.

5.3 Results

5.3.1 Contribution of angular information to C_N and C_W estimation

The contribution of angular information to the model fit in terms of regression R^2 is apparent from Figure 5.1 for C_N and Figure 5.2 for C_W. The coefficients of determination (R^2) increased with additional angular information for all four datasets (SPEC, BNC, CRDR, NBDI) and for both biochemical variables. Adding the data of a second angle as independent variables to the regression analyses is contributing most to increase R^2, thereafter the additional improvement is decreasing steadily as more directional information is added. Regarding C_N regressed on SPEC, R^2 increased by 19 %, 27 % and 32 % (compared to the monodirectional models) when adding data of a second, third and fourth viewing angle, respectively.

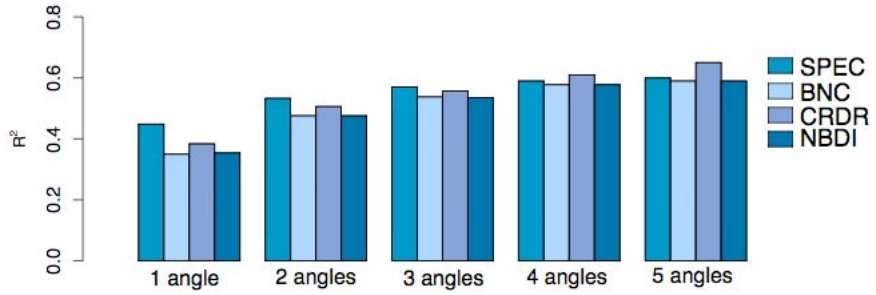

Fig. 5.1. Coefficient of determination (R^2) of nitrogen concentration regressed on the datasets SPEC, BNC, CRDR and NBDI, respectively. R^2 represents the mean of all models with the same number of viewing zenith angles involved. For instance R^2 of one angle stands for the mean of five monodirectional models (± 36°, ±55° and nadir).

The largest increase of R^2 was achieved with the BNC dataset by adding a second angle to the regressions (+36 %). Regarding C_W, the largest increase of R^2 was observed for CRDR; it improved by 25 %, 37 % and 45 % (compared to monodirectional models) when adding data of a second, third and fourth viewing angle, respectively.

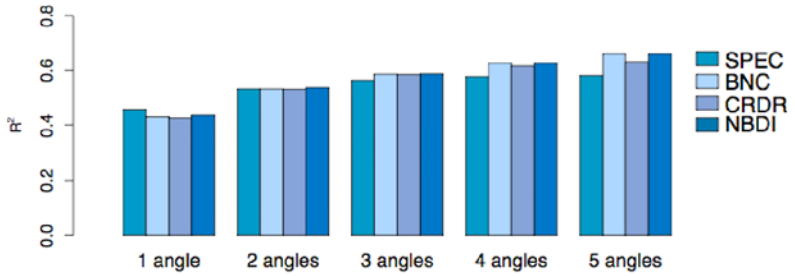

Fig. 5.2. Coefficient of determination (R^2) of water content regressed on the datasets SPEC, BNC, CRDR and NBDI, respectively. R^2 represents the mean of all models with the same number of viewing zenith angles involved. For instance R^2 of one angle stands for the mean of five monodirectional models (± 36°, ±55° and nadir).

Evaluating the contribution of directional information to models based on data from different spectral processing (SPEC, BNC, CRDR, NBDI) revealed interesting variations. For both biochemical parameters, regression models trained from untransformed reflectances (SPEC) performed best in terms of R^2 using data of one angle. Only with information of a second (C_W) and a fourth (C_N) angle added, one or several models developed from transformed data performed better.

5.3.2 Viewing angle combinations for C_N and C_W estimation

In total, 31 regression models were compared for each biochemical parameter and dataset to discover the most promising viewing angle combinations for improved estimates of C_N and C_W. To assess if directional effects are still present after continuum removal the same four different reflectance datasets (SPEC, BNC, CRDR and NBDI) were used. R^2 values varied considerably in all continuum-removed datasets. For instance they ranged from 0.15 (+36°) to 0.5 (-36°) for C_N single-angle models based on BNC (Fig. 5.3) or from 0.27 (+36°) to 0.58 (nadir) for C_W regressed on NBDI (see below).

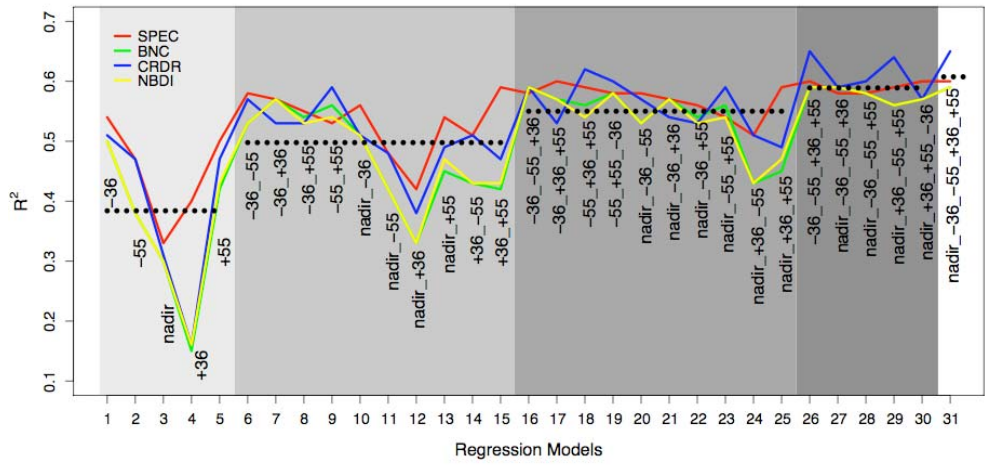

Fig. 5.3. Coefficients of determination (R^2) of leaf nitrogen concentration regressed on data of 31 different viewing angle combinations and four datasets (SPEC, BNC, CRDR, NBDI). The x-axis shows the 31 regression models and the background colors represent the number of angle datasets involved.

Hereafter results are given for C_N starting with single-angle models and continue afterwards with multiangular models. Best results were achieved for C_N trained on single-angle models with data from the nominal -36° angle for all datasets. Models developed from +36° data resulted in the lowest R^2 values for BNC, CRDR and NBDI but not for SPEC, where nadir data generated the lowest model fit.

R^2 values of nadir models among all four datasets ranged from 0.3–0.33, for -36° models from 0.5–0.54. In general, models obtained from -55° and +55° data achieved similar performances. For multi-angle models the combination of off-nadir angles yielded the highest R^2 values. Among all 31 models, maximum R^2 values (and minimum CV-RMSEs) were obtained when using three viewing zenith angles for SPEC (R^2=0.60), BNC (R^2=0.59) and NBDI (0.59), whereas CRDR (0.65) achieved highest model fits when using four viewing zenith angles. The four viewing zenith angles for CRDR were at ±36° and ±55°. Adding data of more than four angles as independent variables to subset selection did not augment the model fit of the best CRDR model any further. It only improved the average fit of models with higher numbers of angles involved.

Figure 5.4 illustrates that cross-validated RMSEs tend to decrease with increasing number of viewing zenith angles. Lowest CV-RMSE (0.376) was obtained from the model based on data of the four nominal angles ±36° and ±55° for CRDR with wavelengths selected at 631 (-36° and +55°), 672 (-55° and +55°) and 728 (+36°) nm. With four angles CV-RMSE was reduced by roughly a third compared to the simple nadir model (CV-RMSE 0.593). For all datasets CV-RMSEs of the best three angle models dropped by more than 0.18 compared to the simple nadir model.

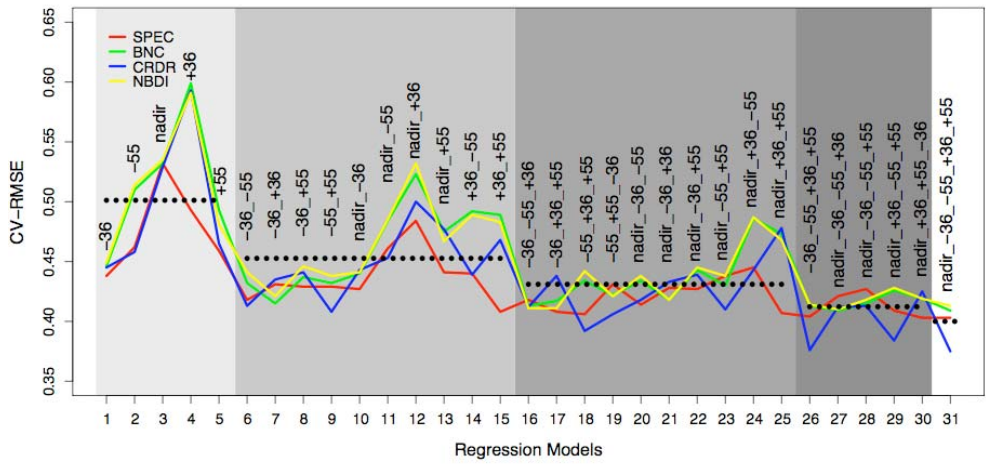

Fig. 5.4. Cross-validated RMSEs of 31 five-term regression models between nitrogen concentration and four spectral datasets (SPEC, BNC, CRDR, NBDI). The x-axis shows the evaluated 31 regression models and the background colors represent the number of angle datasets involved.

Regarding leaf water content estimates, Figure 5.5 shows that for monodirectional models highest model fits were achieved from nadir data (R^2 between 0.53 and 0.58) and lowest fits were obtained from +36° data (R^2 between 0.27 and 0.34) irrespective of spectral processing.

The models developed on backward scattering and nadir data performed better than the models based on forward scattering data.

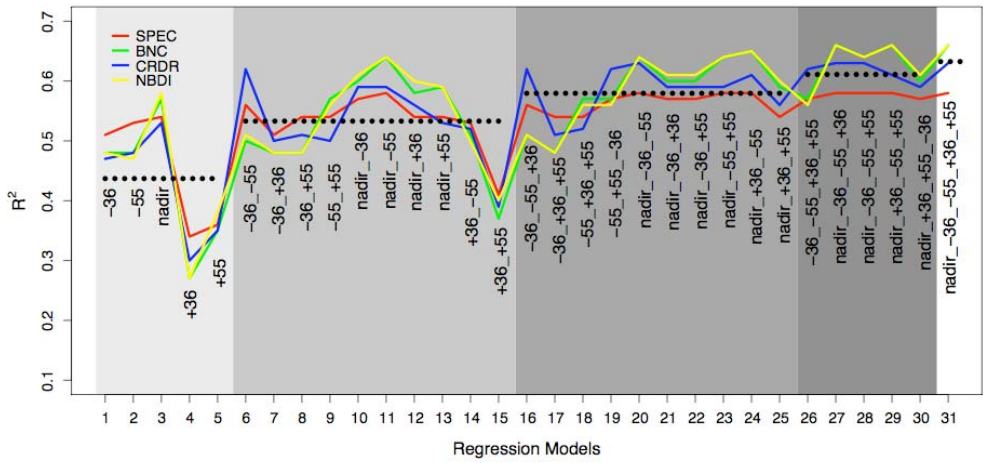

Fig. 5.5. Coefficients of determination (R^2) of leaf water content regressed on data of 31 different viewing angle combinations and four datasets (SPEC, BNC, CRDR, NBDI). The x-axis shows the 31 regression models and the background colors represent the number of angle datasets involved.

Apparent from Figure 5.6 is also the relatively constant curve representing R^2 values of SPEC which means that additional angular information did not improve the regression models. This is in contrast to the transformed datasets, which profited considerably more from adding additional angles. In general, best results were achieved with models using the BNC and the NBDI dataset. For two-angle models, the combination of nadir and -55° viewing zenith angles yielded the highest R^2 values for SPEC, BNC and NBDI (Fig. 5.6).

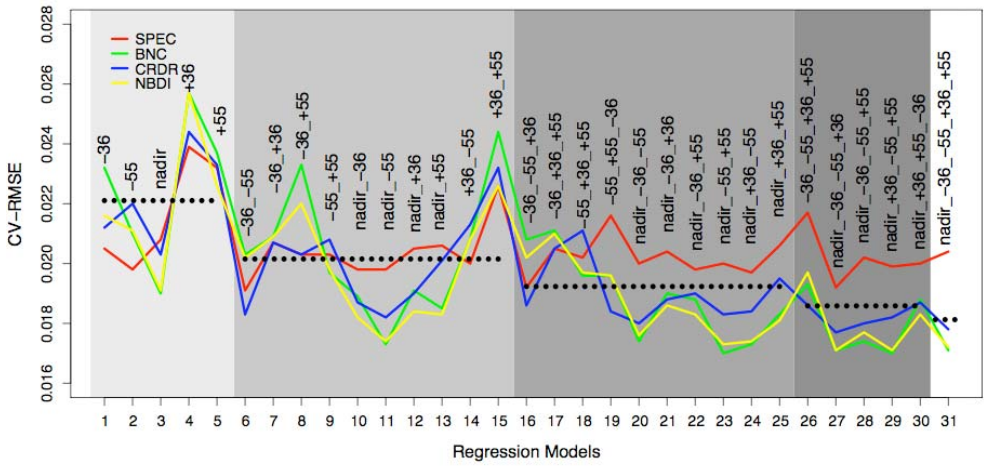

Fig. 5.6. Cross-validated RMSEs of 31 five-term regression models between water content and four spectral datasets (SPEC, BNC, CRDR, NBDI). The x-axis shows the evaluated 31 regression models and the background colors represent the number of angle datasets involved.

Best model fits were obtained already from data of two viewing zenith angles for SPEC (R^2=0.58), from three angles for CRDR (0.63), whereas BNC and NBDI (0.66) achieved maximum R^2 values from four viewing zenith angles (nadir, ±36° and -55°). As with C_N estimates, using data of more than four angles did not increase the coefficients of determination any further. Yet, lowest CV-RMSEs (0.0171) were obtained from models for BNC and NBDI with wavelengths selected at 570 (nadir), 683 (±36°), 728 (-55°) and 735 (-55°) nm. With three and more viewing zenith angles involved in regression modeling, models based on transformed datasets achieved clearly lower RMSEs than those developed on SPEC.

5.4 Discussion

In this study, monodirectional models trained on backward scattering data generally achieved higher R^2 values and lower model errors than those developed on data of the forward scattering direction. The finding that most information for vegetation targets is contained in backward scattering viewing direction reflectance is consistent with previous studies, which found an increase in reflectance for the backward scattering direction in boreal forests but lower reflectance values in the forward scattering direction, due to a combination of gap and backshadow effects (Sandmeier et al., 1998; Deering et al., 1999). These anisotropic effects are more pronounced at high sun zenith angles and are emphasized in high absorbing spectral ranges (e.g. red band) due to the lack of multiple scattering in this wavelength range (Deering et al., 1999). It has also been shown that the canopy hotspot effect has rich information content for vegetation characterization, especially indications of canopy structure (i.e., a shadow is not visible) (Gerstl, 1999; Weiss et al., 2000; Camacho-de Coca et al., 2001; Lacaze et al., 2002). In this analysis the viewing zenith angle of -36° is located closest to the images hotspot. Again it is emphasized that CHRIS images were not recorded in the sun principal plane; the monodirectional models developed on this angular data performed best for C_N irrespective of spectral processing. The minimum reflectance values occurred in the forward scattering directions because the sensor observes the non-illuminated, shaded leaf surfaces (Sandmeier et al., 1998). This is in agreement with the findings of this study, where models based on data of the +36° and +55° angles obtained poor results for C_W. However, for C_N, models developed on data of the +55° angle performed similar to -55° models. From these viewing angles, the sensor's field of view is still dominated by foliar material and – compared to nadir – the shadows seem to have a lower influence than possible soil background effects. For C_N estimates the nadir view direction played a minor role possibly due to shaded background that has strongest influences on the signal for small off-nadir angles (Ni et al., 1999). The large portion of gaps observed in this direction decreases the portion of leaf material seen from the sensor and thus the reflectance values. It was surprising not to see this effect for C_W estimates where the monodirectional models based on nadir data performed best irrespective of spectral processing. A possible explanation for this might be that also influences of non-photosynthetic materials, such as soil or bark, are used as information while C_N estimates are exclusively linked to green plant materials.

Another interesting finding was that C_W models developed on the SPEC dataset showed very stable model fits ($R^2 \approx 0.57$) encompassing all angular combinations (except +36°/+55°)

and an increase of R^2 did not occur when using additional angular data. It is difficult to explain this result. It might be related to the sensor's spectral coverage (442–1019 nm) so that no major liquid water absorption feature could be used in this study. The original reflectance data might not be sufficiently sensitive to changes in water content in the weaker absorption feature around 970 nm. However, for the transformed datasets much more variability in R^2 values was obtained.

Additional uncertainties arose from scaling point field measurements of foliar chemistry to the canopy scale as seen by CHRIS and georegistration. A direct approach (regression modeling) and original laboratory data were used in order to minimize additional sources of error introduced by an intermediate scaling step, for instance with HyMap data. Being aware of the problem, it is suggested that further research should explore the issue of up-scaling between different data sources and scales. With a careful selection of subplots and sampling trees the issue concerning georegistration was partly controlled. However, there remain ambiguities which influence the results that cannot be eliminated completely.

To assess possible directional effects in models based on spectrally transformed data the regression results from three continuum-removed datasets (BNC, CRDR and NBDI) were compared with those from untransformed reflectance values (SPEC). For single-angle models R^2 values varied considerably for both biochemical constituents between viewing angles, indicating that the normalization procedure did not remove all extraneous effects. For C_N, however, it was observed that SPEC performed particularly well for models developed on data based on one or two viewing zenith angles. This indicates that untransformed spectral data contains more additional information related to e.g. tree structures, which may have improved the regression models. Only when using three or more viewing angles, models developed on continuum-removed datasets improved over SPEC data due to contributing information from additional viewing angles.

5.5 Conclusions

This study has investigated the contribution of directional CHRIS data to the estimation of canopy C_N and C_W by assessing R^2 values and CV-RMSEs of regression model fits between the chemical constituents and 31 angular combinations of four spectral datasets. It was discovered that 1) additional information contained in multiangular data improved regression models fits for C_N and C_W estimates and lowered cross-validated RMSEs considerably, 2) strongest effects upon model R^2 can be achieved when adding a second and third viewing zenith angle, 3) monodirectional models developed on the backward scattering viewing directions were generally superior to models based on forward scattering data 4) models based on combinations of off-nadir data performed best for C_N and 5) untransformed reflectance data (SPEC) often outperformed continuum-removed data when using only one viewing zenith angle.

6 Land Cover and Plant Functional Types Classification with Support Vector Machines

6.1 Introduction

Earth's ecosystems and landscapes have been extensively altered in the second half of the 20th through human actions. The most significant change has been the transformation of approximately one quarter of Earth's terrestrial surface to cultivated systems (Millennium Ecosystem Assessment, 2005). Changes in land use and management affect resources critical for human welfare and, in turn, alter climate through feedbacks to the atmosphere (Vitousek et al., 1997; Seneviratne et al., 2006). Detailed information about land use and land cover and their change is therefore critical for climate projections, monitoring systems and ecosystem forecasting. Yet, the measurement of land transformation on a global scale is challenging; changes can be measured more or less directly at a given site, but it is difficult to aggregate these changes regionally and globally (Vitousek et al., 1997). Therefore, it remains one of the future challenges, which can be only solved by remote sensing means (European Space Agency, 2006; National Research Council, 2007). In addition, provision of systematic observations of relevant land cover is one of the major areas identified where remote sensing technology could be applied to support implementation of the Kyoto treaty (Rosenqvist et al., 2003).

Specifying the type of land cover is an important first step in the implementation of a process model. However, most land models developed for use with climate models represent vegetation as discrete biomes. This is, at least for mixed life-form biomes, inconsistent with the leaf-level and whole-plant physiological parameterizations needed to couple these biogeophysical models with biogeochemical and ecosystem dynamics models (Bonan et al., 2002). Therefore, the use of spatially continuous distributions of coexisting plant functional types (PFTs) is a necessary step to link climate and ecosystem models (Bonan et al., 2002; National Research Council, 2007).

Vegetation cover types differ widely in their morphological and ecophysiological attributes and these physiological characteristics influence carbon, nitrogen and water vapor exchange between terrestrial ecosystems and the atmosphere (Running et al., 1999). These differences are the result of adaptations of the plants to specific environments (Reich et al., 1997). Broadleaf deciduous forests, for example, show very different structural and environmental response characteristics from evergreen coniferous forests, even though these vegetation types often occupy the same physiographic regions (Turner et al., 2004). Groups of plants often share similar structural, biochemical and physiological properties and these groups play substantially different roles in determining ecosystem functioning, including carbon and hydrological cycling (Reich et al., 1995; Breshears and Barnes, 1999; Gill and Jackson, 2000; Ollinger et al., 2002; Lovett et al., 2004). It has been shown that the decomposability of leaf litter varies among species (Daubenmire and Prusso, 1963) and that PFTs differ in their sensitivity to climate, land-use and other disturbances and thus play distinct roles in determining rates of ecosystem recovery following disturbance (Hill et al.,

2006). Therefore, physiological differentiation of cover types is important since they control the exchanges between vegetation, soil and atmosphere; and separation of plant functional types are key features in modern global climate models.

Imaging spectroscopy has the capability to detect plant functional types. PFTs are readily revealed through optical properties associated to physiological and structural attributes (Sims and Gamon, 2002; Asner et al., 2005).

In this study support vector machines (SVMs) (section 3.4) were used for classification of multiangular and hyperspectral CHRIS-Proba images obtained from the Vordemwald study site on the Swiss Plateau. SVMs are non-parametric classifiers which do not assume normally distributed input data. They have been successfully used in a range of remote sensing applications, mostly for land cover classifications (Gualtieri et al., 1999; Huang et al., 2002; Pal and Mather, 2006; Koetz et al., 2007). Previous studies demonstrated that classifications based on SVMs gained equal or better results compared to traditional methods such as the maximum likelihood classifier (MLC) (Huang et al., 2002; Pal and Mather, 2003). SVMs are particularly suited for classifications of high dimensional multi source data (Benediktsson et al., 1990). For instance, SVMs were used for the classification of multisensor datasets, consisting of SAR and optical data (Waske and Benediktsson, 2007) or lidar and hyperspectral data (Koetz et al., 2007).

However, so far there has been little attention on the use of SVMs with hyperspectral and multiangular data. Su and co-workers (2007) have successfully used SVMs for the recognition of semi-arid vegetation types using multiangular MISR data and in another study, leaf area index was retrieved with SVM regressions from the same sensor (Durbha et al., 2007). This is the first study investigating the performance of SVMs for classification of spaceborne hyperspectral–directional data. The combined measurements (hyperspectral–directional) from the same sensor allow investigations on the impact of each dimension on classifications.

The objective of this study was to investigate the use of SVMs for land cover and plant functional types classifications with multiangular, hyperspectral data. Two main research questions were addressed: first, how does the SVM classifier perform compared to a standard method (MLC); and second, how does the spectral and directional dimensions influence the classification results. Minor goals were to evaluate the two SVM main strategies to solve multi-class problems (One-Against-All and One-Against-One) and to assess the two approaches for the final training parameter selection from the cross-validated error surface (‘individual parameter set for every binary problem (INDIVIDUAL)’, ‘single parameter set for all binary Problems (MEAN)’).

6.2 Development of a classification scheme and collection of training and validation samples

Prior to SVM classification, a classification scheme was developed in line with the land cover of the study site Vordemwald and a set of training and validation samples was collected (description of study site is given in section 2.1). The classification scheme was generated on the basis of plant functional types defined by Bonan et al. (2002). The study site’s vegetation

types could be partitioned into *broad-leaved deciduous* and *needle-leaved evergreen forest*, *grasslands*, *bare soils* and *crops*. Additionally, the land cover classes *built-up areas* and *water bodies* were added to the scheme (Table 6.1).

Table 6.1. The seven land cover classes of the study site Vordemwald and the number of collected training and validation samples.

Code	**Class**	**Training samples**		**Validation samples**
		SVM	MLC	SVM & MLC
1	Bare soils	95	91	40
2	Crops	100	95	60
3	Grasslands	90	88	40
4	Needle-leaved trees	105	100	70
5	Broad-leaved trees	100	100	70
6	Water bodies	90	85	30
7	Built-up areas	100	100	60

The accuracy of all supervised classification methods considerably depends on the quality of the training samples. In contrary to other classifiers, for a successful SVM training it is important to include mixed pixels at the border of class boundaries because they are most efficient to determine the support vectors and hence the hyperplane between two classes (Foody and Mathur, 2006). Therefore, a purposive sampling strategy was applied, by selecting pixels for each class with a 3 x 3 pixel cross kernel using the *Region of interest (ROI)*-tool in the ENVI image processing package (Research Systems, 2004) and by distributing the pixel crosses evenly across the image (Fig. 6.1).

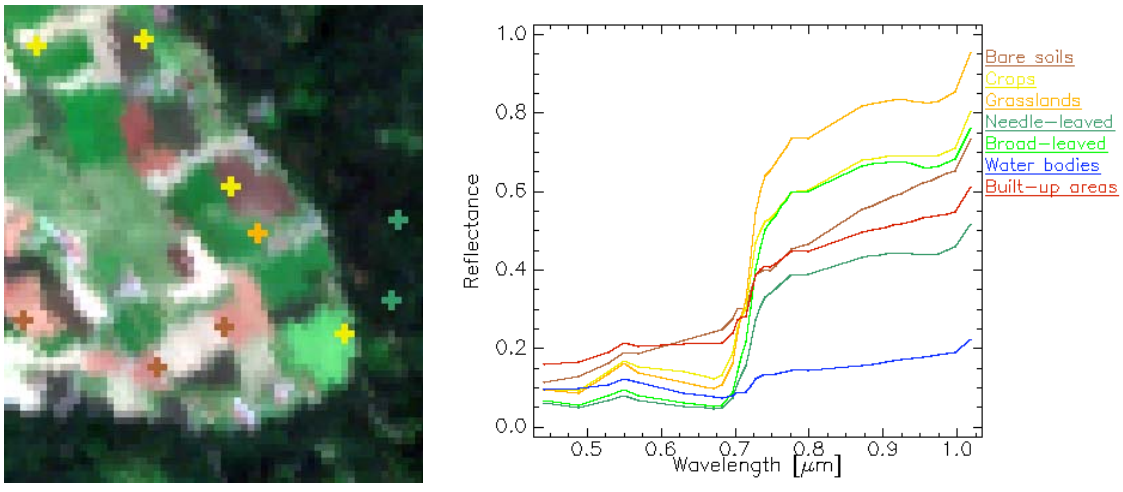

Fig. 6.1. Example of ROIs selected as 3x3 pixel cross kernels along class borders to include mixed pixels in the SVM training (left). Spectral signatures (mean) of training ROIs for seven classes (right).

Purposive sampling is a non-probability sampling method in which elements are chosen based on purpose of the study. The use of a pixel kernel allowed us to cover the internal heterogeneity of each class and to include mixed pixels along with adjacent pure pixels to describe the position of the hyperplane (Koetz et al., 2007). The samples were selected utilizing high-resolution aerial ADS40 data (swisstopo ©), acquired in 2005, a year earlier than the CHRIS data acquisition. This time difference confronted us with problems in selecting training and validation samples, related to crop rotation because separate ground-observed data was not available. For example, a cultivated field in 2005 turned to fallow land in 2006, thus becoming converted to the *grasslands* class. Especially the class *grasslands* was difficult to identify due to its spectral signature being similar to crops. This is expressed in the lower number of samples taken compared to the other classes. Therefore, it was not possible to only rely on ADS40 data when selecting training and validation samples, but also spectral signatures of the CHRIS images had to be considered. Hence, an automatic generation of random samples was not feasible. Roughly 100 samples were taken for each class to train the classifiers and a validation set was generated by sampling additional 370 pixels with the same strategy. With the limited ground data mainly an inter-comparison of different datasets (spectral, directional) and methods was targeted and not an evaluation of the classification quality over the whole image.

In order to compare the SVM results with a standard method the ENVI implemented maximum likelihood classifier (MLC) was used, one of the most popular classifiers in remote sensing (Swain and Davis, 1978). The maximum likelihood procedure is a supervised classification technique that is based on the assumption that the probability density function for each class is multivariate normal (Tou and Gonzalez 1974, Tso and Mather 2001). Descriptions of this classification method are readily available in the literature and hence detailed accounts are not given here.

As mentioned beforehand, the way of selecting training samples depends on the classification method and it impacts the classification result considerably. In general, to successfully train an MLC, rather pure pixels are required as training samples for an explicit separation of land cover classes (and not class borders as for SVMs). Therefore, the selected SVM training samples were slightly adapted for the MLC. Mostly the training samples were moved away from class borders towards the center of the target. Where the target was too small for a 3x3 pixel cross, less pixels were selected, resulting in a smaller number of training samples for MLC (Tab. 1.1). For the validation, the same samples were used as were collected for the SVM approach.

6.3 Development of datasets

To investigate the contribution of spectral and/or directional information to the classification result, five datasets were generated from the preprocessed CHRIS data, acquired in July 2006 over the study site Vordemwald. The datasets differed from each other in terms of their spectral and directional resolutions as presented in Table 6.2. More detailed descriptions are given in section 2.4.2.1.

Table 6.2. Names and descriptions of the five datasets generated for SVM and MLC analyses.

Name of dataset	Description
CHRIS nadir	All 37 bands of CHRIS@nadir
CHRIS nadir TM	CHRIS@nadir convolved to Landsat Thematic Mapper (bands@0.4791, 0.5607, 0.6611, 0.8345 μm)
CHRIS stack TM	CHRIS @nadir, @±36° and @±55° convolved to Landsat Thematic Mapper (bands@0.4791, 0.5607, 0.6611, 0.8345 μm)
CHRIS stack	All 37 bands of CHRIS@nadir, + band 2 (0.489μm) and band 9 (0.6828μm) @±36° and @±55°
CHRIS nadir ANIF	All 37 bands of CHRIS@nadir + ANIF of band 2 (0.489μm), band 9 (0.6828μm) and band 16 (0.7349μm) @±36° and @±55°

6.4 Support vector machines

For all SVM analyses, *imageSVM* (Janz et al., 2007), an IDL based tool for classifying remote sensing images was used. *ImageSVM* applies the library LIBSVM to train the SVMs (Chang and Lin, 2001). LIBSVM is an integrated software for support vector classification, regression and distribution estimation (http://www.csie.ntu.edu.tw/~cjlin/libsvm/index.html).

6.4.1 Grid search, training and classification

The process flow of SVM classifications in *image*SVM is visualized in Figure 6.2. The classification follows a three step approach: 1) a grid search is performed including internal cross-validation to explore the parameter space of the parameters that need to be defined for the training, 2) the training of the SVM used for the classification by considering the information from the grid search and finally 3) the classification of the image data (van der Linden and Janz, 2007). Prior to the grid search it is important to scale the data range of the image data. There are two main advantages for scaling: first, to avoid the case where attributes in greater numeric ranges dominate those in smaller numeric ranges and second, to avoid numerical difficulties during calculation, because *kernel* values (chapter 3.4) usually depend on the inner products of feature vectors, hence large attribute values might cause numerical problems (Hsu et al., 2001). The image data were scaled to the range 0–1 with the routine implemented in *image*SVM.

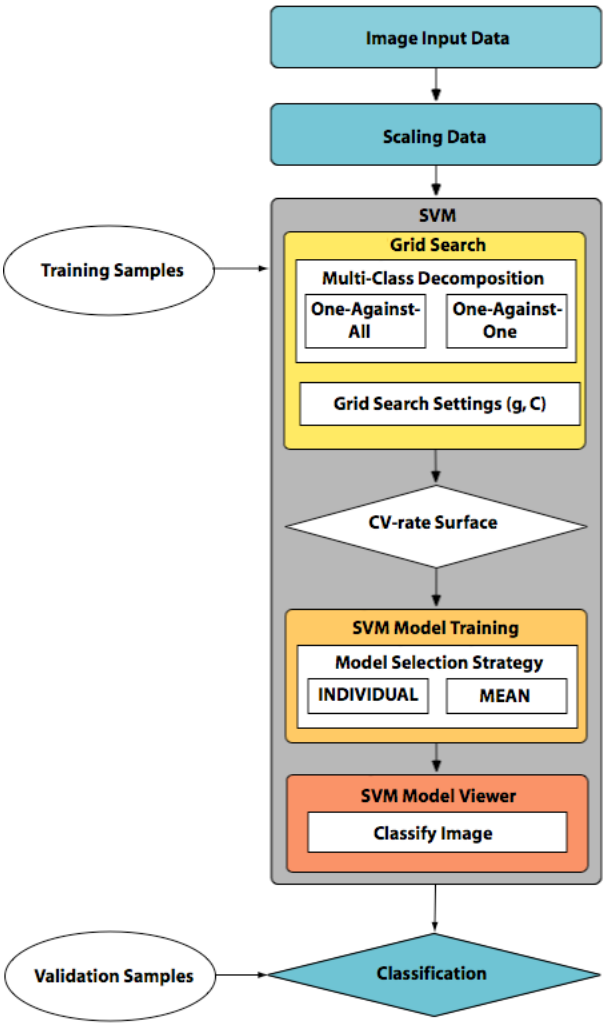

Fig. 6.2. Flowchart of SVM classifications in the software *image*SVM. The classification follows a three-step approach: 1) Grid search, 2) SVM Model Training and 3) SVM Model viewer with classification.

The grid search was started for each dataset with the default RBF *kernel* and regularization parameter settings (g: 0.00001–100000, *C*: 0.1–1000, with a multiplier of 10). Afterwards a 3-fold cross-validation was performed. The *kernel* parameter g (or γ) defines the width of the *kernel* function which implicitly transforms the classification problem into an infinite feature space. The regularization parameter *C* controls the trade-off between the maximization of the margin and the penalization of training errors (margin errors). Therefore, *C* directly limits the influence of the training samples (Burges, 1989). The grid search was conducted for both multi-class strategies, the One-Against-All (OAA) and the One-Against-One (OAO) strategy, to identify their impact on the classifications.

After a first grid search the cross-validation error surfaces were examined whether the parameter margins were approximated. Cross-validation error surfaces show on the x and y axes the *kernel* parameters *C* and g, respectively, and regions with low errors appear towards the center of the image for successful grid searches, otherwise they are shown adjacent to the image edges. Next, a second search was run, either with adjusted or refined settings and a multiplier of two.

The RBF *kernel* was used because it non-linearly maps samples into a higher dimensional space, so that it can handle the case when the relation between class labels and attributes is non-linear. The RBF is one of the most commonly used *kernel* functions. It exhibits less numerical computation difficulties than for instance a polynomial kernel, which has more parameters.

Following a successful grid search, the SVM model training was executed. Two strategies can be chosen to select the final training parameters from the CV error surfaces: first, for every binary problem individual *kernel* parameters (*C*, g) were allocated (INDIVIDUAL) or second, for all binary problems a single parameter set was allocated (MEAN). Both approaches were selected for all datasets to evaluate the strategies' impact on the classifications. After the final training of the SVMs, the datasets were classified and an accuracy assessment of the classifications was conducted with a validation set in ENVI.

6.5 Results and discussion

All SVM and maximum likelihhod classifications were assessed statistically with the overall accuracy (OA) and the Kappa coefficient (*K*). For the comparison of the best nadir-only and multiview-angle results also the Producer and User accuracies were inspected and finally, the results were qualitatively evaluated.

The assessment of all SVM classifications exposed overall accuracies from 72.16 to 79.46 % and Kappa coefficients from 0.672 to 0.757 (Tab. 1.3). Classifications based on the dataset that contains full spectral and directional information (*CHRIS stack)* achieved highest OA and *K* values (OA = 79.46 %, *K* = 0.757). The next best result was achieved with the dataset *CHRIS nadir* (OA = 78.11 %) which was slightly better than the dataset with reduced spectral resolution (*CHRIS nadir TM* OA = 77.30 %). Classifications with ANIF data (*CHRIS nadir ANIF)* were below the expectations.

Investigations on the selection of the two multi-class decompositions (One-Against-All OAA, One-Against-One OAO) showed that for all datasets, best results were achieved with the OAA strategy. Both strategies realized highest Kappa coefficients with the dataset *CHRIS stack* and the lowest with the dataset *CHRIS nadir ANIF*. Regarding the methods to select the final training parameters from the error surface (INDIVIDUAL, MEAN), generally, with a single parameter set for all binary problems (MEAN) best results were achieved for both decomposition strategies (in four of five cases). Interestingly, the only dataset that achieved higher accuracies with the INDIVIDUAL approach realized also the best overall result (*CHRIS stack:* OA = 79.46, *K* = 0.757).

6.5.1 Support vector machine versus maximum likelihood classifications

Our analyses showed that the SVM classifier performed better than the MLC. This result is in accordance with other studies (Huang et al., 2002; Pal and Mather, 2003; Waske and Benediktsson, 2007). However, the evaluation also showed that MLC results differed considerably depending on the strategy of collecting training samples (MLC specific or SVM specific with focus on class borders). As expected, the MLC trained with MLC specific

training samples achieved better results. In this case also the difference to the SVM results was reduced (maximum OAs: SVM = 79.46 %, MLC = 77.84 %) (Tables 6.3 and 6.4). Both classifiers achieved best results with a directional dataset: SVMs with the dataset *CHRIS stack* and MLC with the dataset *CHRIS stack TM*. The dataset containing ANIF information had the lowest classification accuracy when trained with SVMs. This was not the case for MLC, where the dataset *CHRIS nadir* achieved the smallest OA (75.68 %).

Table 6.3. Accuracy assessment of SVM classifications for all datasets and configurations: two multi-class strategies (One-Against-All (OAA), One-Against-One (OAO) strategy) and two approaches to select final parameters from the error surfaces (individual parameter set for every binary problem (INDIVIDUAL), single parameter set for all binary problems (MEAN)). Statistics are given as Overall Accuracy (OA) and Kappa coefficient (*K*).

Dataset	**One-Against-All (OAA)**				**One-Against-One (OAO)**			
	INDIVIDUAL		MEAN		INDIVIDUAL		MEAN	
	OA (%)	*K*	OA (%)	*K*	OA (%)	*K*	OA (%)	*K*
CHRIS nadir	76.22	0.719	78.11	0.741	77.03	0.729	77.57	0.736
CHRIS nadir TM	77.57	0.735	77.84	0.739	73.24	0.683	76.22	0.719
CHRIS stack TM	77.03	0.729	77.30	0.732	75.68	0.712	77.03	0.728
CHRIS stack	79.46	0.757	77.03	0.729	77.84	0.738	75.68	0.712
CHRIS nadir ANIF	74.05	0.694	74.32	0.697	72.16	0.672	73.78	0.690

Table 6.4. Accuracy assessment of MLC classifications, based on SVM specific and MLC specific sampling of training data, respectively. Statistics are given as Overall Accuracy (OA) and Kappa coefficient (*K*).

Dataset	**Maximum Likelihood Classifier**			
	Training samples SVM		Training samples MLC	
	OA (%)	*K*	OA (%)	*K*
CHRIS nadir	75.95	0.716	75.68	0.712
CHRIS nadir TM	74.86	0.704	77.03	0.728
CHRIS stack TM	73.51	0.689	77.84	0.738
CHRIS stack	74.86	0.705	77.03	0.728
CHRIS nadir ANIF	74.05	0.697	76.76	0.726

6.5.2 Spectral versus directional dimension

Quantitative investigations on data with different spectral and directional resolutions showed that classifications based on the dataset *CHRIS stack* were slightly (not significantly) better than classifications based on nadir-only data (for OAA and OAO). These results show that directional data contains additional information which is not inherent in spectral data obtained from nadir. This is in accordance with other studies (Gobron et al., 2000; Su et al., 2007). However, the *CHRIS nadir* (OAA-MEAN) classification (OA = 78.11 %) was still slightly better than the classification based on the TM convolved dataset *CHRIS stack TM* (OA = 77.30 %). This is interesting because both datasets contain bands in the blue and the red wavelength range of the electromagnetic spectrum, where anisotropic effects are most

pronounced for vegetation. It indicates the value of the spectral dimension. In the *CHRIS stack* dataset all 37 narrow bands of the nadir image were available for the classifications whereas the convolved dataset contained only four bands with much broader band-width. However, the OAA result (contradicting the OAO results) achieved with the convolved datasets the *CHRIS nadir TM* classification was better than the *CHRIS stack TM* classification.

The value of the directional data dimension was also investigated with a dataset containing anisotropy factors (ANIF). As demonstrated in section 2.4.2.1.3, the seven land cover types exhibited distinctive ANIFs. However, the ANIF dataset performed below our expectations. In fact, the lowest statistical coefficients were obtained using SVMs on the *CHRIS nadir ANIF* dataset.

Additionally, to the OA and *K* values producer's and user's accuracies were compared for the best nadir-only and multiangular classifications (Table 6.5). For both datasets, the low producer's accuracies for the *grasslands* class are evident. These low values are linked to the difficulties in collecting training samples. As mentioned beforehand, due to crop rotation it was difficult to identify *grassland* samples. Many samples were collected at forest borders, in clearings or orchards. Hence, the *grasslands* class was not well represented by training samples.

Table 6.5. Producer's and User's accuracies for the best SVM *CHRIS nadir* (OAA-MEAN) and SVM *CHRIS stack* (OAA-INDIVIDUAL) classifications.

Land cover	**Producer's Accuracy (%)**		**User's Accuracy (%)**	
	CHRIS nadir (MEAN)	*CHRIS stack* (INDIVIDUAL)	*CHRIS nadir* (MEAN)	*CHRIS stack* (INDIVIDUAL)
Bare soils	100.00	97.50	72.73	68.42
Crops	65.00	71.67	73.58	82.69
Grasslands	45.00	47.50	72.00	79.17
Needle-leaved	84.29	81.43	78.67	80.28
Broad-leaved	77.14	81.43	73.97	72.15
Water bodies	100.00	100.00	96.77	96.77
Built-up areas	81.67	81.67	84.48	87.50

Highest improvements from nadir-only to multiview-angle classifications were obtained in the classes crops (~+9 %) and grasslands (~+7 %). Water bodies were easy to classify since there is only the Aare river intersecting the study site.

6.5.3 Qualitative evaluation

Due to the limited quality of ground-observed data a qualitative inspection of the classifications was inevitable. Even though the statistical values showed a rather small variability among all datasets and methods, the qualitative evaluation revealed considerable differences among the classifications. In particular, there was confusion between the land cover classes *bare soils* and *built-up areas* and also between *grasslands* and *crops*. This confusion did not appear in the statistics. In general, too many pixels were classified as *built-*

up areas, however, with directional information a significant part of the confusion could be resolved. One example is shown in Figure 6.3.

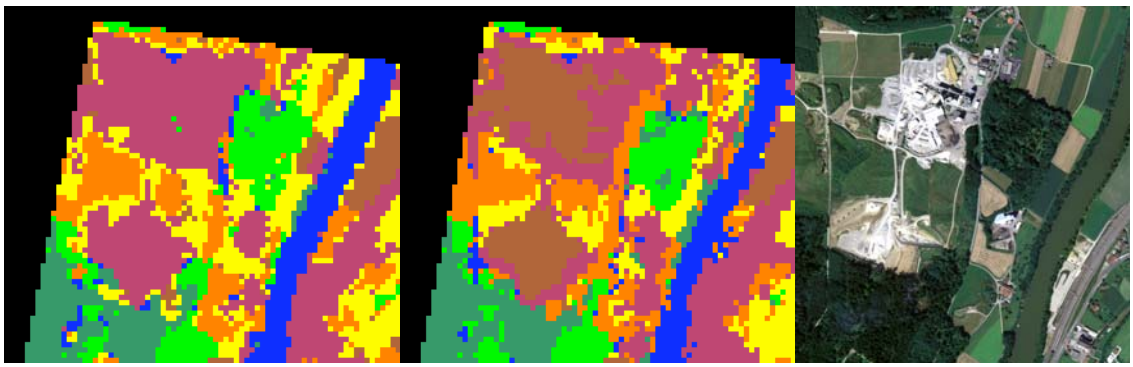

Fig. 6.3. Details of classifications of datasets *CHRIS nadir* (left) *and* CHRIS stack (middle) and ADS40 data (right).

Another problem were the similar spectral signatures of crops and grasslands and the limited available ground data. All this was complicating the generation of training and validation sets. Consequently, in the directional *CHRIS stack* dataset much more pixels were assigned to the *crop* class, whereas in the *CHRIS nadir* dataset they were classified as *grasslands* (Fig. 6.4).

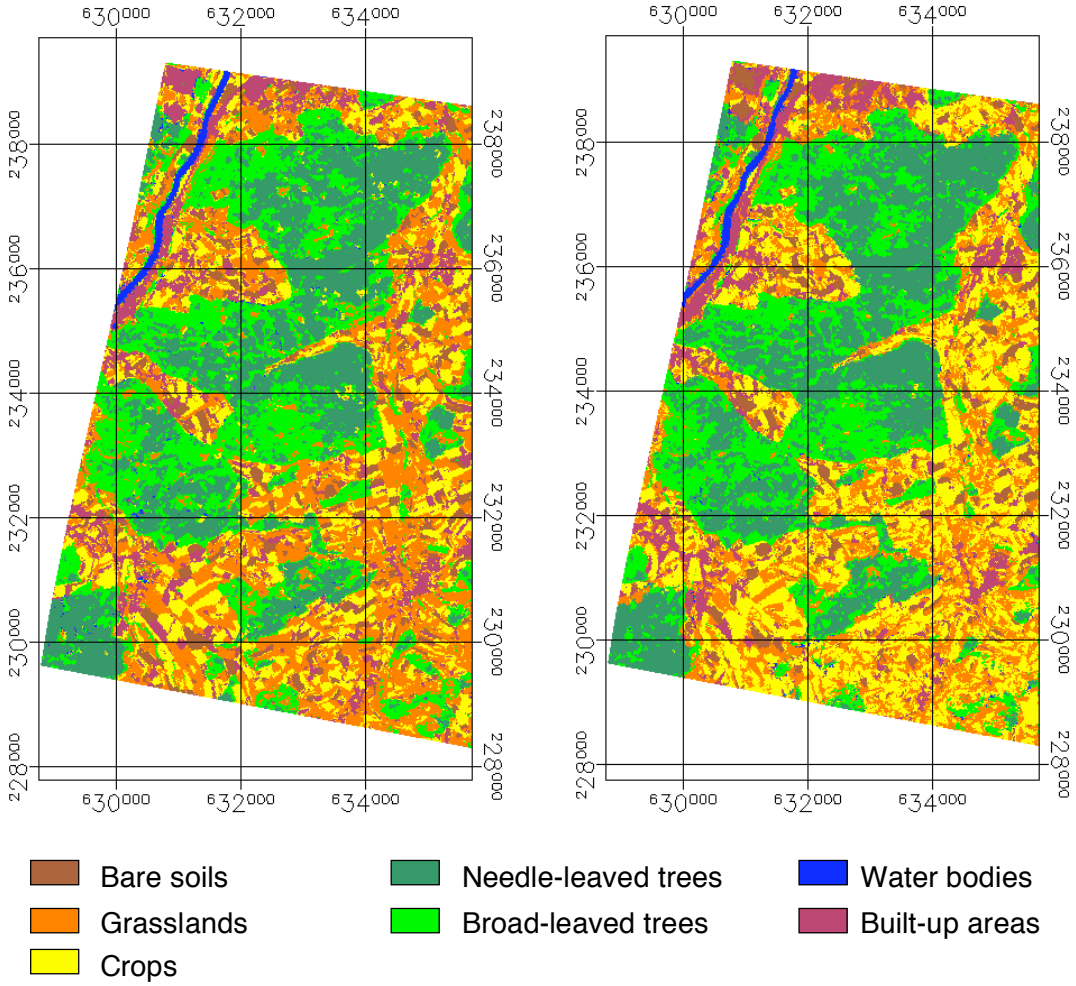

Fig. 6.4. Qualitative comparison between classifications based on *CHRIS nadir* (left) and *CHRIS stack* datasets (right). The different interpretations of *grasslands* versus *crops* are evident in the lower right corner.

The qualitative evaluation demonstrated the importance of well-selected training and validation data. In this study it was not possible to select entirely independent and random validation samples. Hence, the rather small differences between the overall accuracies and Kappa coefficients of different datasets (e.g., *CHRIS nadir–Chris stack*) could not reflect the impressive differences among classifications (see lower right corner of Fig. 6.4).

Another difficulty was the small structured landscape of the study site Vordemwald for an investigation with 18 m pixel spacing. Pure pixels could hardly ever be located in the images and additional geometrical inaccuracies arose from the georegistration (layer stacking) of the five CHRIS images. Originally, each CHRIS image was individually georectified. Pixels of residential areas, for example, showed distinctive vegetation signatures due to the mix of small houses surrounded by gardens and trees.

The dissimilarities between the two classifications in Figure 6.4 are accentuated in a difference image (Fig. 6.5). The class edges appear rather clear in the difference image due to pixel shifts in the co-registered CHRIS images (layer stack).

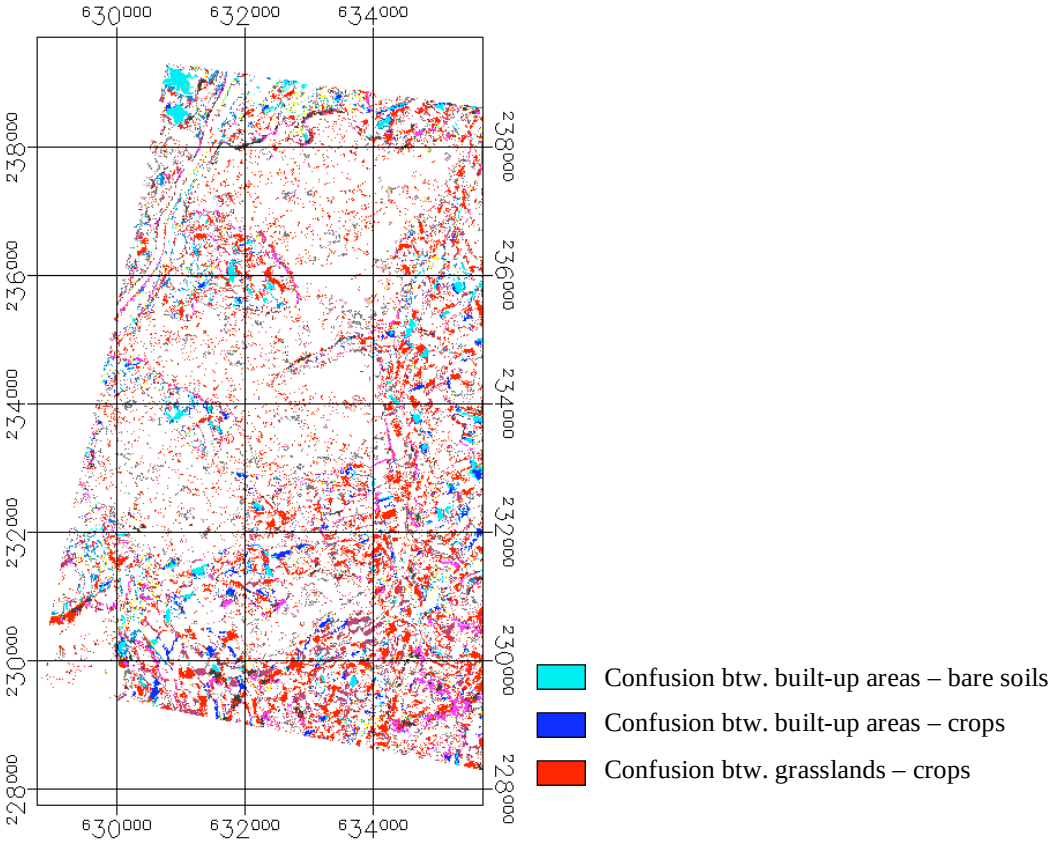

Fig. 6.5. Difference image of *CHRIS nadir* classification and *CHRIS stack* classification (Fig. 6.4). The different interpretations of built-up areas and bare soils (cyan) respectively crops (blue) and grasslands and crops (red) are evident.

6.6 Conclusions

Information about land use and cover and their change is critical for climate projections and ecosystem forecasting and even after many years of research accurate measurements of land

cover change are only available on a case-study basis (European Space Agency, 2006). With the advent of new remote sensing sensors and the opportunity to combine many different information dimensions with non-parametric statistical approaches there have been major improvements in classifications of land cover and plant functional types.

The present study was designed to investigate non-parametric support vector machines for classification of multiangular data. The results of this investigation show that 1) SVMs achieved higher classification accuracies than standard methods such as the maximum likelihood classifier, 2) directional data improved classifications but not always for convolved datasets with reduced spectral resolution, 3) hyperspectral data led to better class discrimination than convolved Landsat TM data with four broad bands, 4) best results were achieved with the SVM multi-class decomposition One-Against-All and 5) generally the SVM MEAN model selection strategy performed best. The findings of this study suggest that multiangular and hyperspectral reflectance and SVM algorithms are important means to improve land cover and vegetation type differentiation.

The statistical classification accuracies did not vary much due to the limited ground data available. However, the qualitative evaluation of the classifications revealed considerable differences among datasets. This emphasizes the importance of a careful and independent selection of training and validation samples inter-linked with high-quality ground data. Future research might explore more refined land cover and plant functional types implicating additional challenges for class discriminations.

7 Conclusions and Main Findings

This research was undertaken to derive ecologically relevant vegetation and land cover attributes from hyperspectral and multidirectional remote sensing data with focus on novel statistical methods. In the first part, this dissertation has investigated the development of inter-regional statistical models over a broad range of tree species to predict foliar biochemistry at the canopy level from airborne hyperspectral data using band-depth analysis and subset algorithms (chapter 4) and further, the impact of multidirectional observations on the predictive accuracy of such models (chapter 5). In the second part of the PhD study, land cover and plant functional types were classified with support vector machines by emphasizing the contribution of the spectral and directional data dimension to classification results (chapter 6).

Returning to the questions posed at the beginning of this study, it is now possible to state that individual tree spectra can be successfully extracted from HyMap images originating from differing test sites and it was possible to train models of sufficient accuracy among multiple study sites and eleven species belonging to three functional types to predict foliar chemistry; the utility of band-depth analysis for estimating biochemistry in mixed forest canopies has been demonstrated and regression models derived from the newly introduced subset selection method (B&B) explained the variation in biochemical concentration better than standard procedures (Huber et al., 2007). The developed regression models allow us to generate regional maps of biochemical concentration, which may serve as an important tool for monitoring forest health and status (Huber et al., 2004).

It was also shown that models, which were solely developed on causal wavebands, performed best in comparisons when predictions were extrapolated to other study sites. This finding suggests the usefulness of using conceptual rather than empirical models for predictive purposes outside of the training area. Currently, there are several conceptual models available (radiative transfer models at the leaf and canopy level), ranging in complexity from simple turbid to realistic ray-tracing models (Goel, 1989). However, none of them is describing all the effects influencing the radiative transfer, in particular in leaves, in a proper way and on the other hand, complex ray-tracing models are usually not-invertible because they need too many input variables (Moreno, 2007). Further research in this area is required to derive exact chemical and structural land cover information. Modern optical spectroradiometers (e.g., APEX) with high measurement precision and radiometric fidelity will help to improve the quality of current conceptual models on the basis of radiative transfer theory.

The results of the study on multidirectional CHRIS data affecting biochemical estimates (C_N and C_W) showed that additional information contained in multiangular data had a clearly positive impact on model accuracy: model fits increased and cross-validated RMSEs declined considerably (Huber et al., 2007). This demonstrates that directional data does not only improve the estimation of structural variables, as shown in previous studies (e.g., Kimes et al., 2006; Armston et al., 2007) but indirectly also biochemical estimates. This linkage originates from the complex structure of vegetation canopies, in particular of forests, where the

reflectance signal is influenced by a broad range of factors including foliar optical properties, canopy structure and viewing geometry (Chen et al., 2000). Further, the study has shown that a) strongest effects upon model R^2 can be achieved when adding a second and third viewing zenith angle, that b) monodirectional models developed on data of the backward scattering viewing directions (-36°, -55°) generally performed well, and that c) all but one monodirectional model performed worst with data of the +36° image. Another finding was that untransformed reflectance data (SPEC) often outperformed continuum-removed data when using only one viewing zenith angle but in turn, when adding data of more viewing zenith angles to develop statistical models, continuum-removed datasets performed better: highest R^2 values were always achieved with continuum-removed datasets with data of four viewing angles involved (CRDR for C_N R^2=0.65; BNC and NBDI for C_W R^2=0.66).

The presented research has examined statistical methods to readily obtain biochemical values from directional data by explicitly using an application-oriented approach. Indeed, many uncertainties and errors with which we have to cope in empirical studies could be either addressed implicitly or removed in purely modeling studies but the use of directional data for vegetation parameter retrieval by inverting radiative transfer models (RTMs) is still in the early stages of development and the behavior of different RTMs regarding directional data is not yet well known. One of the few studies that used real directional data to retrieve chlorophyll content by RTM inversion found only small variation among different angular data, contradicting the findings of this study (Begiebing et al., 2005). Yet, Begiebing and co-workers only discuss nadir and forward looking angles (+36°, +55°) without considering backward scattering data and multiangular information (angular combinations). However, the findings of the current study seem to be consistent with another modeling analysis albeit performed with synthetic data which found that best accuracies were obtained with multiple directions to estimate canopy variables. Chlorophyll content estimation required directions mainly in off-nadir directions for large zenith angles and around the hotspot peak (Weiss et al., 2000).

The performance of different RTMs regarding directional data was recently addressed by Schlerf and co-workers (2007) by comparing the outputs of different canopy reflectance models with real measurements for different wavelengths and multiangular observations. The authors reported good agreement between modeled and measured spectra whereas deviations were generally related to model structure or model parameterization. However, there remain many questions in need of further investigation until environmental applications will normally benefit from multidirectional EO data.

The second part of the dissertation was designed to investigate non-parametric support vector machines (SVM) to classify multidirectional CHRIS data into land cover and plant functional types. Specifying the type of land cover and in particular the physiological differentiation of cover types is important since they control the exchanges between vegetation, soil and atmosphere; and separation of plant functional types are key features in modern global climate models (Nemani and Running, 1996; Prentice et al., 2007). SVM algorithms are well suited for the classification of high-dimensional and multi-sensor data and are rather new to the remote sensing community. The results of this investigation indicate that

SVMs achieve higher classification accuracies than standard methods such as the maximum likelihood classifier. This finding is consistent with those of other studies (e.g., Huang et al., 2002; Waske et al., 2007) and suggests that SVMs should be considered at least as a supplement to standard classifiers. Also this study showed that in general directional data improved classifications and data with higher spectral resolution led to better class discrimination than convolved data with only four wavebands. However, precise multi-scene georegistration is an absolute necessity to achieve higher classification accuracies from multidirectional compared to monodirectional information.

In summary, the findings of this dissertation enhance our understanding of spectrodirectional measurements for practical applications in the field of environmental remote sensing. They highlight the potential of multiangular Earth observations for ecological monitoring and modeling studies as already proclaimed by preparatory studies for the ESA Earth Explorer candidate SPECTRA (Rast, 2004).

8 Outlook

The ability to determine land surface attributes from remote sensing data has evolved considerably in the past few decades mainly due to the advancement of computing environments, analysis techniques and methods. There are basically two approaches– statistical and physical–to assess the vegetation characteristics from the spectral signatures. Statistical methods are widely used, simple and fast to apply and computationally efficient, hence operational techniques largely remain on products derived from empirical studies. However, a drawback of these approaches is that they are usually site-specific and unable to explain causality. Nevertheless, statistical techniques will continue to play an important role in remote sensing of vegetation but in the future, the use of more universal and flexible canopy reflectance models will advance. Further developments in radiative transfer modeling and the availability of multiple, independent information dimensions provided by various Earth observation platforms (e.g., lidar, radar) will enable us to describe and thus solve the radiative transfer equation with increased accuracy and stability. All this will help to derive a robust and comprehensive characterization of the complex and dynamic nature of vegetation canopies and potentially provide more accurate quantitative and continuous estimates of canopy parameters that fulfill the requirements of ecological and technology-enhanced decision making processes and policies. However, only an integrated approach with remote sensing complemented with in situ sensing will allow a more consistent understanding of the relevant processes of vegetated ecosystems and the full Earth system.

Further, future research in remote sensing will also evolve more toward meeting the needs of society and consumers. One promising field toward this direction is ecosystem forecasting. There is a need to improve our knowledge of the socio-environmental system which is only feasible with an interdisciplinary approach and an integrated use of a broad variety of data originating from many different disciplines. Data assimilation will therefore gain in importance.

a) Societal benefits

The inherent purpose of Earth science data has traditionally been to enhance basic theoretical and observational scientific knowledge of Earth processes. However, in recent years consideration of how additional benefits might arise from Earth science data products evolved in particular in informing public understanding of investment in these services (Macauley, 2006). Focus on future remote sensing activities will advance toward meeting societal benefits and consumer needs (Gail, 2007). Several frameworks (GEO, 2005; Global Land Project, 2005) and agencies (NASA, 2005; European Space Agency, 2006; National Research Council, 2007) emphasize the desirability of using EO data in practical applications and public policy decisions, such as disaster and crisis-management support (Voigt et al., 2007) or epidemiology and public health (Tatem et al., 2004). Societal benefit might become a determining factor in selecting the next Earth-observing spacecraft missions and instruments (Macauley, 2006).

b) Ecosystem forecasting

The continuing pressure on ecosystems due to growing human population and improved standards of living is advancing initiatives toward ecological nowcasting and forecasting to optimise natural resource management and provide early warning of biological natural hazards (Clark et al., 2001). The ability to forecast the reciprocal interaction of climate change with the functioning of the biosphere in general and with the terrestrial vegetation in particular, may become of prime importance (Graetz, 1990). Long-term monitoring is an essential component to improve our ability to understand and forecast ecosystem change (Lovett et al., 2007). For the United States, for instance, the National Ecological Observatory Network (NEON - http://neoninc.org) was established and as similar project called "AEON" (Australian Ecosystem Observation Network) is being conceptualised at present. Both are continental-scale research platforms to discover and understand the impacts of climate change, land use change and invasive species on ecology. These platforms will gather long-term data on ecological responses of the biosphere to changes in land use and climate and on feedbacks with the geosphere, hydrosphere and atmosphere. One important future source of spatial and repetitive information to such integrated systems will be spaceborne hyperspectral remote sensing, which will guarantee the retrieval of accurate quantitative key information needed to create informed decision-making processes and outcomes (Asner et al., 2005; Hill et al., 2006). With anticipated launches of next-generation hyperspectral satellites from Germany, South Africa and possibly USA, Canada and Japan in the next five to ten years, combined with possible deployment of spaceborne lidar systems by NASA and others in the same timeframe, the opportunities to further improve remote sensing-derived input to sophisticated Earth system and ecological models are very high.

c) Transdisciplinarity and data assimilation

Due to climate and societal controls on ecosystems, trans-disciplinary linkages are essential for a successful forecasting as well as the capability to integrate a wide variety of data sources at various space and time resolutions (Clark et al., 2001; Nemani et al., 2005). All this requires a grand scientific synthesis across the domains of physics, geology, chemistry and biology but also societal practices (NASA, 2005). One attempt to foster the interrelationships and complexity of the whole coupled socio-environmental system is the international research framework Global Land Project (GLP). The research goal of GLP is to measure, model and understand the coupled human-environment system as part of broader efforts to understand changes in Earth processes and subsequent social, economic and political consequences (Global Land Project, 2005). Integrating socio-economic and socio-cultural components into modeling will certainly take on greater significance.

Integrated approaches with multiple EO sensors enabling the fusion of independent information, complemented with in situ sensing, measurement networks, ecological databases and physical modelling will gain in importance in the future to solve the existing challenges of the land surface outlined by ESA's Earth Science Advisory Committee (European Space Agency, 2006). The systematic combining of information from multiple sensors will enable us to obtain new information from existing sensor technologies (Gail, 2007). The next decade

will likely see rather fewer advances in sensors themselves but rather novel ways of using sensors, combining sensor information and deriving knowledge from that information (Gail, 2007). The optimal exploitation of multiple information dimensions provided by many different sensors and monitoring networks will require further research in the field of data assimilation. This will serve to extract the best possible information out of the observations, in particular those related to a better knowledge of the model and observation error and to maximize the scientific and economic value of EO data (Mathieu and O'Neill, 2007).

One attempt toward this direction is the Terrestrial Observation and Prediction System (TOPS) that facilitates integration of data from satellite, aircraft and ground sensors with weather/climate and application models to expeditiously produce operational nowcasts and forecasts of ecological conditions (Nemani et al., 2005).

The trend towards fusion of independent EO measurements for improved ecology-relevant information is visible in many recent publications (e.g., Treuhaft et al., 2004; Koetz et al., 2006; Bork and Su, 2007; Waske and Benediktsson, 2007; Wulder et al., 2007). In addition, efforts have been undertaken to develop an integrated system – the Carnegie Airborne Observatory (CAO) – to provide already in-flight fusion of imaging spectrometer data with scanning lidar data (Asner et al., 2007). This system endows access to novel and exceptional measurements of ecosystem structure, chemistry, physiology and biodiversity.

References

Akaike, H. (1973). *Information theory as en extension of the maximum likelihood principle.* Proc. of the Second International Symposium on Information Theory, (pp. 267–281). Budapest, Hungary.

Akaike, H. (1974). A new look at the statistical model identification. *IEEE Transactions on Automatic Control*, 19: 716-723.

Armston, J. D., P. F. Scarth, S. R. Phinn and T. J. Danaher (2007). Analysis of multi-date MISR measurements for forest and woodland communities, Queensland, Australia. *Remote Sensing of Environment*, 107: 287.

Asner, G. P. (1998). Biophysical and biochemical sources of variability in canopy reflectance. *Remote Sensing of Environment*, 64: 234-253.

Asner, G. P. (2004). Biophysical Remote Sensing Signatures of Arid and Semiarid Ecosystems. In S. L. Ustin (Ed.), *Remote sensing for natural resource management and environmental monitoring* (pp. 53–109). Hoboken, NJ: John Wiley & Sons.

Asner, G. P., B. H. Braswell, D. S. Schimel and C. A. Wessman (1998). Ecological Research Needs from Multiangle Remote Sensing Data. *Remote Sensing of Environment*, 63: 155-165.

Asner, G. P., J. A. Hicke and D. B. Lobell (2003). Per-Pixel Analysis of Forest Structure. In M. A. Wulder and S. E. Franklin (Eds.), *Remote sensing of forest environments : concepts and case studies* (pp. 209-254). Boston: Kluwer Academic Publishers.

Asner, G. P., D. E. Knapp, T. Kennedy-Bowdoin, M. O. Jones, R. E. Martin, J. W. Boardman, et al. (2007). Carnegie Airborne Observatory: in-flight fusion of hyperspectral imaging and waveform light detection and ranging (wLIDAR) for three-dimensional studies of ecosystems. *Journal of Applied Remote Sensing*, 1: 1-21.

Asner, G. P., R. G. Knox, R. O. Green and S. G. Ungar (2005). The Flora mission for ecosystem composition, disturbance and productivity, U.S. National Academy of Sciences Decadal Survey. http://asnerlab.stanford.edu/highlights/flora/FLORA_NRCDecadalSurvey_2005.pdf (accessed July 2007).

Asner, G. P. and P. M. Vitousek (2005). Remote analysis of biological invasion and biogeochemical change. *PNAS*, 102: 4383-4386.

Banko, G. (1998). A review of Assessing the Accuracy of Classifications of Remotely Sensed Data and of Methods Including Remote Sensing Data in Forest Inventory (pp. 1-42). Laxenburg, Austria: IIASA.

Barnsley, M. J., D. Allison and P. Lewis (1997). On the information content of multiple view angle (MVA) images. *International Journal of Remote Sensing*, 18: 1937-1960.

Barnsley, M. J., J. J. Settle, M. A. Cutter, D. R. Lobb and F. Teston (2004). The PROBA/CHRIS mission: a low-cost smallsat for hyperspectral multiangle observations of the Earth surface and atmosphere. *IEEE Transactions on Geoscience and Remote Sensing*, 42: 1512-1520.

Bartholome, E. and a. S. Belward (2005). GLC2000: a new approach to global land cover mapping from Earth observation data. *International Journal of Remote Sensing*, 26: 1959-1977.

Bazi, Y. and F. Melgani (2006). Toward an optimal SVM classification system for hyperspectral remote sensing images. *IEEE Transactions on Geoscience and Remote Sensing*, 44: 3374-3385.

Begiebing, S., H. Bach and W. Mauser (2007). *Assimilation of Hyperspectral Multi-Directional CHRIS-Data in a Coupled Radiative Transfer and Crop Growth Model*. Proc. of the Envisat Symposium. Montreux, Switzerland.

Begiebing, S., H. Bach, D. Waldmann and W. Mauser (2005). *Analyses of Spaceborne Hyperspectral and Directional CHRIS Data to Deliver Crop Status for Precision*

Agriculture. Proc. of the 5th European Conference on Precision Agriculture. Uppsala, Sweden.

Benediktsson, J. A., P. H. Swain and O. K. Ersoy (1990). Neural Network Approaches Versus Statistical-Methods in Classification of Multisource Remote-Sensing Data. *IEEE Transactions on Geoscience and Remote Sensing,* 28: 540-552.

Bonan, G. B., S. Levis, L. Kergoat and K. W. Oleson (2002). Landscapes as patches of plant functional types: An integrating concept for climate and ecosystem models. *Global Biogeochemical Cycles,* 16: doi: 10.1029/2000GB001360.

Bork, E. W. and J. G. Su (2007). Integrating LIDAR data and multispectral imagery for enhanced classification of rangeland vegetation: A meta analysis. *Remote Sensing of Environment,* 111: 11-24.

Brang, P., W. Schönenberger, E. Ott and B. Gardner (2001). Forests as Protection from Natural Hazards. In J. Evans (Ed.), *The Forests Handbook* (pp. 53–81). Oxford Malden, MA, USA: Blackwell Science.

Breshears, D. D. and F. J. Barnes (1999). Interrelationships between plant functional types and soil moisture heterogeneity for semiarid landscapes within the grassland/forest continuum: a unified conceptual model. *Landscape Ecology,* 14: 465-478.

Briscoe, E. and J. Feldman (2006). *Conceptual Complexity and the Bias-Variance Tradeoff*. Proc. of the Cognitive Science Conference (CogSci), (pp. 1038-1043). Vancouver, Canada.

Brown de Colstoun, E. C. and C. L. Walthall (2006). Improving global scale land cover classifications with multi-directional POLDER data and a decision tree classifier. *Remote Sensing of Environment,* 100: 474-485.

Burges, C. J. C. (1989). A tutorial on support vector machines for pattern recognition. *Data Mining and Knowledge Discovery,* 2: 121-167.

Burnham, K. P. and D. R. Anderson (1998). *Model selection and inference : a practical information-theoretic approach*. New York: Springer.

Camacho-de Coca, F., M. A. Gilabert and J. Melia (2001). *Hot spot signature dynamics in vegetation canopies with varying LAI*. Proc. of the Physical measurements and signatures in remote sensing, (pp. 303-308). Aussois, France.

Carlson, K., G. Asner, R. Hughes, R. Ostertag and R. Martin (2007). Hyperspectral Remote Sensing of Canopy Biodiversity in Hawaiian Lowland Rainforests. *Ecosystems,* 10: 536-549.

Chang, C.-C. and C.-J. Lin (2001). LIBSVM: A Library for Support Vector Machines. http://www.csie.ntu.edu.tw/~cjlin/libsvm (accessed August 2007).

Chapin, F. S. and R. A. Kedrowski (1983). Seasonal Changes in Nitrogen and Phosphorus Fractions and Autumn Retranslocation in Evergreen and Deciduous Taiga Trees. *Ecology,* 64: 376-391.

Chen, J. M., X. Li, T. Nilson and A. H. Strahler (2000). Recent Advances in Geometrical Optical Modelling and its Applications. *Remote Sensing Reviews,* 18: 227-262.

Chen, J. M., J. Liu, S. G. Leblanc, R. Lacaze and J.-L. Roujean (2003). Multi-angular optical remote sensing for assessing vegetation structure and carbon absorption. *Remote Sensing of Environment,* 84: 516-525.

Chopping, M. J., A. Rango, K. M. Havstad, F. R. Schiebe, J. C. Ritchie, T. J. Schmugge, et al. (2003). Canopy attributes of desert grassland and transition communities derived from multiangular airborne imagery. *Remote Sensing of Environment,* 85: 339-354.

Clark, J. S., S. R. Carpenter, M. Barber, S. Collins, A. Dobson, J. A. Foley, et al. (2001). Ecological Forecasts: An Emerging Imperative. *Science,* 293: 657-660.

Clark, M. L., D. A. Roberts and D. B. Clark (2005). Hyperspectral discrimination of tropical rain forest tree species at leaf to crown scales. *Remote Sensing of Environment,* 96: 375-398.

Clark, R. N. and T. L. Roush (1984). Reflectance Spectroscopy: Quantitative Analysis Techniques for Remote Sensing Applications. *Journal of Geophysical Research,* 89: 6329-6340.

Cochrane, M. A. (2000). Using vegetation reflectance variability for species level classification of hyperspectral data. *International Journal of Remote Sensing*, 21: 2075-2087.

Cocks, T., R. Jenssen, A. Stewart, I. Wilson and T. Shields (1998). *The HyMap™ airborne hyperspectral sensor: the system, calibration and performance*. Proc. of the 1st EARSeL Workshop on Imaging Spectroscopy, (pp. 37-42). Zurich.

Cohen, J. (1960). A Coefficient of Agreement for Nominal Scales. *Educational and Psychological Measurement*, 20: 37-46.

Cohen, W. B. and S. N. Goward (2004). Landsat's role in ecological applications of remote sensing. *Bioscience*, 54: 535-545.

Congalton, R. G. and K. Green (1999). *Assesssing the accuracy of remotely sensed data : principles and practices*. Boca Raton: Lewis Publications.

Congalton, R. G., R. G. Oderwald and R. a. Mead (1983). Assessing Landsat Classification Accuracy Using Discrete Multivariate-Analysis Statistical Techniques. *Photogrammetric Engineering and Remote Sensing*, 49: 1671-1678.

Cortes, C. and V. Vapnik (1995). Support-Vector Networks. *Machine Learning*, 20: 273-297.

Cristianini, N. and J. Shawe-Taylor (2000). *An introduction to support vector machines : and other kernel-based learning methods*. Cambridge ; New York: Cambridge University Press.

Curran, P. J. (1989). Remote Sensing of Foliar Chemistry. *Remote Sensing of Environment*, 30: 271-278.

Curran, P. J. (2001). Imaging spectrometry for ecological applications. *International Journal of Applied Earth Observation and Geoinformation*, 3: 305-312.

Curran, P. J., J. L. Dungan, B. A. Macler, S. E. Plummer and D. L. Peterson (1992). Reflectance Spectroscopy of Fresh Whole Leaves for the Estimation of Chemical Concentration. *Remote Sensing of Environment*, 39: 153-166.

Curran, P. J., J. L. Dungan and D. L. Peterson (2001). Estimating the foliar biochemical concentration of leaves with reflectance spectrometry testing the Kokaly and Clark methodologies. *Remote Sensing of Environment*, 76: 349-359.

Cutter, M. A. (2006). HDFclean V2 Help. http://earth.esa.int/object/index.cfm?fobjectid=4409 (accessed June 2007).

Czaplewski, R. L. (2003). Accuracy Assessment of Maps of Forest Condition. In M. A. Wulder and S. E. Franklin (Eds.), *Remote sensing of forest environments : concepts and case studies* (pp. 115-140). Boston: Kluwer Academic Publishers.

Darvishsefat, A. A. (1995). *Einsatz und Fusion von multisensoralen Satellitenbilddaten zur Erfassung von Waldinventuren*. Zurich: Remote Sensing Laboratories, Dept. of Geography, Unibersity of Zurich.

Dash, M. and H. Liu (1997). Feature selection for classification. *Intelligent Data Analysis*, 1: 131-156.

Daubenmire, R. and D. Prusso (1963). Studies of the Decomposition Rates of Tree Litter. *Ecology*, 44: 589-592.

Davidson, M. and P. Vuilleumier (2005). Note on CHRIS Acquisition Procedure and Image Geometry; http://earth.esa.int/includes/resources/dsp_DocDetailsPopUp.cfm?fobjectid=4735 (accessed April 2007).

Dawson, T. P., P. J. Curran, P. R. J. North and S. E. Plummer (1999). The propagation of foliar biochemical absorption features in forest canopy reflectance: A theoretical analysis. *Remote Sensing of Environment*, 67: 147-159.

Deering, D. W., T. F. Eck and B. Banerjee (1999). Characterization of the Reflectance Anisotropy of Three Boreal Forest Canopies in Spring-Summer. *Remote Sensing of Environment*, 67: 205-229.

Defries, R. and L. Bounoua (2004). Consequences of land use change for ecosystem services: A future unlike the past. *GeoJournal*, 61: 345-351.

Defries, R. S. and J. R. G. Townshend (1999). Global land cover characterization from satellite data: from research to operational implementation?. GCTE/LUCC Research Review. *Global Ecology and Biogeography*, 8: 367-379.

Deschamps, P. Y., F. M. Breon, M. Leroy, A. Podaire, A. Bricaud, J. C. Buriez, et al. (1994). The POLDER mission: instrument characteristics and scientific objectives. *IEEE Transactions on Geoscience and Remote Sensing*, 32: 598-615.

Diner, D. J., G. P. Asner, R. Davies, Y. Knyazikhin, J. P. Muller, A. W. Nolin, et al. (1999). New directions in earth observing: Scientific applications of multiangle remote sensing. *Bulletin of the American Meteorological Society*, 80: 2209-2228.

Diner, D. J., J. C. Beckert, G. W. Bothwell and J. I. Rodriguez (2002). Performance of the MISR instrument during its first 20 months in Earth orbit. *IEEE Transactions on Geoscience and Remote Sensing*, 40: 1449-1466.

Diner, D. J., S. W. Boland, E. S. Davis, R. A. Kahn, C. A. Hostetler, R. A. Ferrare, et al. (2007). *Future mission concept for 3-D remote sensing of aerosols from low Earth orbit*. Proc. of the IEEE Aerospace conference. Big Sky, Montana.

Diner, D. J., B. H. Braswell, R. Davies, N. Gobron, J. Hu, Y. Jin, et al. (2005). The value of multiangle measurements for retrieving structurally and radiatively consistent properties of clouds, aerosols, and surfaces. *Remote Sensing of Environment*, 97: 495-518.

Disney, M. I., P. Lewis and M. R. J. North (2000). Monte Carlo ray tracing in optical canopy reflectance modelling. *Remote Sensing Reviews*, 18: 163-196.

Draper, N. R. and H. Smith (1966). *Applied regression analysis*. New York,: Wiley.

Dubey, R. S. (2005). Handbook of photosynthesis. In M. Pessarakli (Ed.), *Books in soils, plants, and the environment* (pp. 717–737). Boca Raton, FL: Taylor & Francis.

Durbha, S. S., R. L. King and N. H. Younan (2007). Support vector machines regression for retrieval of leaf area index from multiangle imaging spectroradiometer. *Remote Sensing of Environment*, 107: 348-361.

Elvidge, C. D. (1990). Visible and near-Infrared Reflectance Characteristics of Dry Plant Materials. *International Journal of Remote Sensing*, 11: 1775-1795.

European Space Agency (2006). The Changing earth : new scientific challenges for ESA's Living Planet Programme. *ESA SP-1304* (p. 83). Noordwijk, The Netherlands: ESA Publications.

Evans, J. R. (1989). Photosynthesis and Nitrogen Relationships in Leaves of C_3 Plants. *Oecologia*, 78: 9-19.

Fassnacht, K. S., W. B. Cohen and T. A. Spies (2006). Key issues in making and using satellite-based maps in ecology: A primer. *Forest Ecology and Management*, 222: 167-181.

Feddema, J. J., K. W. Oleson, G. B. Bonan, L. O. Mearns, L. E. Buja, G. A. Meehl, et al. (2005). The Importance of Land-Cover Change in Simulating Future Climates. *Science*, 310: 1674-1678.

Field, C. and H. A. Mooney (1986). *The photosynthesis–nitrogen relationship in wild plants*. Proc. of the On the economy of plant form and function : proceedings of the Sixth Maria Moors Cabot Symposium, Evolutionary Constraints on Primary Productivity, Adaptive Patterns of Energy Capture in Plants, Harvard Forest., (pp. 25–55). Cambridge [Cambridgeshire] ; New York.

Foley, J. A., R. DeFries, G. P. Asner, C. Barford, G. Bonan, S. R. Carpenter, et al. (2005). Global Consequences of Land Use. *Science*, 309: 570-574.

Foody, G. M. and A. Mathur (2004). A relative evaluation of multiclass image classification by support vector machines. *Geoscience and Remote Sensing, IEEE Transactions on*, 42: 1335-1343.

Foody, G. M. and a. Mathur (2006). The use of small training sets containing mixed pixels for accurate hard image classification: Training on mixed spectral responses for classification by a SVM. *Remote Sensing of Environment*, 103: 179-189.

Fourty, T., F. Baret, S. Jacquemoud, G. Schmuck and J. Verdebout (1996). Leaf optical properties with explicit description of its biochemical composition: Direct and inverse problems. *Remote Sensing of Environment*, 56: 104-117.

Furnival, G. M. and R. W. Wilson (1974). Regressions by Leaps and Bounds. *Technometrics*, 16: 499-511.

Gail, W. B. (2007). Remote sensing in the coming decade: the vision and the reality. *Journal of Applied Remote Sensing*, 1: 1-19.

Gao, B.-C. and A. F. H. Goetz (1994). Extraction of Dry Leaf Spectral Features from Reflectance Spectra of Green Vegetation. *Remote Sensing of Environment*, 47: 369-374.

Gates, D. M., H. J. Gates, J. C. Gates and V. R. Gates (1965). Spectral properties of plants. *Applied Optics*, 4: 11-20.

GENACS Consortium (2005). GMES - Global Monitoring for Environment and Security. http://gmes.info, accessed July 2007.

GEO (2005). GEOSS 10-Year Implementation Plan: Reference Document. In B. Battrick (Ed.) (p. 209). Nordwijk, The Netherlands: ESA Publication Division, ESTEC.

Gerstl, S. A. W. (1999). *Building a global hotspot ecology with Triana data*. Proc. of the Remote Sensing for Earth Science, Ocean, and Sea Ice Applications, (pp. 184-194). Florence, Italy.

Gill, R. A. and R. B. Jackson (2000). Global patterns of root turnover for terrestrial ecosystems. *New Phytologist*, 147: 13-31.

Gitelson, A. A., M. N. Merzlyak and H. K. Lichtenthaler (1996). Detection of red edge position and chlorophyll content by reflectance measurements near 700 nm. *Journal of Plant Physiology*, 148: 501-508.

Global Land Project (2005). Science Plan and Implementation Strategy (p. 64). Stockholm: IGBP Secretariat.

Gobron, N., B. Pinty, M. M. Verstraete, J. V. Martonchik, Y. Knyazikhin and D. J. Diner (2000). Potential of multiangular spectral measurements to characterize land surfaces: Conceptual approach and exploratory application. *Journal of Geophysical Research-Atmospheres*, 105: 17539-17549.

Goel, N. S. (1989). Inversion of Canopy Reflectance Models for Estimation of Biophysical Parameters from Reflectance Data. In G. Asrar (Ed.), *Theory and Applications of Optical remote Sensing* (pp. 205-251). Washington, D.C.: Wiley.

Goetz, a. F. H., G. Vane, J. E. Solomon and B. N. Rock (1985). Imaging Spectrometry for Earth Remote-Sensing. *Science*, 228: 1147-1153.

Goetz, S. J., A. G. Bunn, G. J. Fiske and R. A. Houghton (2005). Satellite-observed photosynthetic trends across boreal North America associated with climate and fire disturbance. *Proceedings of the National Academy of Sciences of the United States of America*, 102: 13521-13525.

Gond, V., D. G. G. de Pury, F. Veroustraete and R. Ceulemans (1999). Seasonal variations in leaf area index, leaf chlorophyll, and water content; scaling-up to estimate fAPAR and carbon balance in a multilayer, multispecies temperate forest. *Tree Physiology*, 19: 673-679.

Goodenough, D. G., J. Y. Li, G. P. Asner, M. E. Schaepman, S. L. Ustin and A. Dyk (2006). *Combining hyperspectral remote sensing and physical modeling for applications in land ecosystems*. Proc. of the IEEE International Geoscience And Remote Sensing Symposium (IGARSS), (p. in Press). Denver, Colorado.

Goodenough, D. G., J. Pearlman, H. Chen, A. Dyk, T. Han, J. Li, et al. (2004). *Forest Information from Hyperspectral Sensing*. Proc. of the IEEE International Geoscience and Remote Sensing Symposium (IGARSS), (pp. 2585–2589). Anchorage, USA.

Goodenough, D. G., H. Tian, J. S. Pearlman, A. Dyk and S. McDonald (2003). *Forest chemistry mapping with hyperspectral data*. Proc. of the IEEE Workshop on Advances in Techniques for Analysis of Remotely Sensed Data, (pp. 395–398). NASA Goddard Visitor Center, Greenbelt, MD, USA.

Gorodetzky, D. (2005). ENVI Function: evf_to_rois.sav.

http://www.ittvis.com/codebank/search.asp?FID=93 (accessed 13 Feb. 2007).

Graetz, D. R. (1990). Remote Sensing of Terestrial Ecosystem Structure: An Ecologist's Pragmatic View. In R. J. Hobbs and H. A. Mooney (Eds.), *Remote Sensing of Biosphere Functioning* (pp. 5-30). New York: Springer-Verlag.

Grassi, G., E. Vicinelli, F. Ponti, L. Cantoni and F. Magnani (2005). Seasonal and interannual variability of photosynthetic capacity in relation to leaf nitrogen in a deciduous forest plantation in northern Italy. *Tree Physiology*, 25: 349-360.

Gualtieri, A., S. R. Chettri, R. Cromp and L. F. Johnson (1999). *Support vector machine classifiers as applied to aviris data*. Proc. of the Eighth JPL Airborne Geoscience Workshop. Pasadena, CA.

Guisan, A. and N. E. Zimmermann (2000). Predictive habitat distribution models in ecology. *Ecological Modelling*, 135: 147-186.

Haglof Inc. http://www.haglofsweden.com (accessed 16 Jan. 2007).

Hapke, B. (1981). Bidirectional Reflectance Spectroscopy - 1. Theory. *Journal of Geophysical Research*, 86: 3039-3054.

Hastie, T., R. Tibshirani and J. Friedman (2001). *The elements of statistical learning : data mining, inference, and prediction*. New York: Springer.

Hearst, M. A. (1998). Support vector machines. *IEEE Intelligent Systems & Their Applications*, 13: 18-21.

Heiskanen, J. (2006). Tree cover and height estimation in the Fennoscandian tundra-taiga transition zone using multiangular MISR data. *Remote Sensing of Environment*, 103: 97-114.

Held, A., C. Ticehurst, L. Lymburner and N. Williams (2003). High resolution mapping of tropical mangrove ecosystems using hyperspectral and radar remote sensing. *International Journal of Remote Sensing*, 24: 2739-2759.

Hill, M. J., G. P. Asner and A. Held (2006). The Bio-geophysical Approach to Remote Sensing of Vegetation in Coupled Human-Environment Systems – Societal Benefits and Global Context. *Spatial Science*, 52: 49-66.

Hocking, R. R. and R. N. Leslie (1967). Selection of the Best Subset in Regression Analysis. *Technometrics*, 9: 531-540.

Hollinger, A., M. Bergeron, M. Maskiewicz, S. Qian, H. Othman, K. Staenz, et al. (2006). *Recent Developments in the Hyperspectral Environment and Resource Observer (HERO) Mission*. Proc. of the IEEE International Conference on Geoscience and Remote Sensing Symposium (IGARSS) (pp. 1620-1623). Denver, Colorado.

Horler, D. N. H., M. Dockray, J. Barber and A. R. Barringer (1983). Red edge measurements for remotely sensing plant chlorophyll content. *Advances in Space Research*, 3: 273-277.

Hruschka, W. R. (1987). Data Analysis: Wavelength Selection Methods. In P. Williams and K. Norris (Eds.), *Near-infrared Technology in the Agricultural and Food Industries* (pp. 35-55). St. Paul, Minnesota, USA: American Association of Cereal Chemists, Inc.

Hsu, C.-W., C.-C. Chang and C.-J. Lin (2001). A practical guide to support vector classification. http://www.csie.ntu.edu.tw/~cjlin/papers/guide/guide.pdf (accessed July 2007).

Huang, C., L. S. Davis and J. R. G. Townshend (2002). An assessment of support vector machines for land cover classification. *International Journal of Remote Sensing*, 23: 725-749.

Huang, Z., B. J. Turner, S. J. Dury, I. R. Wallis and W. J. Foley (2004). Estimating foliage nitrogen concentration from HYMAP data using continuum removal analysis. *Remote Sensing of Environment*, 93: 18-29.

Huber, S., M. Kneubühler, B. Koetz, J. T. Schopfer, K. I. Itten and N. E. Zimmermann (2007). Contribution of Directional CHRIS/Proba Data for Estimating Canopy Biochemistry in Forest. *Journal of Applied Remote Sensing*, Under Review.

Huber, S., M. Kneubühler, A. Psomas, K. Itten and N. E. Zimmermann (2007). Estimating forest canopy biochemistry from hyperspectral data. *Forest Ecology and Management*, Under Review.

Huber, S., J. T. Schopfer, M. Kneubühler, J. Nieke and K. Itten (2004). *A New Approach Using Various Remote Sensing Data for Vegetation Parameter Retrieval as Input to Ecosystem Models.* Proc. of the Envisat & ERS Symposium. Salzburg, Austria.

IPCC (2007). *Climate change 2007: Mitigation. Contribution of Working group III to the Fourth Assessment Report of the Intergovernmental Panel on Climate Change.* Cambridge, United Kingdom and New York, NY, USA: Cambridge University Press.

Jain, A. and D. Zongker (1997). Feature selection: Evaluation, application, and small sample performance. *IEEE Transactions on Pattern Analysis and Machine Intelligence*, 19: 153-158.

Janz, A., S. van der Linden, B. Waske and P. Hostert (2007). *imageSVM - A user-oriented tool for advanced classification of hyperspectral data using support vector machines*. Proc. of the 5th EARSeL workshop on Imaging Spectroscopy. Bruges, Belgium.

Johansen, K., N. C. Coops, S. E. Gergel and Y. Stange (2007). Application of high spatial resolution satellite imagery for riparian and forest ecosystem classification. *Remote Sensing of Environment*, 110: 29-44.

Johnson, L. F. and C. R. Billow (1996). Spectrometric estimation of total nitrogen concentration in Douglas-fir foliage. *International Journal of Remote Sensing*, 17: 489-500.

Kellenberger, T. W. (1996). *Erfassung der Waldfläche in der Schweiz mit multispektralen Satellitenbilddaten*. Zurich: Remote Sensing Laboratories, Dept. of Geography, University of Zurich.

Kimes, D. S., K. J. Ranson, G. Sun and J. B. Blair (2006). Predicting lidar measured forest vertical structure from multi-angle spectral data. *Remote Sensing of Environment*, 100: 503-511.

Kneubühler, M. (2002). Spectral Assessment of Crop Phenology Based on Spring Wheat and Winter Barley. *RSS Vol. 38* (p. 149). Zurich: University of Zurich, Switzerland.

Kneubühler, M., B. Koetz, S. Huber, J. T. Schopfer, R. Richter and K. Itten (2006). *Monitoring Vegetation Growth using Multitemporal CHRIS/PROBA Data*. Proc. of the IGARSS, (pp. 2677-2680). Denver, USA.

Koetz, B., M. Kneubühler, S. Huber, J. T. Schopfer and F. Baret (2007). *LAI Estimation Based on Multi-temporal CHRIS/PROBA Data and Radiative Transfer Modelling*. Proc. of the Envisat Symposium. Montreux, Switzerland.

Koetz, B., F. Morsdorf, T. Curt, S. van der Linden, L. Borgniet, D. Odermatt, et al. (2007). *Fusion of imaging spectrometer and lidar data using support vector machines for land cover classification in the context of forest fire management*. Proc. of the 10th ISPMSRS. Davos, Switzerland.

Koetz, B., F. Morsdorf, G. Sun, K. J. Ranson, K. Itten and B. Allgower (2006). Inversion of a lidar waveform model for forest biophysical parameter estimation. *IEEE Geoscience and Remote Sensing Letters*, 3: 49-53.

Koh, L. P. (2007). Impacts of land use change on South-east Asian forest butterflies: a review. *Journal of Applied Ecology*, 44: 703-713.

Kokaly, R. F. (2001). Investigating a physical basis for spectroscopic estimates of leaf nitrogen concentration. *Remote Sensing of Environment*, 75: 153-161.

Kokaly, R. F. and R. N. Clark (1999). Spectroscopic determination of leaf biochemistry using band-depth analysis of absorption features and stepwise multiple linear regression. *Remote Sensing of Environment*, 67: 267-287.

Kokaly, R. F., D. G. Despain, R. N. Clark and K. E. Livo (2003). Mapping vegetation in Yellowstone National Park using spectral feature analysis of AVIRIS data. *Remote Sensing of Environment*, 84: 437-456.

Kurz, W. and M. Apps (2006). Developing Canada's National Forest Carbon Monitoring, Accounting and Reporting System to Meet the Reporting Requirements of the Kyoto Protocol. *Mitigation and Adaptation Strategies for Global Change*, 11: 33-43.

Lacaze, R., J. M. Chen, J. L. Roujean and S. G. Leblanc (2002). Retrieval of vegetation clumping index using hot spot signatures measured by POLDER instrument. *Remote Sensing of Environment,* 79: 84-95.

Lawrence, R. and M. Labus (2003). Early detection of Douglas-Fir beetle infestation with subcanopy resolution hyperspectral imagery. *Western Journal of Applied Forestry,* 18: 202-206.

Lawrence, R. L., S. D. Wood and R. L. Sheley (2006). Mapping invasive plants using hyperspectral imagery and Breiman Cutler classifications (randomForest). *Remote Sensing of Environment,* 100: 356-362.

Lenney, M. P., C. E. Woodcock, J. B. Collins and H. Hamdi (1996). The status of agricultural lands in Egypt: The use of multitemporal NDVI features derived from Landsat TM. *Remote Sensing of Environment,* 56: 8-20.

Leuschner, C., K. Backes, D. Hertel, F. Schipka, U. Schmitt, O. Terborg, et al. (2001). Drought responses at leaf, stem and fine root levels of competitive Fagus sylvatica L. and Quercus petraea (Matt.) Liebl. trees in dry and wet years. *Forest Ecology and Management,* 149: 33.

Levins, R. (1966). Strategy of Model Building in Population Biology. *American Scientist,* 54: 421-431.

LI-COR (1987). LI-3100 Area Meter Instruction Manual. Lincoln, NE, USA: LI-COR.

LI-COR (1992). LAI-2000 Plant Canopy Analyser. Instruction manual. Lincoln, NE, USA: LICOR.

Lovett, G. M., D. A. Burns, C. T. Driscoll, J. C. Jenkins, M. J. Mitchell, L. Rustad, et al. (2007). Who needs environmental monitoring? *Frontiers in Ecology and the Environment,* 5: 253-260.

Lovett, G. M., K. C. Weathers, M. A. Arthur and J. C. Schultz (2004). Nitrogen cycling in a northern hardwood forest: Do species matter? *Biogeochemistry,* 67: 289-308.

Macauley, M. K. (2006). Ascribing Societal Benefit to Environmental Observations of Earth from Space. The Multiangle Imaging SpectroRadiometer (MISR) (pp. 1-30). Washington, DC: Resources for the future.

Macauley, M. K. and D. J. Diner (2007). Ascribing societal benefit to applied remote sensing data products: an examination of methodologies based on the Multi-angle Imaging SpectroRadiometer experience. *Journal of Applied Remote Sensing,* 1: 1-20.

Martin, M. E. and J. D. Aber (1994). Analysis of forest foliage III: Determining nitrogen, lignin and cellulose in fresh leaves using near infrared reflectance data. *Journal of Near Infrared Spectroscopy,* 2: 25-32.

Martin, M. E. and J. D. Aber (1997). High spectral resolution remote sensing of forest canopy lignin, nitrogen, and ecosystem processes. *Ecological Applications,* 7: 431-443.

Mathieu, P.-P. and A. O'Neill (2007). Data assimilation: From photon counts to Earth System forecasts. *Remote Sensing of Environment*: Article in press.

Matson, P. A., L. F. Johnson, C. Billow, J. R. Miller and R. Pu (1994). Seasonal Patterns and Remote Spectral Estimation of Canopy Chemistry across the Oregon Transect. *Ecological Applications,* 4: 280-298.

McLellan, T. M., J. D. Aber, M. E. Martin, J. M. Melillo and K. J. Nadelhoffer (1991). Determination of Nitrogen, Lignin, and Cellulose Content of Decomposing Leaf Material by near-Infrared Reflectance Spectroscopy. *Canadian Journal of Forest Research-Revue Canadienne De Recherche Forestiere,* 21: 1684-1688.

McPherson, R. A. (2007). A review of vegetation--atmosphere interactions and their influences on mesoscale phenomena. *Progress in Physical Geography %R 10.1177/0309133307079055,* 31: 261-285.

McRoberts, R. E. and E. O. Tomppo (2007). Remote sensing support for national forest inventories. *Remote Sensing of Environment,* 110: 412-419.

Melillo, J. M., J. D. Aber and J. F. Muratore (1982). Nitrogen and Lignin Control of Hardwood Leaf Litter Decomposition Dynamics. *Ecology,* 63: 621-626.

Merrill, W. and E. B. Cowling (1966). Role of Nitrogen in Wood Deterioration - Amounts and Distribution of Nitrogen in Tree Stems. *Canadian Journal of Botany*, 44: 1555-1580.

Meyer, D., M. M. Verstraete and B. Pinty (1995). The effect of surface anisotropy and viewing geometry on the estimation of NDVI from AVHRR. *Remote Sensing Reviews*, 12: 3-27.

Millennium Ecosystem Assessment (2005). *Ecosystems and human well-being : synthesis*. Washington, DC: Island Press.

Miller, A. J. (2002). *Subset selection in regression*. Boca Raton: Chapman & Hall/CRC.

Minnaert, M. (1941). The reciprocity principle in lunar photometry. *Astrophysical Journal*, 93: 403-410.

Mitten, L. G. (1970). Branch-and-Bound Methods - General Formulation and Properties. *Operations Research*, 18: 24-34.

Mooney, H. a., P. M. Vitousek and P. a. Matson (1987). Exchange of Materials between Terrestrial Ecosystems and the Atmosphere. *Science*, 238: 926-932.

Moreno, J. (2007). Advanced Optical Theory - 2: Retrieval of Information. http://earth.esa.int/landtraining07/D1LA5-Moreno.pdf (accessed Nov. 2007). *ESA Advanced Training Course on Land Remote Sensing*. 2–7 September 2007, Lisbon, Portugal.

Moss, D. M. and B. N. Rock (1991). *Analysis of Red Edge Spectral Characteristics and Total Chlorophyll Values for Red Spruce (Picea Rubens) Branch Segments from Mt. Moosilauke, NH, USA.* Proc. of the IEEE Geoscience and Remote Sensing Symposium (IGARSS), (pp. 1529-1532). Espoo, Finland.

Murray, I. and P. C. Willliams (1987). Chemical Principles of Near-Infrared Technology. In P. Williams and K. Norris (Eds.), *Near-infrared Technology in the Agricultural and Food Industries* (pp. 17-31). St. Paul, Minnesota, USA: American Associaton of Cereal Chemists, Inc.

Mutanga, O., A. K. Skidmore, L. Kumar and J. Ferwerda (2005). Estimating tropical pasture quality at canopy level using band depth analysis with continuum removal in the visible domain. *International Journal of Remote Sensing*, 26: 1093-1108.

Mutanga, O., A. K. Skidmore and H. H. T. Prins (2004). Predicting in situ pasture quality in the Kruger National Park, South Africa, using continuum-removed absorption features. *Remote Sensing of Environment*, 89: 393-408.

Myneni, R. B., J. Ross and G. Asrar (1989). A Review on the Theory of Photon Transport in Leaf Canopies. *Agricultural and Forest Meteorology*, 45: 1-153.

Narendra, P. M. and K. Fukunaga (1977). Branch and Bound Algorithm for Feature Subset Selection. *IEEE Transactions on Computers*, 26: 917-922.

NASA (2005). NASA earth observations serving society (p. 28 p.). Washington, DC: NASA.

National Research Council, Space Studies Board (2007). *Earth Science and Applications from Space: National Imperatives for the Next Decade and Beyond*. Washington, DC: National Academies Press.

Nemani, R. and S. W. Running (1996). Implementation of a hierarchical global vegetation classification in ecosystem function models. *Journal of Vegetation Science*, 7: 337-346.

Nemani, R. R., P. Votava, A. R. Michaelis, M. A. White, F. Melton, C. Milesi, et al. (2005). Terrestrial Observation and Prediction System (TOPS): Developing ecological nowcasts and forecasts by integrating surface, satellite and climate data with simulation models. http://ecocast.arc.nasa.gov/content/view/106/134/ (accessed July 2007).

Ni, W., C. E. Woodcock and D. L. B. Jupp (1999). Variance in Bidirectional Reflectance over Discontinuous Plant Canopies. *Remote Sensing of Environment*, 69: 1-15.

Nieke, J., K. I. Itten, W. Debryun and APEX Team (2005). *The Airborne Imaging Spectrometer APEX: From Concept to Realisation.* Proc. of the 4th EARSeL Workshop on Imaging Spectroscopy. Warsaw.

Norris, K. H., R. F. Barnes, J. E. Moore and J. S. Shenk (1976). Predicting Forage Quality by Infrared Reflectance Spectroscopy. *Journal of Animal Science,* 43: 889-897.

Ollinger, S. V., M.-L. Smith, M. E. Martin, R. A. Hallett, C. L. Goodale and J. D. Aber (2002). Regional variation in foliar chemistry and N cycling among forests of diverse history and composition. *Ecology,* 83: 339-355.

Pal, M. and P. M. Mather (2003). *Support Vector classifiers for Land Cover Classification*. Proc. of the Map India Conference. New Delhi, India.

Pal, M. and P. M. Mather (2006). Some issues in the classification of DAIS hyperspectral data. *International Journal of Remote Sensing,* 27: 2895-2916.

Pan, Y. D., J. Horn, J. Jenkins and R. Birdsey (2004). Importance of foliar nitrogen concentration to predict forest productivity in the Mid-Atlantic region. *Forest Science,* 50: 279-289.

PCI Geomatics (2006). OrthoEngine, User's Guide Version 10.0.

Penuelas, J., J. A. Gamon, A. L. Freeden, J. Merino and C. Field (1994). Reflectance indices associated with physiological changes in nitrogen and water-limited sunflower leaves. *Remote Sensing of Environment,* 48: 135–146.

Peterson, D. L., J. D. Aber, P. A. Matson, D. H. Card, N. Swanberg, C. A. Wessman, et al. (1988). Remote-Sensing of Forest Canopy and Leaf Biochemical Contents. *Remote Sensing of Environment,* 24: 85-127.

Phinn, S. R., C. Menges, G. J. E. Hill and M. Stanford (2000). Optimizing Remotely Sensed Solutions for Monitoring, Modeling, and Managing Coastal Environments. *Remote Sensing of Environment,* 73: 117-132.

Piedallu, C. and J.-C. Gegout (2005). Effects of forest environment and survey protocol on GPS accuracy. *Photogrammetric Engineering and Remote Sensing,* 71: 1071-1078.

Pielke Sr, R. A. (2005). Atmospheric Science: Land Use and Climate Change. *Science,* 310: 1625-1626.

Pinty, B., J. L. Widlowski, N. Gobron, M. M. Verstraete and D. J. Diner (2002). Uniqueness of multiangular measurements - Part I: An indicator of subpixel surface heterogeneity from MISR. *IEEE Transactions on Geoscience and Remote Sensing,* 40: 1560-1573.

Prentice, C., A. Bondeau, W. Cramer, S. P. Harrison, T. Hickler, W. Lucht, et al. (2007). Dynamic Global Vegetation Modeling: Quantifying Terrestrial Ecosystem Responses to Large-Scale Environmental Change. In J. G. Canadellet al (Eds.), *Terrestrial ecosystems in a changing world* (pp. 175-192). Berlin; New York: Springer.

R Development Core Team (2005). R: A language and environment for statistical computing. R Foundation for Statistical Computing. (pp. 299-314). Vienna, Austria.

Rast, M. (2004). SPECTRA - Surface Processes and Ecosystem Changes Through Response Analysis (p. 74). ESTEC, Nordwijk, the Netherlands: ESA Publication Division.

Reich, P. B., B. D. Kloeppel, D. S. Ellsworth and M. B. Walters (1995). Different Photosynthesis-Nitrogen Relations in Deciduous Hardwood and Evergreen Coniferous Tree Species. *Oecologia,* 104: 24-30.

Reich, P. B., M. B. Walters and D. S. Ellsworth (1997). From tropics to tundra: Global convergence in plantfunctioning. *PNAS,* 94: 13730-13734.

Research Systems (2004). ENVI User's Guide.

Richter, R. (1998). Correction of satellite images over mountainous terrain. *Applied Optics,* 37: 4004–4015.

Richter, R., A. Muller, M. Habermeyer, S. Dech, K. Segl and H. Kaufmann (2005). Spectral and radiometric requirements for the airborne thermal imaging spectrometer ARES. *International Journal of Remote Sensing,* 26: 3149-3162.

Richter, R. and D. Schlaepfer (2002). Geo-atmospheric processing of airborne imaging spectrometry data. Part 2: atmospheric/topographic correction. *International Journal of Remote Sensing,* 23: 2631-2649.

Rock, B. N., T. Hoshizaki and J. R. Miller (1988). Comparison of Insitu and Airborne Spectral Measurements of the Blue Shift Associated with Forest Decline. *Remote Sensing of Environment,* 24: 109-127.

Rosenqvist, A., A. Milne, R. Lucas, M. Imhoff and C. Dobson (2003). A review of remote sensing technology in support of the Kyoto Protocol. *Environmental Science & Policy*, 6: 441-555.

Roughgarden, J., S. W. Running and P. A. Matson (1991). What Does Remote Sensing Do For Ecology? *Ecology*, 72: 1918-1922.

Running, S. W., D. D. Baldocchi, D. P. Turner, S. T. Gower, P. S. Bakwin and K. A. Hibbard (1999). A global terrestrial monitoring network integrating tower fluxes, flask sampling, ecosystem modeling and EOS satellite data. *Remote Sensing of Environment*, 70: 108-127.

Sandmeier, S. and D. W. Deering (1999). Structure Analysis and Classification of Boreal Forests Using Airborne Hyperspectral BRDF Data from ASAS. *Remote Sensing of Environment*, 69: 281-295.

Sandmeier, S., C. Muller, B. Hosgood and G. Andreoli (1998). Physical Mechanisms in Hyperspectral BRDF Data of Grass and Watercress. *Remote Sensing of Environment*, 66: 222-233.

Schaepman, M. E. (2007). Spectrodirectional remote sensing: From pixels to processes. *International Journal of Applied Earth Observation and Geoinformation*, 9: 204-223.

Schimel, D. S., J. I. House, K. A. Hibbard, P. Bousquet, P. Ciais, P. Peylin, et al. (2001). Recent patterns and mechanisms of carbon exchange by terrestrial ecosystems. *Nature*, 414: 169-172.

Schläpfer, D. (2005). Parametric Geocoding (PARGE), User Guide, Version 2.2: ReSe Applications Schläpfer, Wil (SG) & Remote Sensing Laboratories, University of Zurich.

Schläpfer, D., B. Koetz, S. Gruber and F. Morsdorf (2003). *The influence of DEM characteristics on preprocessing of DAIS/ROSIS data in high altitude alpine terrain*. Proc. of the 3rd EARSeL Workshop on Imaging Spectroscopy, (pp. 133-139). Herrsching, Germany.

Schläpfer, D., J. Nieke and K. I. Itten (2007). Spatial PSF Nonuniformity Effects in Airborne Pushbroom Imaging Spectrometry Data. *IEEE Transactions on Geoscience and Remote Sensing*, 45: 458-468.

Schläpfer, D. and R. Richter (2002). Geo-atmospheric processing of airborne imaging spectrometry data. Part 1: parametric orthorectification. *International Journal of Remote Sensing*, 23: 2609-2630.

Schlerf, M. and J. Hill (2005). *Estimation of forest biophysical characteristics through coupled atmosphere-reflectance model inversion using hyperspectral multi-directional remote sensing data – A contribution to future forest inventory strategies*. Proc. of the 3rd ESA CHRIS/Proba Workshop. Frascati, Italy.

Schlerf, M., J. Hill, H. Buddenbaum, W. Werner and G. Schüler (2005). *Assessment of Vegetation Nitrogen Status from Hyperspectral Laboratory and Image Data*. Proc. of the The 9th International Symposium on Physical Measurements and Signatures in Remote Sensing (ISPMSRS), (pp. 60–63). Beijing, China.

Schlerf, M., W. Verhoef, H. Buddenbaum, J. Hill, C. Atzberger and A. K. Skidmore (2007). *Comparing Three Canopy Reflectance Models with Hyperspectral Multi-Angular Satellite Data*. Proc. of the The 10th International Symposium on Physical Measurements and Signatures in Remote Sensing (ISPMSRS). Davos, Switzerland.

Schölkopf, B., A. J. Smola, R. C. Williamson and P. L. Bartlett (2000). New support vector algorithms. *Neural Computation*, 12: 1207-1245.

Schönermark, M. v., B. Geiger and H.-P. Röser (2004). *Reflection properties of vegetation and soil : with a BRDF data base*. Berlin: Wissenschaft und Technik Verlag.

Schopfer, J. T., S. Huber, T. Schneider, W. A. Dorigo, N. Oppelt, D. Odermatt, et al. (2007). *Towards a Comparison of Spaceborne and Ground-based Spectrodirectional Reflectance Data*. Proc. of the Envisat Symposium 2007. Montreux, Switzerland.

Schwarz, M. and N. E. Zimmermann (2005). A new GLM-based method for mapping tree cover continuous fields using regional MODIS reflectance data. *Remote Sensing of Environment*, 95: 428-443.

Secretariat of the Convention on Biological Diversity. (2006). *Global biodiversity outlook 2*. Montreal: Secretariat of the Convention on Biological Diversity.

Seneviratne, S. I., D. Luthi, M. Litschi and C. Schar (2006). Land-atmosphere coupling and climate change in Europe. *Nature,* 443: 205.

Serrano, L., J. Penuelas and S. L. Ustin (2002). Remote sensing of nitrogen and lignin in Mediterranean vegetation from AVIRIS data: Decomposing biochemical from structural signals. *Remote Sensing of Environment,* 81: 355-364.

Sharpe, P. J. H. (1990). Forest modeling approaches: compromises between generality and precision. In R. K. Dixonet al (Eds.), *Process modeling of forest growth responses to environmental stress* (pp. 180-190). Portland, OR: Timber Press.

Shi, H. R., F. D. Zhuang and Z. Niu (2003). Effects of spectral transformations in statistical modeling of leaf biochemical concentrations. *In: IEEE Workshop on Advances in Techniques for Analysis of Remotely Sensed Data*: 263-266.

Sims, D. A. and J. A. Gamon (2002). Relationships between leaf pigment content and spectral reflectance across a wide range of species, leaf structures and developmental stages. *Remote Sensing of Environment,* 81: 337-354.

Solomon, S., D. Qin, M. Manning, R. B. Alley, T. Berntsen, N. L. Bindoff, et al. (2007). *Technical Summary. In: Climate Change 2007: The Physical Science Basis. Contribution of Working Group I to the Fourth Assessment Report of the Intergovernmental Panel on Climate Change* Cambridge, United Kingdom and New York, NY, USA: Cambridge University Press

Stern, N. (2007). *The economics of climate change : the Stern review*. Cambridge, UK ; New York: Cambridge University Press.

Strand, H., R. Höft, J. Strittholt, L. Miles, N. Horning, E. Fosnight, et al. (Eds.) (2007). *Sourcebook on Remote Sensing and Biodiversity Indicators*. Montreal: Secretariat of the Convention on Biological Diversity.

Stricker, N. C. M., A. Hahne, D. L. Smith, J. Delderfield, M. B. Oliver and T. Edwards (1995). ATSR-2: The evolutionin its design from ERS-1 to ERS-2. *ESA Bulletin,* 83: 32-37.

Stuffler, T., C. Kaufmann, S. Hofer, K. P. Forster, G. Schreier, A. Mueller, et al. (2007). The EnMAP hyperspectral imager--An advanced optical payload for future applications in Earth observation programmes. *Acta Astronautica,* 61: 115-120.

Su, L., M. J. Chopping, A. Rango, J. V. Martonchik and D. P. C. Peters (2007). Support vector machines for recognition of semi-arid vegetation types using MISR multi-angle imagery. *Remote Sensing of Environment,* 107: 299-311.

Swain, P. H. and S. M. Davis (1978). *Remote sensing : The quantitative approach*. London ; New York: McGraw-Hill International Book Co.

Swiss Federal Office of Meteorology and Climatology MeteoSchweiz (2006). http://www.meteoschweiz.ch/web/en/climate/recent_climate_development/letzte_monate.reg6.stationBUS.html (accessed Feb. 2007).

Tatem, A. J., S. J. Goetz and S. I. Hay (2004). Terra and Aqua: new data for epidemiology and public health. *International Journal of Applied Earth Observation and Geoinformation,* 6: 33-46.

Toutin, T. (2004). Review article: Geometric processing of remote sensing images: models, algorithms and methods. *International Journal of Remote Sensing,* 25: 1893-1924.

Treuhaft, R. N., B. E. Law and G. P. Asner (2004). Forest attributes from radar interferometric structure and its fusion with optical remote sensing. *Bioscience,* 54: 561-571.

Trimble (2005). GPS Pathfinder Office Software V3.10.

Tsai, F. and W. Philpot (1998). Derivative Analysis of Hyperspectral Data. *Remote Sensing of Environment,* 66: 41-51.

Turner, D. P., M. Guzy, M. A. Lefsky, W. D. Ritts, S. Van Tuyl and B. E. Law (2004). Monitoring forest carbon sequestration with remote sensing and carbon cycle modeling. *Environmental Management,* 33: 457-466.

Turner, D. P., S. V. Ollinger and J. S. Kimball (2004). Integrating remote sensing and ecosystem process models for landscape- to regional-scale analysis of the carbon cycle. *Bioscience,* 54: 573-584.

Underwood, E., S. L. Ustin and D. DiPietro (2003). Mapping nonnative plants using hyperspectral imagery. *Remote Sensing of Environment,* 86: 150-161.

United Nations (2002). *Report of the World Summit on Sustainable Development : Johannesburg, South Africa, 26 August-4 September 2002*. New York: United Nations.

United Nations Environment Programme (2007). *Global Environment Outlook – environment for development (GEO-4)*: UNEP.

Ustin, S. L., D. A. Roberts, J. A. Gamon, G. P. Asner and R. O. Green (2004). Using imaging spectroscopy to study ecosystem processes and properties. *Bioscience,* 54: 523-534.

Ustin, S. L., M. O. Smith, S. Jacquemoud, M. M. Verstraete and Y. Govaerts (1999). Geobotany: Vegetation Mapping for Earth Sciences. In A. N. Rencz (Ed.), *Remote Sensing for the Earth Sciences: Manual of Remote Sensing* (pp. 189-248): John Wiley & Sons, Inc.

Ustin, S. L., P. J. Zarco-Tejada, S. Jacquemoud and G. P. Asner (2004). Remote Sensing of the Environment: State of the Science and New Directions. In S. L. Ustin (Ed.), *Remote sensing for natural resource management and environmental monitoring* (pp. 679–729). Hoboken, NJ: John Wiley & Sons.

van der Linden, S. and A. Janz (2007). imageSVM-Support Vector Machine Classification for Remote Sensing Image Data (preliminary) Manual (pp. 1-13): Geomatics Department, Humboldt-Universität zu Berlin.

Vapnik, V. N. (2000). *The nature of statistical learning theory*. New York: Springer.

Vitousek, P. M., H. A. Mooney, J. Lubchenco and J. M. Melillo (1997). Human domination of Earth's ecosystems. *Science,* 277: 494-499.

Voigt, S., T. Kemper, T. Riedlinger, R. Kiefl, K. Scholte and H. Mehl (2007). Satellite Image Analysis for Disaster and Crisis-Management Support. *IEEE Transactions on Geoscience and Remote Sensing,* 45: 1520-1528.

Waske, B. and J. A. Benediktsson (2007). Fusion of Support Vector Machines for Classification of Multisensor Data. *IEEE Transactions on Geoscience and Remote Sensing,* Accepted.

Waske, B., G. Menz and J. A. Benediktsson (2007). *Fusion of Support Vector Machines for Classifying SAR and Multispectral Imagery from Agricultural Areas*. Proc. of the IGARSS. Barcelona, Spain.

Weisberg, S. (1980). *Applied linear regression*. New York: Wiley.

Weiss, M., F. Baret, R. B. Myneni, A. Pragnere and Y. Knyazikhin (2000). Investigation of a model inversion technique to estimate canopy biophysical variables from spectral and directional reflectance data. *Agronomie,* 20: 3-22.

Wessman, C. A., J. D. Aber, D. L. Peterson and J. M. Melillo (1988). Remote-Sensing of Canopy Chemistry and Nitrogen Cycling in Temperate Forest Ecosystems. *Nature,* 335: 154-156.

Wickland, D. E. (1991). Mission to Planet Earth: The Ecological Perspective. *Ecology,* 72: 1923-1933.

Widlowski, J. L., B. Pinty, N. Gobron, M. M. Verstraete and A. B. Davis (2001). Characterization of surface heterogeneity detected at the MISR/TERRA subpixel scale. *Geophysical Research Letters,* 28: 4639-4642.

Widlowski, J. L., B. Pinty, N. Gobron, M. M. Verstraete, D. J. Diner and A. B. Davis (2004). Canopy structure parameters derived from multi-angular remote sensing data for terrestrial carbon studies. *Climatic Change,* 67: 403-415.

Wulder, M. A., T. Han, J. C. White, T. Sweda and H. Tsuzuki (2007). Integrating profiling LIDAR with Landsat data for regional boreal forest canopy attribute estimation and change characterization. *Remote Sensing of Environment,* 110: 123-137.

Yoder, B. J. and R. E. Pettigrew-Crosby (1995). Predicting Nitrogen and Chlorophyll Content and Concentrations from Reflectance Spectra (400-2500nm) at Leaf and Canopy Scales. *Remote Sensing of Environment,* 53: 199-211.

Zimmermann, N. E., T. C. Edwards, G. G. Moisen, T. S. Frescino and J. A. Blackard (2007). Remote sensing-based predictors improve distribution models of rare, early successional and broadleaf tree species in Utah. *Journal of Applied Ecology,* 44: 1057-1067.

Acknowledgements

A major part of the research relevant for the presented dissertation was granted by the Swiss National Science Foundation project no. 200020-101517.

I would like to acknowledge all the contributors for their highly appreciated support, dedication and interest to accomplish this PhD thesis. I greatly appreciate the willingness of Martin Schlerf (ITC, The Netherlands) to review this thesis and contribute an external expertise of the work.

My gratitude goes to my promoter and supervisor Prof. Klaus Itten for his confidence, commitment and generous support during the past years to make this project possible. I would like to express my appreciation to Dr. Niklaus Zimmermann (WSL), my second supervisor, who substantially helped in organizing, conducting and financing the fieldwork to kick-off the PhD project. I highly appreciated his expertise and enthusiasm during the time of this work. I deeply acknowledge Dr. Mathias Kneubühler, my team leader and co-adviser, for sharing know-how, in particular in CHRIS matters and his advisory support in many difficult situations.

A special thanks goes to my colleagues Andi Hüni, who contributed not only with prompt reviewing and commenting to many of my scientific texts but also with narrating adventurous mountaineering stories in the coffee breaks (Cheers, Andi!), Dr. Ben Koetz, who significantly supported this research with many scientific discussions and advices, Achilleas Psomas who captivated with his cheerful nature and extensively supported me in field and lab work (Efharisto poli, Achilleas!), Dr. Daniel Schläpfer, whose expertise in radiometric data processing was indispensable for the correction of the hyperspectral imagery and Jürg Schopfer, whose company I highly appreciated during all these years. It was very helpful and inspiring to have him as a room mate. I say thank you to all my colleagues at RSL and GIUZ for their manifold support and for the pleasant and motivating atmosphere. Thank's all of you!

I would also like to acknowledge the tree climber Melch Kümin and the many individuals for their important contribution to field and lab work in 2004, the lab technicians Bruno Kägi and René Husi (Institute of Environmental Sciences, University of Zurich) who helped me with the laboratory work at the University of Zurich and Christian Ginzler (WSL) for his support in GPS matters.

Finally, I wish to express my appreciation to my family and friends who contributed to my overall wellbeing.

Silvia Huber Zurich, December 2007

Curriculum Vitae

Name	Silvia Huber Gharib
Date and place of birth:	2 April 1976, Wädenswil ZH (Switzerland)
Nationality:	Swiss

January 1996	Secondary school, Kantonsschule Zürich-Enge (Zurich, Switzerland) Matriculation ('Abitur') Type Economy.
Oct. 1997–Jan. 2003	University of Zurich (Zurich, Switzerland) Master of Science in Geography (Minor subjects: Agro-ecology and Geology at the Swiss Federal Institute of Technology, Zurich) MSc thesis: 'Interannual Vegetation Analysis of an Agricultural Area in Spain Using Imaging Spectroscopy Data'.
Oct. 2003–March 2008	University of Zurich (Zurich, Switzerland) PhD studies at the Remote Sensing Laboratories (RSL) on the 'Estimation of Ecologically Relevant Land Cover Variables from Imaging Spectroscopy', granted by the Swiss National Science Foundation.

Personal Bibliography

Peer reviewed journals

Huber, S., Kneubühler, M., Psomas, A., Itten, K., & Zimmermann, N.E. (2008). Estimating Biochemistry in Mixed Forests from HyMap Data using Band-Depth Analyses and Subset Regression Algorithms. *Forest Ecology and Management*, 256: 491-501.

Huber, S., Kneubühler, M., Koetz, B., Schopfer, J.T., Itten, K.I., & Zimmerman, N.E. (2008). Contribution of Directional CHRIS/Proba Data for Estimating Canopy Biochemistry in Forest. *Journal of Applied Remote Sensing. Under Review*.

Psomas, A., Kneubühler, M., **Huber, S.**, Itten, K.I., & Zimmermann, N.E. (2007). Analysis of Seasonal and Annual Spectral Characteristics for the Discrimination of Grassland Habitats. *Remote Sensing of Environment. Under Review.*

Kneubühler, M., Koetz, B., **Huber, S.**, Zimmermann, N.E. & Schaepman, M.E. (2007). Space-based Spectro-doirectional Measurements for the Improved Estimation of Ecosystem Variables. *Canadian Journal of Remote Sensing. Accepted*.

Conference and workshop contributions

2007

Huber, S., Kneubuehler, M., Koetz, B., Schopfer, J.T., Zimmerman, N.E., & Itten, K.I. (2007). The potential of spectrodirectional CHRIS/PROBA data for biochemistry estimation. In H. Lacoste & L. Ouwehand (Eds.), *Envisat Symposium*, 23–27 April 2007, Montreux, Switzerland: ESA Communication Production Office, ESTEC, Noordwijk, The Netherlands.

Koetz, B., Kneubühler, M., **Huber, S.**, Schopfer, J.T., & Baret, F. (2007). LAI Estimation Based on Multi-temporal CHRIS/PROBA Data and Radiative Transfer Modelling. In H. Lacoste & L. Ouwehand (Eds.), *Envisat Symposium*. Montreux, Switzerland: ESA Communication Production Office, ESTEC, Noordwijk, The Netherlands.

Schopfer, J.T., **Huber, S.**, Schneider, T., Dorigo, W.A., Oppelt, N., Odermatt, D., et al. (2007). Towards a Comparison of Spaceborne and Ground-based Spectrodirectional Reflectance Data. In H. Lacoste & L. Ouwehand (Eds.), *Envisat Symposium 2007*. Montreux, Switzerland: ESA Communication Production Office, ESTEC, Noordwijk, The Netherlands.

Huber, S., Kneubühler, M., Koetz, B., Schopfer, J.T., Zimmerman, N.E., & Itten, K.I. (2007). Estimating nitrogen concentration from directional CHRIS/Proba data. In *Proc. of the 10th International Symposium on Physical Measurements and Signatures in Remote Sensing (ISPMSRS)*, 12–14 March 2007, Davos, Switzerland, pp. 462-467.

Visscher von Arx, A., **Huber, S.**, Kneubühler, M., & Itten, K.I. (2007). Leaf area index estimates obtained for mixed forest using hemispherical photography and HyMap data. In *Proc. of the 10th International Symposium on Physical Measurements and*

Signatures in Remote Sensing (ISPMSRS), 12–14 March 2007, Davos, Switzerland, pp. 456-461.

Koetz, B., Kneubühler, M., **Huber, S.**, Schopfer, J.T., & Baret, F. (2007). Radiative Transfer Model Inversion based on Multi-Temporal CHRIS/Proba Data for LAI Estimation. In In *Proc. of the 10th International Symposium on Physical Measurements and Signatures in Remote Sensing (ISPMSRS)*, 12–14 March 2007, Davos, Switzerland, pp. 344-349.

2006

Huber, S., Kneubühler, M., Koetz, B., Schopfer, J.T., Zimmermann, N.E., & Itten, K.I. (2006). Canopy Biochemistry Estimation Using Spectrodirectional CHRIS Data. In *J.A. Sobrino (Ed.), Second Recent Advances in Quantitative Remote Sensing* (pp. 314-319). Servicio de Publicaciones. Universitat de Valencia, Spain.

Kneubühler, M., Koetz, B., **Huber, S.**, Schopfer, J.T., Richter, R., & Itten, K.I. (2006). Monitoring Vegetation Growth using Multitemporal CHRIS/PROBA Data. In *Proc. of IEEE International Geoscience and Remote Sensing Symposium (IGARSS)*, 31 July- 04 August 2006, Denver, Colorado.

Kneubuehler, M., Koetz, B., **Huber, S.**, Schopfer, J.T., Richter, R., & Itten, K.I. (2006). CHRIS/PROBA Data Analysis at the Swiss Midlands Testsite, In *Proc. of the 4th CHRIS/PROBA Workshop*, 19–21 September 2006, Frascati, Italy.

2005

Huber, S., Schopfer, J.T., Kneubühler, M., Nieke, J., & Itten K.I. (2005). A New Approach Using Various Remote Sensing Data for Vegetation Parameter Retrieval as Input to Ecosystem Models. In *Proc. of the CEReS International Symposium on Remote Sensing*, 13–14 December 2005, Chiba University, Japan, pp. 209-212.

Huber, S., Zimmermann, N.E., Kneubühler, M., Psomas, A., & Itten, K.I. (2005). Estimating Nitrogen in Mixed Forests from HyMap Data using Band-Depth Analysis and Branch-and-Bound Algorithm. In *Proc. of the 9th International Symposium on Physical Measurements and Signatures in Remote Sensing (ISPMSRS)*, 17–19 October 2005, Beijing, China, pp. 533-535.

Huber, S., M. Kneubühler, N.E. Zimmermann and K.I. Itten (2005). Potential of Spectral Feature Analysis to Estimate Nitrogen Concentration in Mixed Canopies. In *B. Zagajewski and M. Sobczak (Eds.), Imaging Spectroscopy. New Quality in Environmental Studies* (pp. 255-262). Warsaw: EARSeL & Warsaw University.

2004

Huber, S., Schopfer, J.T., Kneubühler, M., Nieke J., & Itten, K.I. (2004). A New Approach Using Various Remote Sensing Data for Vegetation Parameter Retrieval as Input to Ecosystem Models. In *Proc. of the ENVISAT & ERS Symposium* 6–10 September 2004, Salzburg, Austria: ESA Communication Production Office, ESTEC, Noordwijk, The Netherlands.

Schaepman-Strub, G., Painter, P., **Huber, S.**, Dangel, S., Schaepman, M.E., Martonchik, J.V., et al. (2004). About the importance of the definiton of reflectance quantities - results of case studies. In *Proc. of the XXth International Society for Photogrammetry and Remote Sensing (ISPRS) Congress*, 12–23 July 2004, Istanbul, Turkey, pp. 361-366.

2003

Schaepman, G., Schaepman, M.E., **Huber, S., &** Itten, K.I. (2003). Retrieval of vegetation parameters from hyperspectral imaging sensor data. Draft Final, Report of Phase III January 2001– July 2003, RSL, University of Zurich, Zurich, pp. 1-76.